Master's thesis

NTNU
Norwegian University of Science and Technology
Faculty of Information Technology and Electrical Engineering
Department of Electric Power Engineering

Erlend Øye

# A Practical Application of an Active Distribution Grid Planning Framework in Relation to a Pilot Area for New Energy Solutions

Master's thesis in Energy and Environmental Engineering
Supervisor: Kjell Sand
Co-supervisor: Eivind Solvang and Iver Bakken Sperstad

June 2021

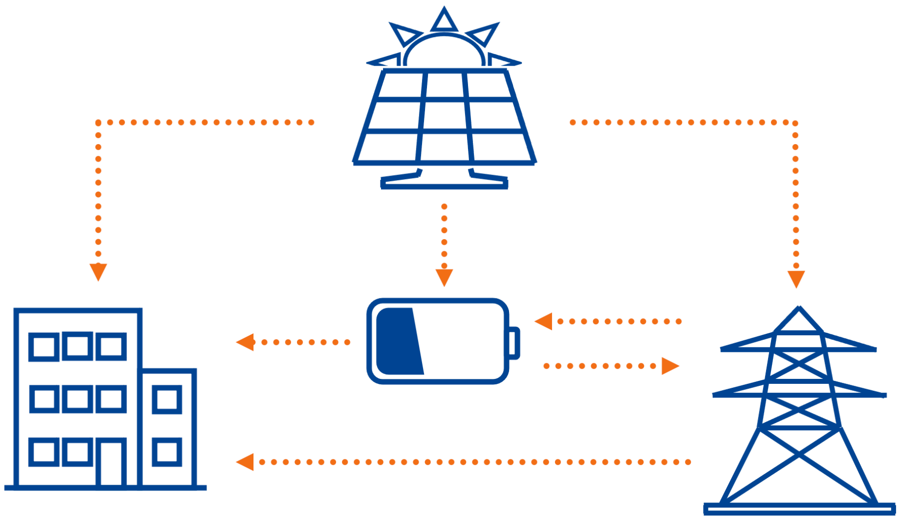

NTNU
Norwegian University of
Science and Technology

Erlend Øye

# A Practical Application of an Active Distribution Grid Planning Framework in Relation to a Pilot Area for New Energy Solutions

Master's thesis in Energy and Environmental Engineering
Supervisor: Kjell Sand
Co-supervisor: Eivind Solvang and Iver Bakken Sperstad
June 2021

Norwegian University of Science and Technology
Faculty of Information Technology and Electrical Engineering
Department of Electric Power Engineering

NTNU
Norwegian University of
Science and Technology

# Preface

This master's thesis work was performed during the spring of 2021 at the Department of Electric Power Engineering, NTNU, and is a continuation of the work performed in the specialization project during the fall of 2020. The task itself is proposed by SINTEF Energy Research and Nordlandsnett (from here on referred to by their new name: Arva), and is related to the Centre for Intelligent Electricity Distribution (CINELDI), where SINTEF Energy Research serves as the host institution.

Regarding the work, I would like to thank my supervisors Kjell Sand (vice dean for innovation at NTNU), Eivind Solvang (senior research scientist at SINTEF Energy Research) and Iver Bakken Sperstad (research scientist at SINTEF Energy Research) for superb guidance throughout the project.

Second, I would like to thank Tarjei Benum Solvang and the rest of Arva, for valuable input and discussions related to the task.

Finally, a big thank you to Pål Ivar Hansen (Volue) for arranging for me to learn NETBAS first-hand at Volue and to Reidar Ognedal (Volue) for essential help related to the use of NETBAS.

Erlend Øye

Trondheim, June 2021
Erlend Øye

**Abstract**

The work performed is based around the development of an area in Bodø, referred to as Molobyen, and is related to the FME CINELDI pilot project *Development area Molobyen*. The overall objective has been to investigate alternative ways of connecting this area to the grid, considering both technical and economic aspects, with a focus on including flexibility solutions (e.g. batteries). In order to do so, a grid planning framework combining elements from traditional grid planning and from active grid planning frameworks in the research literature, has been proposed. Also, to capture the operational benefits of batteries, a model for battery optimal dispatch was developed.

By utilizing time series from an energy system analysis performed in FME ZEN, load demand and solar PV generation of the area were modelled, before alternatives for connecting the area to the grid were defined. If these alternatives included batteries, the model for battery optimal dispatch was utilized. From there on, power flow analyses were performed in order to ensure no technical constraint violations, as well as to calculate power losses. For several alternatives, PV generation turned out to be the dimensioning factor of nearby transformers and cables, as large amounts of power were fed back to the grid during summer months. Due to this, some alterations had to be made to the traditional approach for calculating cost of losses. By also calculating investment costs, socio-economic analyses were performed and the different system solutions ranked.

The most promising system solution involving batteries was only about 3% more expensive than the optimal solution, which involved upgrading nearby transformers. However, it suffered from not being capable of reducing the maximum loading of nearby transformers, caused by PV generation, sufficiently. Hence, to connect the area of Molobyen to the grid, the more traditional approach of upgrading the nearby transformers appeared as a better solution, both from a technical and economic perspective.

Finally, the main contributions of this work are related to the proposed grid planning framework, the model for battery optimal dispatch and the method for calculating cost of losses.

**Sammendrag**

Oppgaven er relatert til utbyggingen av et område i Bodø, kalt Molobyen, og er tilknyttet FME CINELDIs pilotprosjekt *Development area Molobyen*. Målet med oppgaven har vært å undersøke ulike måter å koble Molobyen til distribusjonsnettet på, basert på tekniske og økonomiske betraktninger. Det foreligger også et fokus på bruk av fleksibilitetsløsninger, som batterier. Som en følge av dette, har et rammeverk for nettplanlegging, som kombinerer elementer fra tradisjonell nettplanlegging og fra planlegging av aktive distribusjonsnett i forskningslitteraturen, blitt etablert. Det er også utviklet en optimeringsmodell for bruk av batteri, for å kartlegge operasjonelle fordeler ved batteribruk i nettet.

Ved å benytte tidsserier fra en energisystemanalyse, utført i FME ZEN, har forventet lastbehov og solcelleproduksjon for Molobyen blitt modellert. Videre, så har ulike alternativer for å koble området til omkringliggende nett blitt definert, hvorpå det er gjennomført lastflytanalyser. Hovedformålet med disse har vært å sørge for sikker drift av nettet, samt å beregne tap, for de ulike alternativene. Fra disse analysene ble det klart at det for flere av alternativene, var høy solcelleproduksjon som førte til maksimal belastning i nærliggende kabler og transformatorer. Spesielt i sommermånedene ble store mengder kraft sendt tilbake ut på nettet. Som en følge av dette, måtte den tradisjonelle metoden for å beregne tapskostnader justeres. Deretter ble investeringskostnader for de ulike alternativene beregnet og samfunnsøkonomiske analyser gjennomført, hvorpå de ulike systemløsningene kunne rangeres.

Den mest lovende systemløsningen som inkluderte bruk av batteri, var omtrent 3% dyrere enn den optimale løsningen, som omhandlet oppgradering av transformatorer. Fra et økonomiske perspektiv er systemløsningene dermed sammenliknbare, men fra et teknisk perspektiv var ikke nevnte batteriløsning i stand til å redusere maksimal belastning av nærliggende transformatorer tilstrekkelig. Dermed vil den mer tradisjonelle løsningen (oppgradering av trafoer) være å foretrekke, både fra et teknisk og økonomisk perspektiv.

Avslutningsvis, de viktigste bidragene fra dette arbeidet omhandler det etablerte rammeverket for nettplanlegging, optimeringsmodellen for batteribruk og den reviderte metoden for å beregne tapskostnader.

# Table of contents

# 1 Introduction

## 1.1 Passive and Active Distribution Grid Planning

The electricity power system is currently experiencing substantial changes, due to the introduction of distributed energy resources (DER), increased penetration of variable renewable energy sources (VRES), and increased deployment of advanced information and communication technologies (ICT). Among other elements, DER includes distributed generation (DG), typically utilizing VRES, and an increased installed capacity of such DG causes the power generation to become less predictable, which again leads to challenges related to the distribution grid planning and operation. These challenges are made more complex as also the load demand becomes less predictable. This is due to the rise of new types of "high power, low energy"-equipment, e.g. induction cookers and heat pumps, as well as fast chargers for electrical vehicles (EVs). However, these challenges can be mitigated, for instance through the use of energy storage systems (ESSs) in combination with DG. Regardless, it is critical to incorporate such active measures into the grid planning process.

Traditional distribution grid planning is based around a "fit-and-forget"-approach, but due to the challenges described above, this approach could turn out to be outdated. Although it would probably satisfy energy demand and technical requirements, such an approach would require major investments, as well as probably leaving the grid largely under-utilized. Thus, this passive approach to distribution grid planning should be replaced by a more active grid planning, utilizing the rise of ICT used in the power system and the flexibility introduced by active measures. The need for this transition, or change, of framework is emphasized in both [1], [2] (or [3]), [4], and [5].

Klyapovskiy, et al. [1] describe a distribution grid in transition, mainly due to the rise of DER and new types of "high power, low energy"-equipment. If a new planning strategy is not adopted, the traditional "worst-case" planning algorithm, used in passive distribution networks, will cause a substantial under-utilization of the grid. However, this can be avoided by including active elements/measures in the grid planning process. Thus, "a generic multi-stage planning framework for incorporating the flexibility from active elements in the distribution grid planning is proposed", which "facilitates the transition from passive to active distribution networks" [1, p.66]. The framework includes all planning stages, from data collection to implementation plan. In addition, the two methods, passive and active distribution network planning, are compared through an example, showing how the latter can make for significant savings.

Sperstad, et al. [2] also emphasize a distribution grid in transition, and that the long-term distribution grid planning frameworks used today will not be able to account for DER or active grid measures. Further, even though there exist algorithms and methods handling this challenge, they are seldom used in practice. Thus, a framework facilitating the transition from passive to active distribution grid planning, is presented. In addition, a test case is provided to illustrate the gains and benefits from the proposed framework and its probabilistic methodologies.

Tønne [4] emphasizes that the electric distribution system is undergoing major changes, making the traditional "fit-and-forget" approach for dimensioning the grid both expensive and challenging to meet. At the same time, he points out that the increasing number of sensors and ICT equipment in the distribution grid will create huge amounts of data, that could and should be actively utilized in the distribution grid planning process. As a result, a probabilistic method for load and generation modelling is proposed, with probabilistic network calculations (power flow) performed with Monte Carlo simulations. By comparing this probabilistic method with the traditional one, it is concluded that the probabilistic method both reduces over-investment in grid capacity and prevents a significant under-utilization of the grid.

Pilo, et al. [5] investigate traditional approaches used in distribution grid planning, from which it is concluded that the traditional "fit-and-forget" approach is no longer satisfactory. From this, the different requirements for realizing the transition towards an active distribution system (ADS) are investigated. Some of these requirements are that the distribution grid operation and planning stage can no longer be separate tasks, ICT systems must be actively accounted for in the grid planning process, and load demand must be modelled using time-dependent models in order to capture the operational aspect. As such, a new framework and methodologies for short, medium and long term models for ADS planning, are identified.

Finally, an essential part of both passive and active grid planning frameworks, is mapping investment costs. In this context, REN's *Planleggingsbok for kraftnett: Kostnadskatalog distribusjonsnett* [6] should be highlighted as a relevant source.

## 1.2 Batteries as Active Grid Measures

Active measures are frequently mentioned as a way of handling the fluctuating production from renewable energy sources, or simply to defer grid reinvestments. Such active measures can be energy storage systems, for instance in terms of battery energy storage systems (BESSs). The span of applications for which BESSs can be used is wide, and includes load levelling, provision of ancillary services, and grid reinvestment deferral. However, from a grid planning perspective, the use of BESSs are not commonly included. As stated in [7], "the lack of established computational methods for including BESSs in grid planning is a barrier for taking published research-based models into practice".

Although there are no established methods for including BESSs in grid planning, there are several methods and papers on the topic. Some of these are [7], [8] and [9].

Sperstad, et al. [7] provide an overview of real-world BESS projects for grid applications, along with computational methods for including the storage systems in grid planning. At the same time, it is emphasized that although there exist several such methods in the research literature, there are not many examples where they are applied in practice. As such, there is a clear gap between research-based grid planning and grid planning in practice, preventing the research-based methods from being utilized. The reasons for this are then discussed, before recommendations on how to reduce the gap are provided. The key recommendations are based around the structure and content of the current methods, emphasizing that they should handle timing, sizing and siting of the BESS installations. Equally important, they must clearly capture the expected future development in the triggers causing a need for performing grid planning. At last, the operational benefits of the BESS must be realistically modelled, in order to perform robust cost-benefit analyses.

Li, et al. [8] provide an extensive overview of the different models and methods for planning of active distribution systems (ADSs). With a high penetration of DERs, such as ESSs, traditional grid planning frameworks have become unsuitable. Hence, in order to obtain models well suited for ADS planning, the main features, or problems, causing traditional planning to be unsuitable, are analyzed. This includes, for instance, integration of DGs and ESSs and handling of high-level uncertainties. In ADS planning, it is important that these are included and handled as a part of the planning process, with suggested approaches being probabilistic multi-scenario based approaches and multi-level programming.

Sand, et al. [9] present methods for performing cost-benefit analyses regarding investment decisions related to battery installations in the distribution grid. Technical considerations are also included, as these are important for, for instance, mapping losses related to the batteries. Further, examples performing these cost-benefit analyses are presented, along with results and experiences from real-life applications/projects. From one of these, it was revealed that the use of batteries as a temporary solution to defer grid reinvestments, was profitable. This utilization of batteries is also emphasized as one of the main differences between batteries and traditional grid investments.

## 1.3 Introduction to Molobyen

The work is related to the FME CINELDI pilot project *Development area Molobyen*. More specifically, the work is based around the power supply situation related to the development of a new area, referred to as Molobyen. The area is located on the north-west coastline of Bodø, and is shown in Figure 1. To cover the increased power demand related to this project, district heating (DH), solar photovoltaic (PV), and the electric distribution grid will be utilized. The use of solar PV is important in this context, as there is a focus on the application of new energy solutions, in order to obtain something close to a zero emission neighbourhood (ZEN). It should also be added that there is practically no existing grid in the area of Molobyen, thus new grid must be constructed. More general information on Molobyen is provided in Section 2.1.


Figure 1: The area to be developed, Molobyen, is located within the dashed red line. The buildings within this line are not currently constructed. The figure is a modified version of [10, p.6].

### 1.4 Scope and Objective

In the "fit-and-forget"-approach, used in the traditional passive distribution grid planning methodology, the grid is dimensioned according to worst-case operating conditions. In Norway, this typically involves calculating the loading of the grid during the winter, when the consumption is at its highest level. However, with the rise of e.g. DG and ESS, the time of maximum loading may be shifted in time. Also, load demand is not necessarily the dimensioning factor of the grid anymore, as generation from DG may be considerable higher than consumption at certain points of time, causing power to be fed back to the grid. This needs to be accounted for in the grid planning process, and thus a more active grid planning approach is required.

For the development of Molobyen, it is essential to ensure that capacity requirements and voltage limits of the existing grid, as well as of the grid to be built, are satisfied. However, there is not one, unique way of ensuring such satisfactory operation. Several alternative ways of connecting the loads and PV to the existing grid may exist. These alternatives should be mapped and power flow analyses should be performed, in order to ensure safe operation. At the same time, the investments to ensure this must be cost-efficient. It should benefit both the grid company and customers of the grid company. Thus, typically the overall goal of distribution grid planning processes is to obtain an optimal socio-economic solution. Based on this, the objective of the master's thesis can be stated:

> *Investigate alternative ways of how the loads and solar PV of Molobyen can be connected to the grid, taking into consideration both technical and economic aspects, in order to obtain an optimal system solution. The use of flexibility solutions, such as ESSs, should be examined.*

Finally, the use of probabilistic methods, typically emphasized in the context of active distribution grid planning, is considered out of scope.

## 1.5 Contributions

Certain parts of the work in this thesis can be performed according to methods from existing grid planning frameworks, both from the current operation of grid companies and from the research literature. Other parts have posed more challenges, as new methods had to be developed. Some of the more important new methods, or parts, are listed below:

- *Grid planning framework:* A suiting grid planning framework, combining elements from passive and active grid planning, is developed. The focus on utilizing time series is prominent, as well the use of active measures in the grid. The framework is presented in Figure 8, Section 5.
- *Battery optimal dispatch model:* As batteries are considered utilized, a model capturing the operational benefits of batteries is developed. The model, presented

in Section 5.4, is based around optimizing battery dispatch, i.e. controlling when the battery should charge and discharge.

- *Calculation of cost of losses:* If the maximum power loss in a system is due to local generation, the cost of losses should not be calculated as if load demand caused this power loss. This is accounted for, with the method presented in Section 5.6.2.

## 1.6 Relation to the Specialization Project

This thesis is as an extension of the work carried out in the course *TET4520 - Electric Power Engineering and Energy Systems, Specialization Project*, or more simply *the specialization project*, the fall of 2020. Due to this, certain parts of the theory, background and methodology of the specialization project will also apply to the master's thesis and, thus, be included in the master's thesis. Although very few sections remain identical to the ones in the specialization project, several have been modified for the purpose of this thesis. The sections concerned by this, are:

- Sections 1.1 (several paragraphs added), 1.3 (modified, figure added), 1.4 (modified, new objective) and 1.7 (heavily modified).
- Sections 2.1, 2.2, 2.3: Text and tables as in specialization project, figures are modified for the purpose of this thesis.
- Section 4.1: Slightly modified.
- Section 5.1: Modified, new figure added.
- Section 5.2: Most text and tables as in specialization project, figures are modified for the purpose of this thesis.
- Section 5.3.1: Some text as in specialization project, but is heavily modified (e.g. several new alternatives added).
- Section 5.3.2: Modified.
- Appendix A: Same as in specialization project.

## 1.7 Work Process and Thesis Structure

For the specialization project, the work started off with a literature review on distribution grid planning, as this was the main topic of the project. Having conducted such a review, it was important to gain case-specific information on the area of Molobyen, as well as on the current supply situation. This information was gained through a continuous dialogue with the grid operators of the area, Arva, both through digital meetings and e-mails. In parallel with this, it was critical to learn how to use the software NETBAS, in order to perform power flow analyses. Thus, several days were spent at the offices of the developer of NETBAS, Volue. By gaining insight in the functionalities offered by the software, along with the case-specific information, alternatives for connecting the new area to the existing grid could be defined. Then, at last, power flow analyses were performed, in order to check for potential constraint violations of the respective alternatives.

The work performed in the master's thesis, the spring of 2021, began with a literature review on the use of batteries for grid applications, as it early on became apparent that this could be an interesting element to include in the grid planning process. From there on, much of the time were spent developing a model for battery optimal dispatch, in MATLAB. Further, several new alternatives had to be developed and defined. Power flow analyses were performed to ensure that also these ensured safe operation, according to the limits set. Having ensured this, the costs related to the different alternatives were mapped, before socio-economic analyses were performed in DYNKO. From these, the optimal system solution was obtained.

The remainder of the thesis is structured as follows: In Section 2, relevant background information on Molobyen and theory related to distribution grid planning, are presented. More theory are provided in Sections 3 and 4: First, regarding technical and economic considerations regarding batteries and optimization, then regarding software used in the thesis. In Section 5, the grid planning framework developed is presented. From there on, technical and socio-economic analyses are performed according to the framework, with results and evaluations presented in Section 6. Finally, more general considerations, along with limitations, are discussed in Section 7, before conclusions and suggestions for future work are made in Section 8.

# 2 Molobyen and Distribution Grid Planning Frameworks

## 2.1 Background Information on Molobyen

The work is based around the development of a new area, on the north-west coastline of Bodø. The area is referred to as *Molobyen*, and will contain office spaces, a hotel, and 600 apartments, as illustrated in Figure 1. Further, it will work as a pilot for a larger project, called *New city-new airport, Bodø* [11]. Hence, one of the main focus areas of Molobyen will be on new energy solutions to obtain something close to a ZEN. In this context, DH and solar PV are highly important. Regarding DH, a resolution adopted in 2011 for certain parts of Bodø, including the area of Molobyen, states that new buildings with areas above $500m^2$ will automatically be offered connection to the heat network [12]. This is the case for the buildings of Molobyen, and so DH will be utilized. Through meetings held with Bodø Energi (BE) Varme AS, it was revealed that DH will cover the power demand related to space heating (SH), domestic hot water (DHW), and cooling. Regarding solar PV, the roofs of the buildings will be covered with solar panels, in order to reduce energy use and power demand.

During the spring of 2020, an energy system analysis on the energy use of the buildings to be constructed was performed, in FME ZEN; the Research Centre on Zero Emission Neighbourhoods in Smart Cities [13]. For this purpose, the dynamic building simulation tool *IDA Indoor Climate and Energy (IDA ICE)* [14], was utilized. By also including *ASHRAE Weather Data* [15] for Bodø, the expected solar PV production from the rooftop PVs were obtained. The results from this energy system analysis, being expected load demand and PV production for a year, are used as a basis for the load and generation modelling in this thesis.

Further, the results from the analysis were investigated in work performed by the author, as a summer intern for SINTEF Energy Research [16], the summer of 2020. In Table 1, the most important findings are listed: By utilizing solar PV and DH, the maximum load demand is reduced from $3.93MW$ to $0.61MWh$, while the net energy use is reduced from $8535MWh$ to $1285MWh$. Only utilizing DH, reduces the maximum demand to $0.62MW$. Thus, PV does not manage to substantially reduce the maximum load demand, which is expected due to PV production and maximum load demand being negatively correlated (for northern parts of the world). The duration curves for the three supply situations mentioned, are shown in Figure 2. Observe that for a large share of the year, when utilizing DH and PV, substantial amounts of power are fed back to the grid (yellow graph becomes negative). As the maximum power flow to the grid is larger than maximum power flow from the grid ($0.61MW$), solar PV becomes the dimensioning factor of this grid.

Table 1: Energy use and maximum power demand of Molobyen for different supply situations, as seen from the electricity distribution grid. Also, see Figure 2.

| | Energy use | Maximum power |
|---|---|---|
| No DH or PV (blue) | 8535MWh | 3.93MW |
| With DH (orange) | 3433MWh | 0.62MW |
| With DH and PV (yellow) | 1285MWh | 0.61MW |

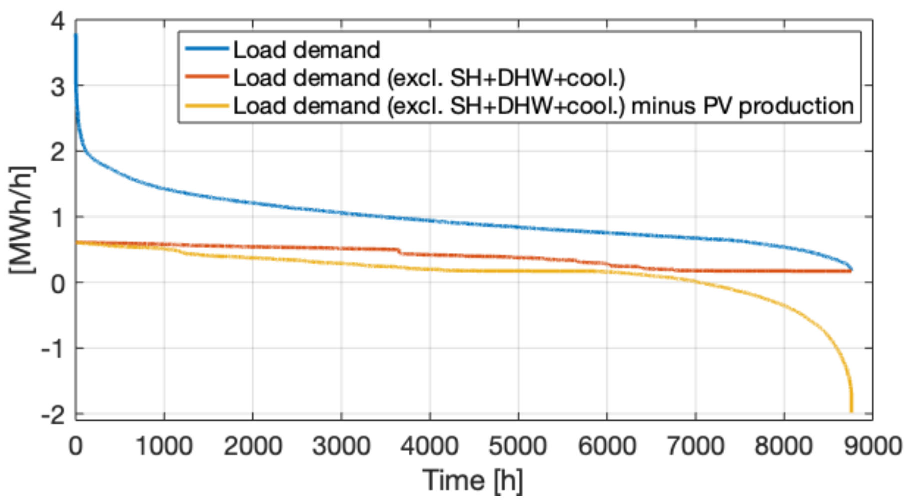


Figure 2: Duration curves for total building related power demand (blue), power demand if DH (covering SH, DHW, cooling) is considered (orange), and power demand if DH and solar PVs are included (yellow).

## 2.2 Passive and Active Distribution Grid Planning

### 2.2.1 Passive Distribution Grid Planning

Distribution grids are, in general, dimensioned to handle the worst-case operating scenarios, both regarding loads and voltage drops. As such, the use of and need for active measures are negligible. This approach is typically referred to as the ”fit and forget”-approach, and is highly deterministic (i.e. uncertainties are not extensively considered). The approach is illustrated in Figure 3, with the different stages elaborated below. The descriptions are mainly based on [17].

**Definition of planning study (motivation, scope, premises)**
In the first stage, the motivation of the study is established. Typically, the motivation involves closing the gap between the current and the desired situation, or more simply solving an existing or future problem in the grid. From this, the term ”problem” is defined [17, p.4]:

$$Problem \;=\; Desired\ situation \;-\; Current\ situation$$

For the planning study to turn out successful, a thorough definition of the problem and the system boundaries are essential. This involves [17]:

- Establishing an overview of the planning area in consideration
- Identification and description of the problem
- Clarification of expectations with different actors
- Clarification of what parts of the grid are to be affected
- Description of goals and criteria
- Consideration of the time horizon for the analysis
- Consideration of what analyses and simulations that should be performed, and to what extent
- Clarify terminology

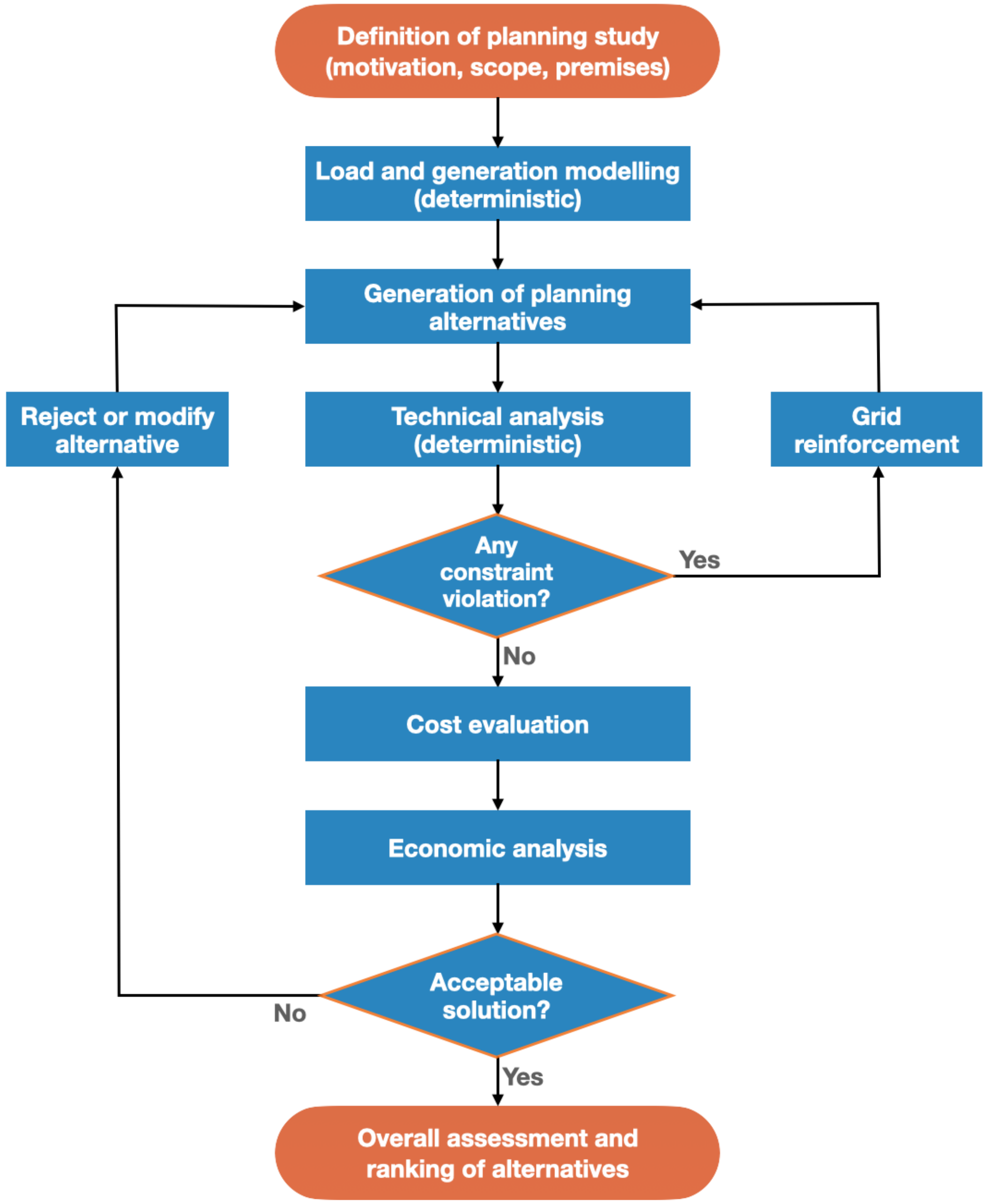


Figure 3: General planning framework used for passive distribution grid planning, based on figures found in [2], [4], [5] and [17].

**Load and generation modelling (deterministic)**
The purpose of the power grid is to connect power generation and consumption. As the generation should match the load demand, it is essential to have knowledge on the size and location of the generating units and loads, yearly variation, and expected future development [17].

In the deterministic "fit-and-forget"-approach, only the worst-case operating states are considered: the case of maximum (peak) demand without generation and the case of minimum demand with maximum generation. The maximum power demand is typically found through the use of standard variation curves for a given consumer (e.g. household, industry, office etc.), in combination with utilization times and Velander coefficients [4].

**Generation of planning alternatives**
There may be several combinations of measures that can be applied to solve a grid problem, i.e. close the gap between the desired and current situation. Thus, combinations of measures, or alternatives, are created and tested. It should be noted that this is an iterative process, meaning that alternatives not satisfying technical constraints or cost-related demands are either rejected or modified. As a result, new alternatives may be created.[17]

**Technical analysis (deterministic)**
As several grid planning alternatives have been developed, technical analyses must be performed. The main goal of these analyses is to ensure that the alternatives are feasible, i.e. that they satisfy different limits and restrictions. If the results are non-satisfactory, new alternatives should be developed (e.g. by introducing an increased capacity of a line violating voltage limits). Also, the results can be used for estimating operational costs, through finding the network losses.

The idea is to map the different properties important for comparing and ranking the different alternatives. Several analytical tools can be used for this matter, including [2][17]:

- Power flow analysis

- Power quality analysis
- Short circuit analysis
- Reliability analysis
- Risk analysis
- Transient and stability analysis

**Cost evaluation**

As Norwegian distribution grid companies are required by law to develop the grid in a socio-economic rational manner [18], the different costs related to the different alternatives must be mapped. These costs include [17]:

- Investment costs
- Costs of losses
- Interruption costs
- Environmental costs
- Congestion costs
- Operation & maintenance (O&M) costs

Not all cost elements are necessarily included in each analysis. The purpose of the analysis decides what costs are included.

**Economic analysis**

In the economic analysis the main goal is to find the alternatives or measures minimizing the overall costs, for a given period of analysis. By adding together the overall costs over the years in the analysis period, for all of the combinations of measures and implementation times, the economic analysis provides a basis for deciding both which measures to implement and to what time. Thus, the objective will be to choose the optimal path throughout the period of analysis, and to implement the correct measures in each time interval [17]. This is illustrated in Figure 4.

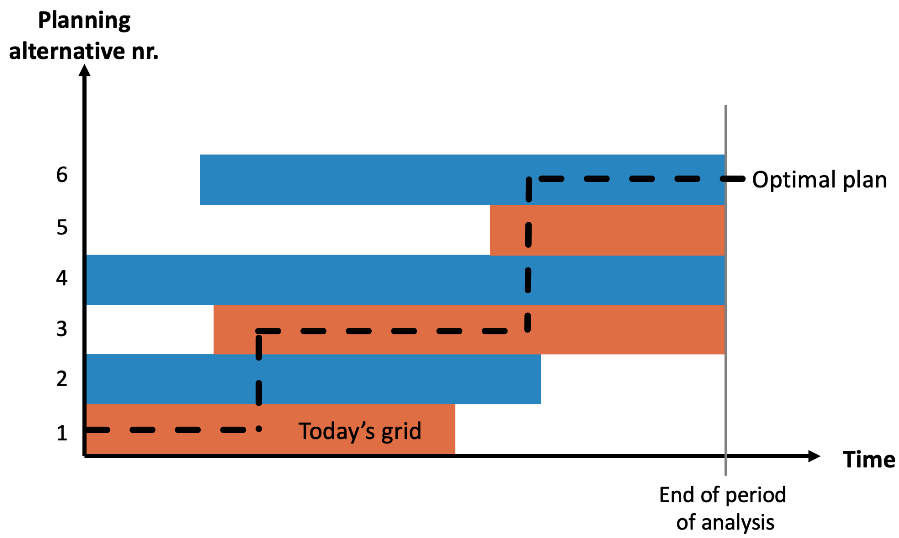


Figure 4: Optimal order of implementation of measures. Figure based on [17, p.7].

**Overall assessment and ranking of alternatives**

In the final step, the most economic beneficial alternatives are chosen and further evaluated based on the uncertainty in the underlying data (typically through sensitivity analyses), the impact of elements that are hardly quantified and the flexibility in the plans regarding the uncertainty in the underlying data. Based on this, a proposal of measures to be implemented, and the timing of them, is created. [17, p.7]

### 2.2.2 Active Distribution Grid Planning

With the rise of DER and new types of "high power, low energy"-equipment, this passive approach to distribution grid planning may turn out to be outdated. Although this approach would probably be capable of meeting load demand and satisfying technical requirements, major investments would be required, and these could leave the grid largely under-utilized. Thus, this passive approach to distribution grid planning should be replaced by a more active grid planning, utilizing the rise of ICT used in the power system and the flexibility introduced through DG and ESS. Again, the need for this transition, or change, of framework is emphasized in both [1], [2], [4], and [5]. Based on several of these, an active distribution grid planning framework is presented in Figure 5.

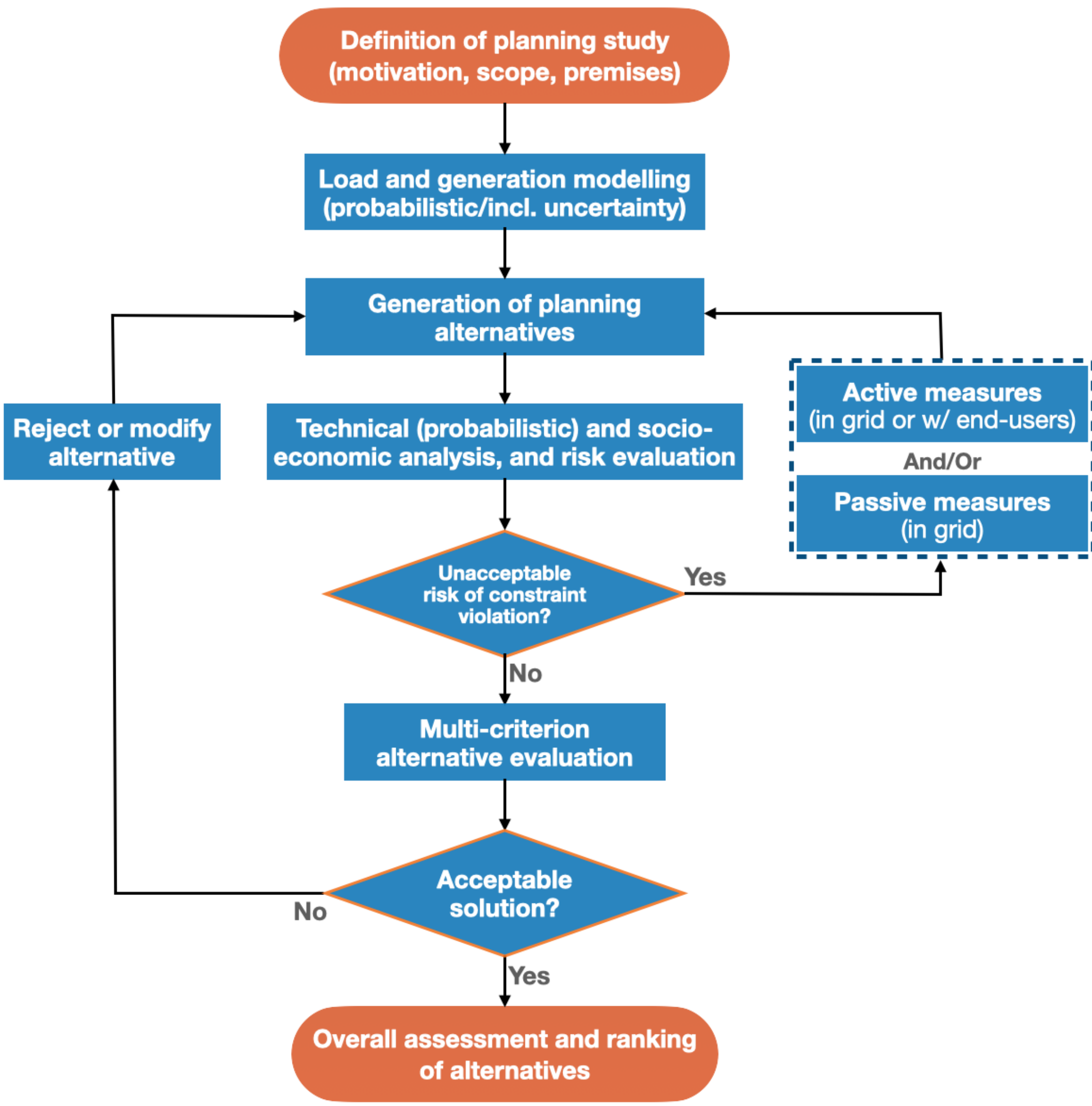


Figure 5: General planning framework used for active distribution grid planning, based on figures found in [2], [4] and [5].

The main differences from the passive approach are found within *load and generation modelling*, *technical analysis*, *multi-criterion alternative evaluation*, and *active measures*. These will be briefly discussed below.

For the load and generation modelling, it is emphasized that there should be developed, or modelled, daily and yearly variation curves for both load and generation. Also, typical operating conditions should be recognized, in order to create models for uncertainty, i.e. the relative probability of an operating condition occurring.[2][4].

For the technical analysis, [2] and [4] emphasize that uncertainties should be modelled by probability density functions, from which probabilistic power flow calculations, or e.g. Monte Carlo simulations, can be performed. By also considering consequences of different outcomes, the technical analysis turns into a risk analysis, from which decisions can be made by the decision maker.

Multi-criterion alternative evaluation is based around the inclusion of several other criteria in the evaluation of the alternatives. As opposed to the traditional approach only considering minimizing the socio-economic costs, multi-criterion evaluation also considers e.g. aesthetics and environmental consequences of the grid measures. [2] [4]

Active measures simply refers to the possibility of utilizing other measures than traditional passive measures, such as building new lines or substations, in order to satisfy different constraints. An example of an active measure, is the use of ESS.

## 2.3 Power Flow Analysis

A fundamental element in the grid planning process, is the power flow (or load flow) analysis. The objectives, in this context, are typically to check for overloads (capacity issues), voltage problems and identify locations of network reinforcements [19]. In the following, the power flow problem will be discussed, along with voltage and capacity limits.

### 2.3.1 The Power Flow Problem

To obtain a power flow model, data on the loads, generating units, transmission lines, and transformers, are required. From this, mathematical models on the different components are established. By solving the non-linear nodal power balance equations, Equation (24) in Appendix A, all relevant system quantities can be obtained. This includes bus voltages, voltage drops, power flows, and power losses [20, p.1]. The power flow problem is addressed more extensively in Appendix A.

### 2.3.2 Voltage Limits

To secure a satisfactory level of quality of the power supplied to consumers, national and international regulations on the quality of supply are developed. The term *quality of electricity supply* is defined by IEC (International Electrotechnical Commission) [21] as the "collective effect of all aspects of performance in the supply of electricity". This includes the continuity of supply, voltage quality and commercial quality [22]. In Norway, the requirements related to these are specified in the *Norwegian regulation of quality of supply* [23] (in Norwegian: *Forskrift om leveringskvalitet i kraftsystemet*, commonly referred to as FoL). For the continuity of supply, there are no quantified requirements. For the voltage quality, however, numerous requirements related to the different voltage phenomena deferring voltage quality, have been set. These phenomena include the voltage frequency, supply voltage variations, voltage unbalance, harmonic voltages, along with others; all of them making the voltage magnitude or waveform deviate from ideal values [22]. According to [24] and [25], the most important phenomenon deferring voltage quality is supply voltage variations. Thus, this phenomenon is further emphasized, in the context of low voltage grids, i.e. grids with voltages below 1kV.

Supply voltage variations refers to slow variations in the r.m.s. value of the voltage at the supply terminal, for a given time interval. In the Norwegian regulation of quality of supply, it is specified that the 1 minute r.m.s. value of the voltage, should be kept within an interval of $\pm 10\%$ of the nominal voltage at the supply terminal, 100% of the time [23]. For comparison, the corresponding European Standard, EN 50160:2010 [26, p.11], states that:

"Under normal operating conditions:

- during each period of one week 95% of the 10 min mean r.m.s. values of the supply voltage shall be within the range of $U_n \pm 10\%$; and
- all 10 min r.m.s. values of the supply voltage shall be within the range of $U_n + 10\% / - 15\%$".

As can be seen, this is less strict than the Norwegian requirements, both in terms of the time interval from which the mean r.m.s. value is calculated and in terms of limit violation acceptance (0% of the time vs 5% of a week).

### 2.3.3 Capacity Limits

Both overhead lines, cables, and transformers are designed with a certain power transfer capacity. Several factors come into play to determine this capacity, with temperature limits being one of the most important factors in this context. For overhead lines and cables, this will be the major limiting factor for the ampacity, i.e. the maximum current a conductor can carry continuously without violating temperature limits [27]. From the ampacity, in combination with voltage rating, it follows a power transfer capacity. Also, for transformers, temperature plays an important role in deciding capacity. For transformers this capacity rating is typically given in volt-ampere (VA).

The main objective of the above is not to give an insight in how the different capacity limits are decided, but to emphasize that there are capacity restrictions related to the lines, cables, and transformers. Further, it should be noted that there are consequences of violating these limits. For the overhead lines and cables, an operating condition causing these to be overloaded, can cause overheating. This can reduce the lifetime of the line (or cable) and, in worst case, destroy it. Also for transformers, overloading may lead to overheating, which again reduces the lifetime. Thus, in general, overloading should be avoided. However, as new loads and generators are connected to the grid, times of overloading may occur for existing components. This does not necessarily mean that, for instance, a transformer should be replaced with a higher rated transformer, as overloading for short periods may not be considered a major problem. In [28], it was shown that, under certain operating conditions, a transformer can be overloaded considerably for short periods with little loss in life.

As a final note, what is considered an acceptable overloading of both overhead lines, cables, and transformers, may vary. The owner of the components, typically grid companies, establishes these limits.

# 3 Batteries and Optimization

## 3.1 Batteries: Technical and Economic Considerations

With an increased load demand and an increased penetration of VRES, several challenges arise for the power grid and heavy grid reinvestments may be required. An alternative to heavy reinvestments, however, is the use of ESSs, for instance batteries, as such systems have the ability of providing both load levelling and balancing of VRES [7]. This can prove particularly beneficial for northern parts of the world, where solar PV is utilized, as peak load demand and peak PV production will be close to negatively correlated [29].

In this section, first some technical considerations regarding batteries are made, before the economic aspect is investigated.

### 3.1.1 Technical Considerations

A BESS consists of four main parts [9]:

- *The battery pack:* A cluster of battery modules (a module is a cluster of battery cells). Decides how much energy can be stored in the BESS, i.e. the capacity rating of the system.

- *The battery management system:* Ensures safe operation, through monitoring and controlling the battery cells.

- *The supervisory control system:* Decides when the battery should charge/discharge, with what current and at what rate. It is dependent on measurements from the grid as input, in order to perform these tasks.

- *The power conversion system:* Converts the battery voltage from DC to AC, in order for the battery to be connected to the grid. The converters typically represent the limiting factor regarding the power rating of the BESS.

The correlation between these four parts are illustrated in Figure 6.

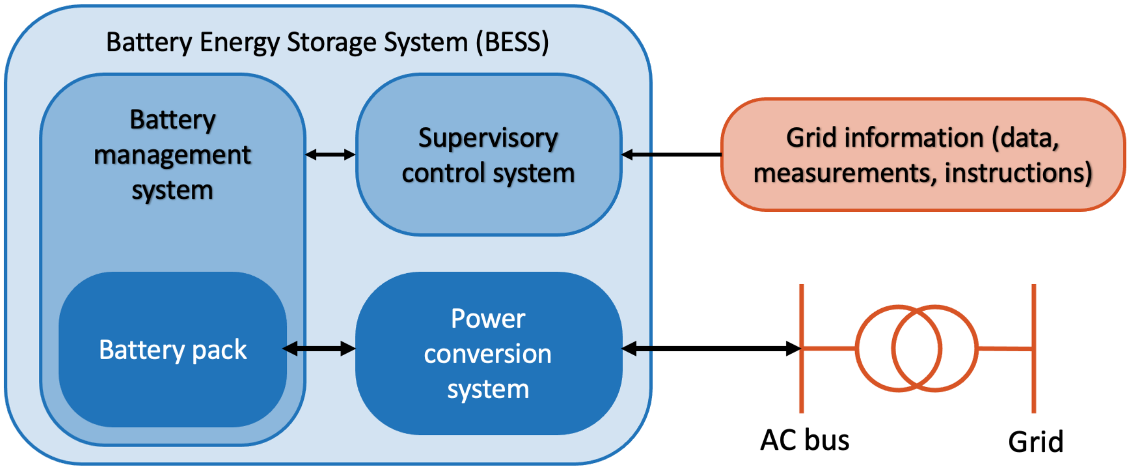


Figure 6: The different parts of a BESS. The figure is a replication of Figure 2.1 in [9].

Further, some key terms related to the BESSs are listed and explained below [9]:

- *Cycle:* Charging or discharging a battery from an initial state of charge (SOC), back to the same state within one charging and discharging.
- *Degradation:* Ageing of the battery, both due to time (calendar) and use (cycles), causes a reduction in battery capacity (power and energy). This is referred to as degradation.
- *State of health (SOH):* SOH refers to the amount of available energy capacity left in the battery. SOH is reduced due to degradation,
- *Lifetime:* Can be measured in years and cycles. A battery can be utilized until it has been reduced to a certain SOH, typically 80%.
- *State of charge (SOC):* The percentage of maximum battery energy capacity utilized, at a given time. Lithium-ion batteries should typically be operated at a SOC between 10 and 90%, in order to reduce degradation.
- *Round-trip efficiency:* Ratio of energy retrieved from the storage device and energy put into it. As such, both charge and discharge efficiencies are accounted for.

Several battery technologies exist, varying in both power rating, storage capacity, efficiency, lifetime, degradation, and costs. The most popular one as of 2020 is the lithium-ion battery, as it has a high energy density, high efficiency and long lifetime [9]. These parameters, along with several others, are listed in Table 2. Also, typical values for lithium-ion batteries are presented, with all values according to [9].

Table 2: Li-ion battery parameters. Values found in [9, p.53]

| Parameter | Value |
|---|---|
| Power rating | $0 - 100kW$ |
| Efficiency | 90% |
| Lifetime | $5 - 15$ years |
| Cyclic lifetime | $1000 - 10000$ cycles |
| Suitable storage time | minutes-days |
| Response time | seconds |
| Energy density | $75 - 200Wh/kg$ |
| Power density | $500 - 2000W/kg$ |
| Costs: $\$/kW$ | 1200-4000 |
| Costs: $\$/kWh$ | 600-2500 |
| Costs: $\$/kWh/cycle$ | 15-100 |

Several of the parameters listed can hardly be quantified with exact numbers. For instance, the lifetime is both dependent on age and usage, in addition to ambient temperature and SOC [9]. There is also a significant uncertainty related to battery costs. This is further discussed in Section 3.1.2.

Some considerations should also be made regarding the power rating listed in Table 2. [9] uses the article *Overview of current development in electrical energy storage technologies and the application potential in power system operation* [30] to find the power rating listed. Although, at the same time, [30] also states that the power rating could be between 1 and $100MW$. In addition, the lithium-ion battery pack currently utilized at e.g. Hornsdale Power Reserve has a rating of $100MW/129MWh$, with a $50MW/64.5MWh$ expansion under construction [31]. Hence, having any power rating between 0 and $100MW$ appears to be highly feasible, in terms of technical considerations.

### 3.1.2 Economic Considerations

As the development within the battery industry is moving fast, some considerations should be made regarding battery costs. The costs listed in Table 2 are found in [9], published November 2020. However, [9] has apparently extracted these values from [30], published in 2015, which again has used [32], published in 2009, to obtain the values. Thus, the current battery costs can be expected to be far below the listed values. As is also stated in [9], according to calculations from Bloomberg New Energy Finance (BloombergNEF) [33], the cost of a lithium-ion battery pack has been reduced from about $1200\$/kWh$ in 2010 to $156\$/kWh$ in 2019. Here, the 2010-value aligns pretty well with the interval listed in Table 2, while the 2019-value is reduced to a quarter of the minimum MWh-cost in the table. This supports the use of a lower battery cost value than what is listed in the table. Note: The values provided by BloombergNEF are volume-weighted average values.

The calculations performed by BloombergNEF should give a good estimate of the current battery costs. In addition, looking at the actual battery costs specified by battery manufacturers should give some highly valuable insight. These costs are, however, typically not made available unless a purchase is to be made or direct contact is initiated. Nevertheless, as late as October 2020, CleanTechnica [34] has quoted Elon Musk on the Tesla Megapack, stating that the battery pack of the Tesla Megapack comes at a cost less than $200\$/kWh$. Including power electronics and servicing over 15 to 20 years, the price increases to around $300\$/kWh$. This is higher than the calculations performed by BloombergNEF [33], but this is expected as BloombergNEF do not only consider batteries for grid applications when finding their average battery costs. For instance, the use of batteries for EVs are also included in these calculations. The cost estimates of the Tesla Megapack is, on the other hand, more relevant for only specific applications, as the Megapack is suited for utilities and heavy industrial users [34]. Thus, a lithium-ion battery pack price of 200$\$/kWh$ appears as a reasonable estimate of the current price. Including power electronics and servicing, an overall price of 300$\$/kWh$ should be used.

Furthermore, some considerations should be made regarding future battery prices. Again, BloombergNEF's annual battery price survey of 2019 [33] found a reduction in lithium-ion battery pack prices from 1200$\$/kWh$ in 2010 to 156$\$/kWh$ in 2019. The same survey also states that reaching an average price of 100$\$/kWh$ by 2024 looks promising, while there is more uncertainties related to the expected further reduction from 100$\$/kWh$ to 61$\$/kWh$ by 2030.

In BloombergNEF's latest annual battery price survey [35], released December 2020, the numbers above are alternated to some extent. Current lithium-ion battery pack prices have seen a further reduction, reaching 137$\$/kWh$ in 2020. A new minimum was also reached, with battery pack prices below 100$\$/kWh$, for e-buses in China, being reported. Further, the average price (including passenger EVs, e-buses, commercial EVs and stationary storage) is still looking to reach an expected 100$\$/kWh$ by 2024, with the 2023 average value expected to be 101$\$/kWh$. The expected price for 2030 mentioned in the 2019 survey [33], is expected to be even lower in the 2020 survey [35], now estimated at 58$\$/kWh$. The results from this survey, along with CleanTechnica's findings, are illustrated in Figure 7. Note: The volume-weighted average, mentioned in the figure, is simply the average value over a given time horizon [36].

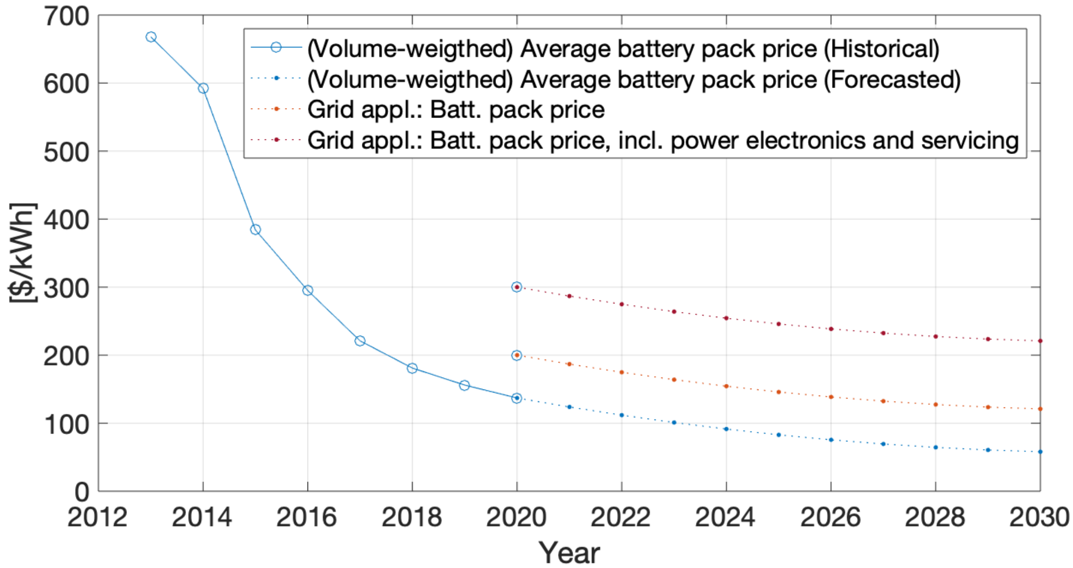


Figure 7: Lithium-ion battery pack prices: The solid line represents actual historical values, while the dotted lines represent forecasted values. The dotted blue line is based on the 2023 and 2030 projections by BloombergNEF [35]. The orange and red line do also utilize these projections, but are based on CleanTechnica's findings [34] regarding current prices.

The yearly values are also summarized in Table 3. The prices for the years 2021-2022 and 2024-2029 are found through *spline interpolation*, using the forecasted values from BloombergNEF [35] as a starting point. In addition, the costs related to power electronics and servicing are assumed constant throughout all years.

Table 3: Lithium-ion battery pack prices: The values in the column *Average price* are based on findings by BloombergNEF [35]. The last two columns uses findings by CleanTechnica [34] as starting points, and follows the same price projections as reported by BloombergNEF [35].

| Year | Average price | Grid appl. price | Grid appl. price, incl. power electronics and service |
|---|---|---|---|
| | [$\$/kWh$] | [$\$/kWh$] | [$\$/kWh$] |
| 2013 | 668 | - | - |
| 2014 | 592 | - | - |
| 2015 | 384 | - | - |
| 2016 | 295 | - | - |
| 2017 | 221 | - | - |
| 2018 | 181 | - | - |
| 2019 | 156 | - | - |
| 2020 | 137 | 200 | 300 |
| 2021 | 124 | 187 | 287 |
| 2022 | 112 | 175 | 275 |
| 2023 | 101 | 164 | 264 |
| 2024 | 91 | 154 | 254 |
| 2025 | 83 | 146 | 246 |
| 2026 | 76 | 139 | 239 |
| 2027 | 69 | 132 | 232 |
| 2028 | 64 | 127 | 227 |
| 2029 | 61 | 124 | 224 |
| 2030 | 58 | 121 | 221 |

## 3.2 Optimization

In general, "optimization is the maximization or minimization of a function $[f(x)]$, subject to constraints $[c_i(x)]$ on its variables $[x]$" [37]. Mathematically, this can be formulated as in Equation (1):

$$\begin{aligned} &\min_{x \in R^n} f(x) \\ &s.t.\ c_i(x) = 0, \qquad i \in \varepsilon \\ &\qquad c_i(x) \geq 0, \qquad i \in I \end{aligned} \tag{1}$$

Here, $I$ refers to the set of indices for inequality constraints and $\varepsilon$ to the set of indices for equality constraints.

There are several types of optimization problems, mainly based on how their objective function and constraints are defined. Three of the more important types are linear programming (LP) problems, quadratic programming (QP) problems and nonlinear programming (NLP) problems. These are compared below:

- LP: linear objective function and linear constraints.
- QP: quadratic objective function and linear constraints.
- NLP: non-linear objective function and/or non-linear constraints.

In addition to their formulation, they also differ in complexity and efforts needed to find an optimal solution. LPs are *convex* problems, which means that a local solution is also the global solution, i.e. if you find a solution, it must be the optimal solution. For QPs and NLPs, this is not necessarily the case. Particularly, "general nonlinear problems, both constained and unconstrained, may possess several local solutions that are not global solutions" [37]. Due to this, several iterations and large computational efforts are typically required in order to obtain the optimal (global) solution for NLPs.

# 4 Tools

The most prominent softwares used in this work are NETBAS, MATLAB and DYNKO. These are briefly introduced below.

## 4.1 NETBAS

NETBAS, based on the geographic information system (GIS) framework, is a solution for both planning, analyzing, operating and maintaining the power grid, and is widely used in Norwegian grid companies [38] [39]. The possibilities of planning and analyzing are important, as they provide the opportunity of modifying and expanding the grid, on which power flow analyses can be performed. These features will be extensively used in the project work to map potential capacity and voltage limit issues, in order to obtain a technically feasible grid. Note: NETBAS is developed by Volue, which was previously named Powel AS.

In addition, different modules/simulation tools, within NETBAS, can be used to perform the power flow analyses. In this thesis, the module "Timesanalyse" (or "hourly analysis") is extensively used. This module allows for power flow analyses to be run for any desired time interval, with the results being on an hourly format. For the purpose of Molobyen, this time interval is set to an entire year, simulating operation of the grid from January $1^{st}$ to December $31^{st}$, for the year in consideration. As such, results on the yearly variation in e.g. transformer loading, can be obtained.

## 4.2 MATLAB

MATLAB is a matrix-based programming language for data analytics, for developing algorithms and for creating models and applications [40]. In this thesis, its main areas of use are for creating and solving optimization models, and for data processing and visualization.

## 4.3 DYNKO

DYNKO is used for grid planning processes, with the aim of deciding what investments should be made and to what time. To obtain this, dynamic programming is utilized to minimize the sum ($K_{tot}$) of investment costs ($I$), costs of losses ($K_{losses}$), and interruptions costs ($K_{inter}$) (Equation (2)), for a given period of analysis, for all possible combinations of grid investment alternatives.

$$min\ K_{tot} = \sum I + \sum K_{losses} + \sum K_{inter} \tag{2}$$

All costs are referred to present time, i.e. present values are used to decide what investments should be made and to what time they should be made. Present values are calculated as in Equation (3). Potential residual values are also accounted for.

$$K_0 = \sum_{i=1}^{n} \frac{k_i}{(1 + \frac{r}{100})^{i-1}} \tag{3}$$

Here, $K_0$ is the present value of all costs within the period of analysis, $n$, $k_i$ the costs in year $i$ and $r$ the discount rate.

# 5 Proposed Grid Planning Framework

The proposed framework is presented in Figure 8, and combines elements from the frameworks in Figures 3 and 5. The following subsections will follow the same structure as this framework, and will be presented in relation to Molobyen. However, all results from calculations and simulations (optimization, technical and economic analyses), are presented in Section 6.

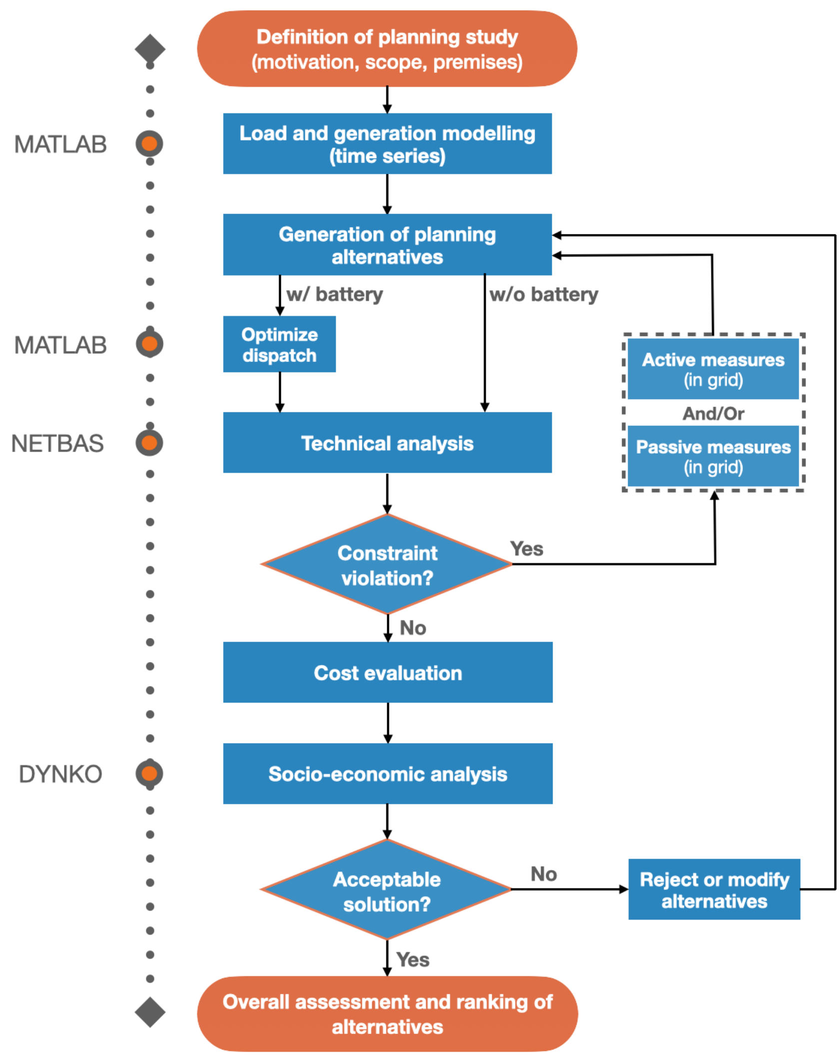


Figure 8: Methodology of the thesis, along with software used in the different stages.

## 5.1 Definition of Planning Study

The single-line diagram of the radial of the 10.7$kV$ grid, which is going to be connected to the new loads of Molobyen, is shown in Figure 9. Transmission data of the different cable sections are shown in Table 4.

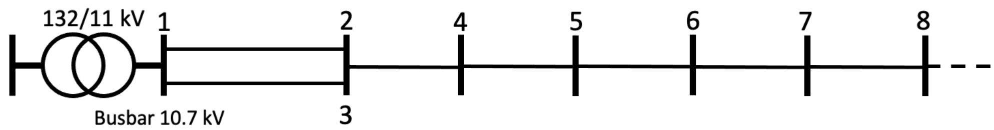


Figure 9: Single-line diagram of the 10.7kV grid to be connected to Molobyen.

Table 4: Transmission data related to Figure 9.

| Section | Length | Type |
|---|---|---|
| 1-2 | 0.955km+ 0.698km | TXSP AL 1x3x240mm$^2$+ TSLE AL 3x1x240mm$^2$ |
| 1-3 | 0.139km+ 0.387km | TSLF AL 3x1x240mm$^2$+ TSLF AL 3x1x240mm$^2$ |
| 2-4 | 0.107km+ 0.009km | TSLF AL 3x1x240mm$^2$+ TSLF AL 3x1x240mm$^2$ |
| 4-5 | 0.011km+ 0.117km | TSLF AL 3x1x240mm$^2$+ TSLF AL 3x1x240mm$^2$ |
| 5-6 | 0.067km+ 0.065km | TSLF AL 3x1x240mm$^2$+ TSLF AL 3x1x240mm$^2$ |
| 6-7 | 0.150km | TSLE AL 3x1x240mm$^2$ |
| 7-8 | 0.140km | DKBA AL 1x3x240mm$^2$ |

Buses 7 and 8 are important. Both are located close to the area of Molobyen and are, as such, potential candidates for supplying the increased load demand from the new buildings. To reduce computational efforts and time, the system boundary of the problem is defined to cover these two buses, the loads currently connected to them, and the new buildings of Molobyen. This is shown in Figure 31, Appendix B. A zoomed-in version of this figure is shown in Figure 10. As can be observed, there are several loads currently connected to substations 7 and 8.

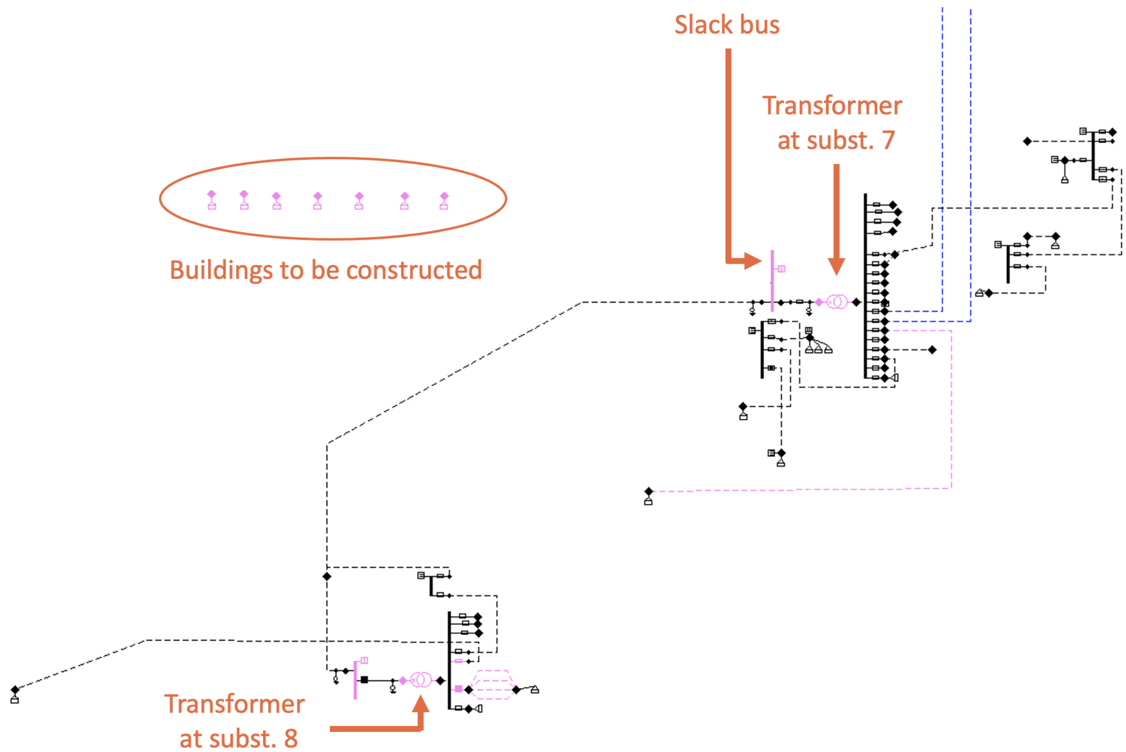


Figure 10: System boundary of the planning study. Note: Some of the loads connected to substation 7 are not shown in this figure. The entire system boundary is shown in Figure 31, Appendix B.

For clarity, from here on, Figure 11 will be representative of Figure 10 (and Figure 31). It captures the most important parts within the system boundary, being the buildings to be constructed and the nearby buses (or substations). Although the loads currently connected to the buses are not explicitly shown, these are under no circumstances neglected. It could be noted that the relative position of the buildings and buses in Figure 11 replicate the actual, future geographical situation. However, the actual locations are not provided, as this is classified as sensitive information.

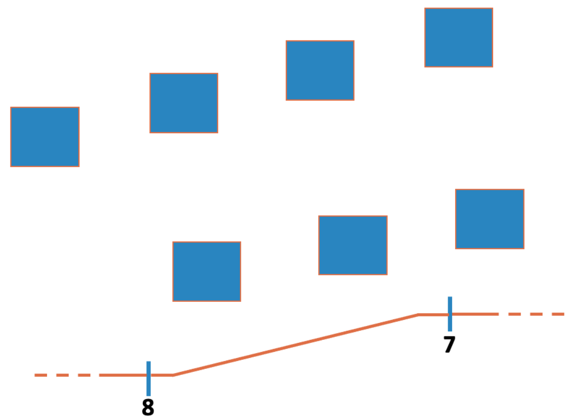


Figure 11: System boundary. The blue boxes represent the buildings to be constructed in Molobyen. Note: the loads currently supplied by buses 7 and 8 are not depicted in the figure.

Further, relevant data on the transformers of the MV/LV substations at buses 7 and 8, are listed in Table 5. From this, it is observed that there are still some capacity not being utilized, which can be used to supply the new loads of Molobyen. Also, two of the loads currently supplied by substation 7, are located in the exact area of where the new buildings of Molobyen are to be constructed. These are assumed demolished, making considerable more transformer capacity become available at substation 7, as the maximum power demand of these two loads are $194kW$ and $102kW$, both at $cos\phi = 0.98$.

Table 5: Transformer data of the transformers located at substations 7 and 8.

| Substation | Rating | Voltage ratio, $V_p/V_s$ | Capacity utilized |
|---|---|---|---|
| 7 | 800kVA | 10.5/0.24kV | 67% |
| 8 | 500kVA | 10.5/0.24kV | 46% |

## 5.2 Load and Generation Modelling

Each building to be constructed is modelled as a combination of a load demand and solar PV production:

- Load: Maximum demand, with daily and yearly variation curves.
- PV: Maximum production, with a yearly variation curve and monthly time of sunrise.

This is summarized in Figure 12, and will be expanded upon in the following sections, Sections 5.2.1 and 5.2.2.

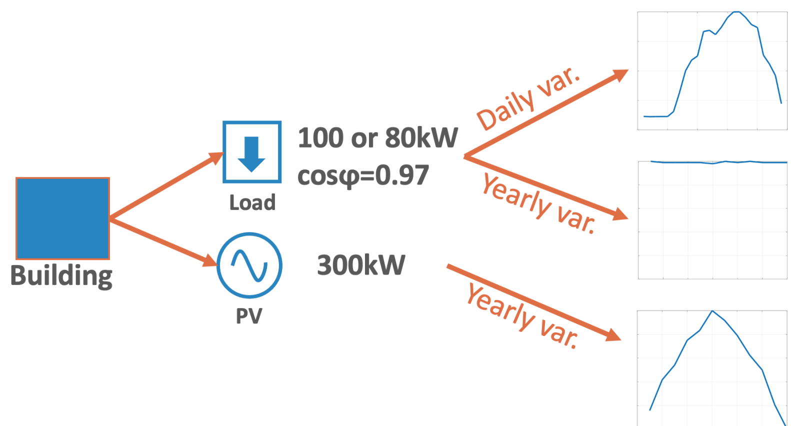


Figure 12: Load and generation modelling of each building in Molobyen.

### 5.2.1 Load Modelling

The different buildings illustrated in Figure 11, will not be constructed at the same time. The construction will be performed in stages, referred to as construction stages. Due to this, the different buildings, and the roof-top solar PV of the respective buildings, will come into operation at different points of time. Which buildings are included in the different construction stages, as well as the order of the stages, are defined in [10] and illustrated in Figure 13.

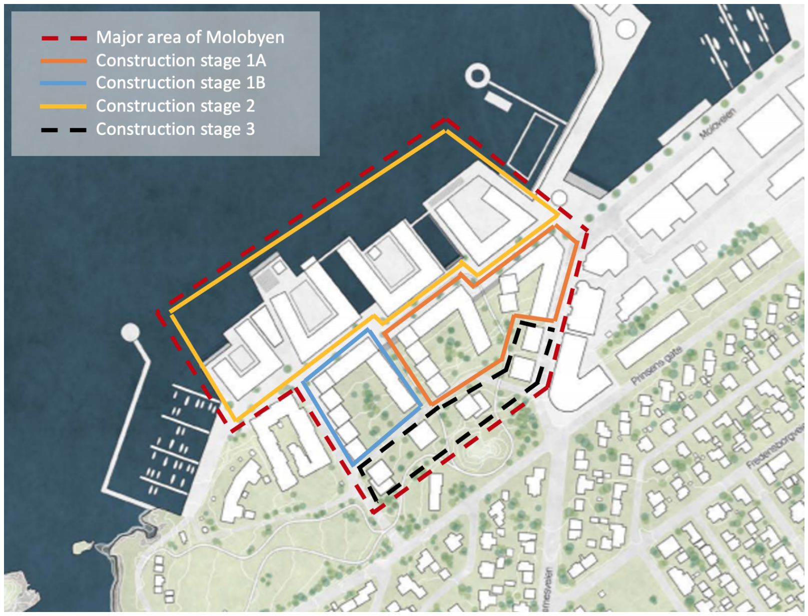


Figure 13: Construction stages defined for Molobyen. The figure is a modified version of [10, p.6].

As illustrated in the figure, the construction of Molobyen will take place through four construction stages, namely stage 1A, 1B, 2, and 3. In stage 1A, two major buildings will be constructed. The corresponding numbers for stages 1B and 2, are one and four buildings, while in stage 3 only several smaller buildings will be constructed. To simplify load modelling, only the seven major buildings will be modelled in NETBAS. From this, it follows that construction stage 3 is neglected in terms of being a construction stage. However, the total load demand and PV generation found in the energy system analysis [13], remain the same. I.e. construction stage 3 is neglected, but the load demand and PV generation from it are not.

Based on the above discussion, *the buildings to be constructed in Molobyen are modelled as seven loads, representing the seven major buildings to be built during construction stages 1A, 1B and 2*. Further, the buildings (load and solar PV) of stage 1A are defined to come into operation in 2024, stage 1B in 2026 and stage 2 in 2030. This will be elaborated in Section 5.3.

The total power demand of the loads of Molobyen, with DH considered, was found to be $0.62MW$, see Table 1. This power demand is divided between the seven buildings: *The three buildings closest to the buses (stage 1A and 1B) are modelled with a maximum power demand of* $100kW$*, while the four furthest from the buses (stage 2) have a maximum power demand of* $80kW$*, all with a power factor of* $cos(\phi) = 0.97$. Which buildings are closest and furthest from the buses can be seen in Figure 11; see also Figure 13. This makes for a total consumption of $0.62MW$. With the maximum power demand of each building defined, the daily and yearly consumption patterns must be modelled.

Daily consumption patterns vary based on season and on whether or not it is a weekday or a weekend. In NETBAS, this variation is handled through the possibility of defining four different daily consumption patterns: one for weekdays with low loading, one for weekdays with high loading, one for weekends with low loading, and one for weekends with high loading. As such, the model is capable of replicating the actual consumption pattern of any day, as these four patterns makes it able to differ between, e.g., the consumption on a Tuesday (weekday) during the summer (low loading) and a Saturday (weekend) during the winter (high loading).

For the case of Molobyen, DH will cover the demand related to SH, DHW and cooling. This leaves little variation in the daily consumption patterns throughout the year. The consumption patterns become independent of both day and season. Thus, the same daily consumption pattern will be used for all the four pattern variations. The pattern is obtained by looking into the data from the simulations of the energy system analysis [13], and is presented in Figure 14b. This will be the daily consumption pattern of all the seven loads in Molobyen.

For comparison, an average household in Bodø has the daily consumption pattern shown in Figure 14a, on a typical weekday in the winter. The data point values used in this pattern, are extracted from NETBAS for the Bodø area. As can be observed, the patterns have some similarities, such as two peaks and relatively low consumption during the night. However, the pattern is not perfectly replicated. The main reason for this is that consumption pattern for Molobyen does not include SH and DHW.

Another reason is that the buildings of Molobyen do not solely consist of apartments, or households. In the energy system analysis [13], also a hotel and office spaces are included, although apartments account for the major share of the power demand.

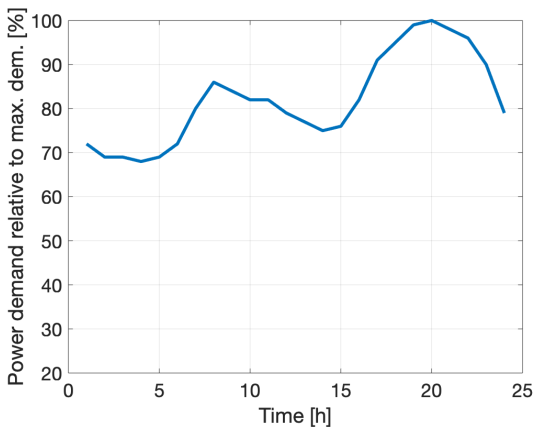


(a) Households, Bodø (high loading, weekday).

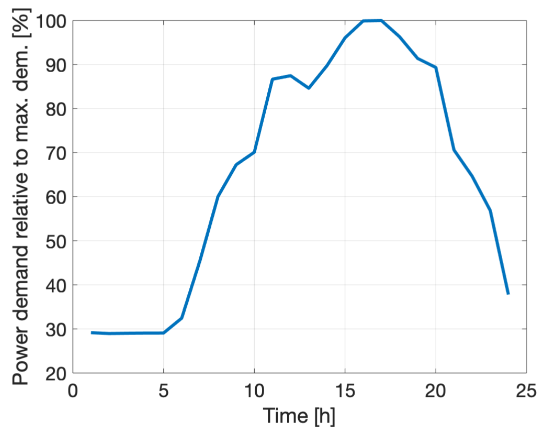


(b) Buildings to be constructed, Molobyen

Figure 14: Daily consumption patterns of households/buildings in the Bodø area.

For the yearly consumption pattern, the consumption is typically high in the winter months and low in the summer months. This is mainly due to an increased heating demand in the cold months of the year. However, as DH will cover this heating demand, the yearly consumption pattern of Molobyen deviates severely from this pattern. The variation throughout the year becomes close to zero, as shown in Figure 15.

### 5.2.2 Generation Modelling

From the energy system analysis [13], the yearly time profile/variation of solar PV production, for a given installed PV capacity, is obtained. This is presented in Figure 16a. Based on this, each building in Molobyen is modelled to have a maximum PV production of 300kW, along with the same relative time profile as presented in Figure 16a. This yields a maximum production of 2.1MW, and the total yearly PV production of Molobyen becomes as in Figure 16b.

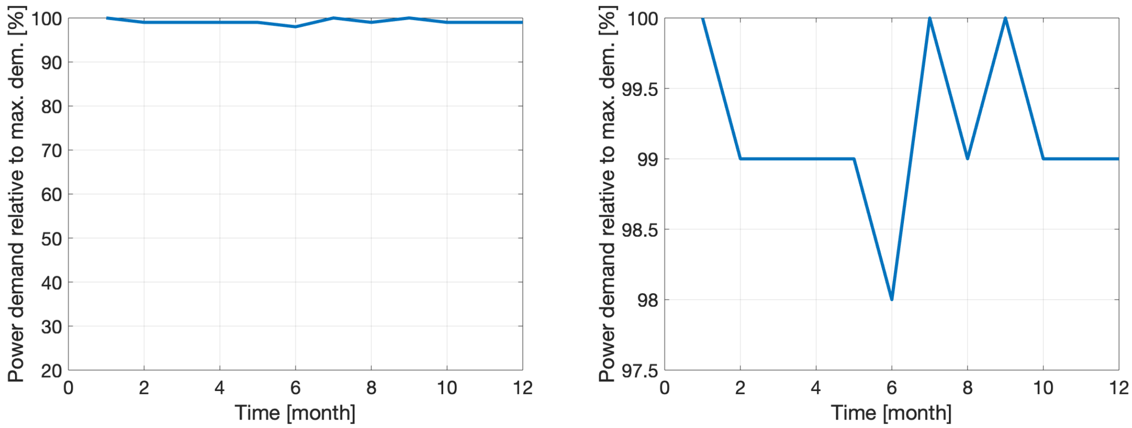


(a) Y-axis between 0 and 1.

(b) Y-axis between 0.975 and 1.

Figure 15: Yearly consumption pattern of the buildings of Molobyen.

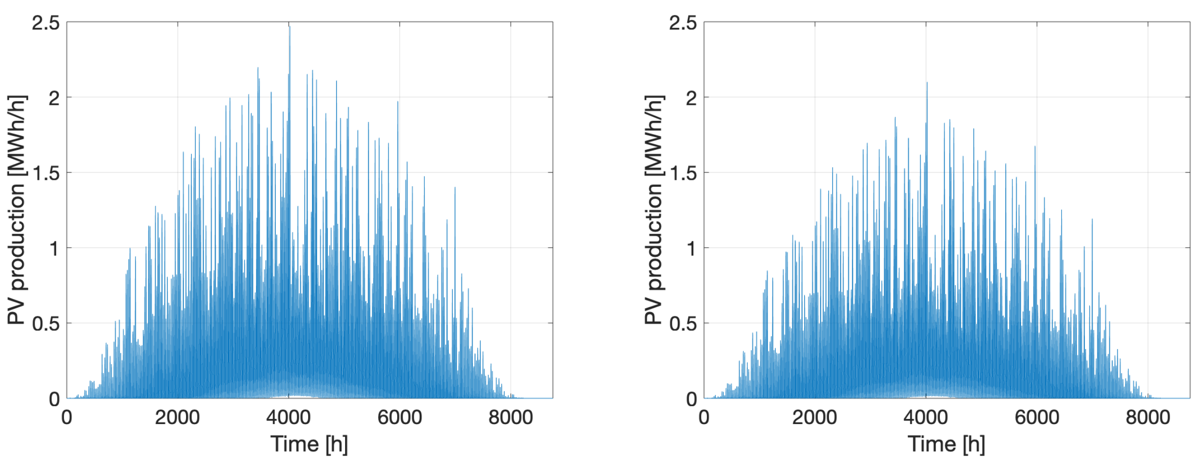


(a) With original installed capacity.

(b) With reduced installed capacity.

Figure 16: Yearly prod. from solar PV. Max. prod.: (a) 2.47MWh/h, (b) 2.10MWh/h.

Ideally, the time series presented graphically in Figure 16b should be used to model the PV production in NETBAS, however this functionality was not made available due to inadequate licenses. Hence, the PV production had to be replicated through values on the monthly maximum and minimum production, along with the time of sunrise for the different months. These values are obtained through inspection of the curve in Figure 16b, and are presented in Table 6. Note that the time of sunrise is presented in two of the columns. The first of these, *Actual*, represents the values extracted from the curve, while the second, *NETBAS*, represents the standard values set by NETBAS. Due to certain restrictions within the software, the time of sunrise cannot be changed, and so the standard values are utilized.

Table 6: Relative production from PVs (max.=2.1MWh/h) and time of sunrise, used in NETBAS to replicate Figure 16b. The column *NETBAS* is used instead of *Actual*, due to certain restrictions within NETBAS.

| Month | % of yearly max Max/Min | Sunrise [h]: Actual | Sunrise [h]: NETBAS |
|---|---|---|---|
| Jan. | 15.8/0.0 | 10:00 | 10:00 |
| Feb. | 41.7/0.0 | 09:00 | 08:30 |
| Mar. | 54.2/0.0 | 07:00 | 07:30 |
| Apr. | 75.0/0.0 | 04:00 | 06:15 |
| May | 83.3/0.0 | 02:00 | 05:00 |
| June | 100.0/0.0 | 00:00 | 03:40 |
| July | 91.7/0.0 | 00:30 | 04:10 |
| Aug. | 79.2/0.0 | 02:00 | 05:20 |
| Sept. | 62.5/0.0 | 04:00 | 06:40 |
| Okt. | 50.0/0.0 | 06:30 | 08:15 |
| Nov. | 20.8/0.0 | 08:30 | 09:00 |
| Dec. | 0.0/0.0 | 11:00 | 10:30 |

## 5.3 Generation of Planning Alternatives

In this section, the different planning alternatives are defined, before some general comments on the process of generating these are provided.

### 5.3.1 Planning Alternatives

Several measures or alternatives may be adapted to satisfy the capacity requirements and voltage limits. Common measures are grid reinforcements and reinvestments, grid expansion and utilization of power reserves [41]. As there is close to no existing grid in the area of what is to become Molobyen, the nearby grid must be expanded to also cover this part of Bodø. Several alternatives, and the combination of them, will be investigated. Here, the term *alternative* is defined as a combination of measures, being *valid* for a certain period of time. The period for which an alternative is valid, is decided by the years it offers connections to all buildings currently constructed. This will be further elaborated below. The combination of alternatives are referred to as a *system solution*, and is characterized by its capability of satisfying load demand and handling PV production throughout the whole period of analysis.

First, the different measures are defined, see Table 7, and illustrated, see Figure 17. In the table and the figure, the loads are denoted LBx-y. Here:

- *LB* refers to "leilighetsblokk" (apartment block)
- $x$ refers to construction stage (1A, 1B or 2)
- $y$ refers to the building number within a construction stage

Also, by the standard used by Arva, all cables from substations to loads are chosen to be $1kV$ cables with cross-sections of $240mm^2$. As can be seen from Table 7, all these connection points are operated with two cables in parallel. This is simply to achieve a maximum cable loading of 60%, as this is the standard, or limit, set by Arva in the planning phase.

In Figure 17, it should be emphasized that the orange cables are MV cables, while the black cables are LV cables. This implies that there are MV/LV transformers within the substations at buses 7, 8 and 9. For substations 7 and 8, this could be observed in Figure 10. It should also be added that this, Figure 17, is simply an illustrative figure to showcase all the different measures. The actual current supply situation, however, can be presented as in Figure 18: There are no existing grid and the seven buildings have not yet been constructed, as illustrated by the grey placeholders.

Table 7: Different measures to handle the new loads of Molobyen. See also Figure 17.

| Meas. | Description of measure | Trans. dist. |
|---|---|---|
| $A$ | 2 new cables ($1kV$, $240mm^2Al$) from substation 7 to LB1A-1 | 0.135km |
| $B$ | 2 new cables ($1kV$, $240mm^2Al$) from substation 7 to LB1A-2 | 0.073km |
| $C$ | 2 new cables ($1kV$, $240mm^2Al$) from substation 8 to LB1B-1 | 0.119km |
| $D$ | 2 new cables ($1kV$, $240mm^2Al$) from substation 7 to LB2-1 | 0.136km |
| $E$ | 2 new cables ($1kV$, $240mm^2Al$) from substation 7 to LB2-2 | 0.083km |
| $F$ | 2 new cables ($1kV$, $240mm^2Al$) from substation 8 to LB2-3 | 0.119km |
| $G$ | 2 new cables ($1kV$, $240mm^2Al$) from substation 8 to LB2-4 | 0.120km |
| $H$ | 2 new cables ($1kV$, $240mm^2Al$) from substation 9 to LB1A-1 | 0.109km |
| $I$ | 2 new cables ($1kV$, $240mm^2Al$) from substation 9 to LB1A-2 | 0.026km |
| $J$ | 2 new cables ($1kV$, $240mm^2Al$) from substation 9 to LB1B-1 | 0.059km |
| $K$ | 2 new cables ($1kV$, $240mm^2Al$) from substation 9 to LB2-1 | 0.105km |
| $L$ | 2 new cables ($1kV$, $240mm^2Al$) from substation 9 to LB2-2 | 0.046km |
| $M$ | 2 new cables ($1kV$, $240mm^2Al$) from substation 9 to LB2-3 | 0.068km |
| $N$ | 2 new cables ($1kV$, $240mm^2Al$) from substation 9 to LB2-4 | 0.117km |
| $O$ | Upgrade transformers at subst. 7 and 8 to 1250kVA and 800kVA, resp. | |
| $P$ | New substation (subst. 9) with a transformer capacity of 1250kVA +$12kV$ cable from subst. 7 to 9 | 0.109km |
| $Q$ | New substation (subst. 9) with a transformer capacity of 1600kVA +$12kV$ cable from subst. 7 to 9 | 0.109km |
| $R$ | $0.015MW/0.015MWh$ and $0.13MW/0.13MWh$ battery at LV side of subst. 7 and 8, resp. | |
| $S$ | $0.53MW/0.53MWh$ battery at LV side of subst. 9 ($80\% loading$) | |
| $T$ | $0.06MW/0.06MWh$ battery at LV side of subst. 9 ($100\% loading$) | |

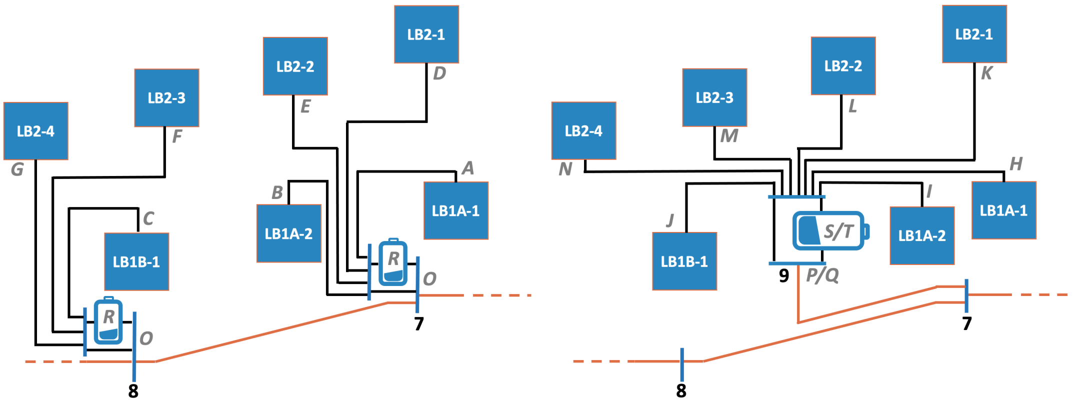


(a) Measures A-G, R & O  (b) Measures H-N, S, T, P & Q

Figure 17: Illustration of the different measures (denoted by grey capital letters). Note: orange cables represent MV cables, while the black ones are LV cables.

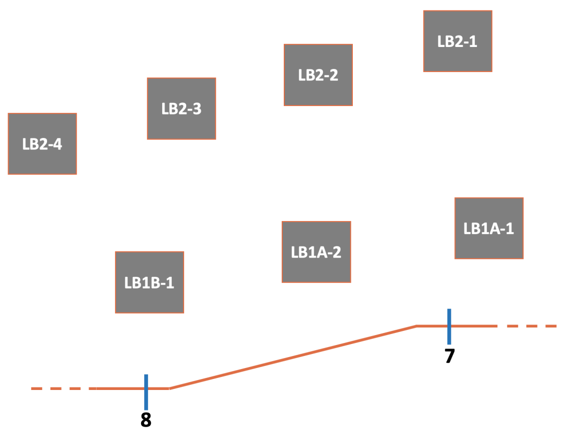


Figure 18: Current supply situation.

With the presented measures in mind, the alternatives can be presented, see Table 8. Again, these are combinations of measures and, based on these combinations, they have different periods for which they are valid. For instance, alternative 2 only offers connections between bus 7 and the buildings of construction stage 1A. As the loads of this stage become operative in 2024, and the load of stage 1B becomes operative in 2026, alternative 1 will be valid from 2024 to 2025. From 2026, a new alternative involving a connection to the load of stage 1B (here: alternative 3) must be adopted. Moreover, in 2030, when the four last buildings come into operation, alternatives offering connections to these must be adopted, e.g. alternative 4. As such, going from alternative 1 to 2 in 2024, from 2 to 3 in 2026 and from 3 to 4 in 2030, represent a system solution. This is illustrated in Figure 19. Again, grey buildings are placeholders for buildings not yet constructed.

Table 8: Alternatives, i.e. combinations of measures, to handle the new loads of Molobyen.

| Alt. | A | B | C | D | E | F | G | H | I | J | K | L | M | N | O | P | Q | R | S | T | Years valid |
|---|---|---|---|---|---|---|---|---|---|---|---|---|---|---|---|---|---|---|---|---|---|
| 1 | | | | | | | | | | | | | | | | | | | | | 2023-2023 |
| 2 | X | X | | | | | | | | | | | | | | | | | | | 2024-2025 |
| 3 | X | X | X | | | | | | | | | | | | | | | | | | 2026-2029 |
| 4 | X | X | X | X | X | X | X | | | | | | | | | | | | | | 2030-2037 |
| 5 | X | X | X | X | X | X | X | | | | | | | | X | | | | | | 2030-2037 |
| 6 | X | X | X | X | X | X | X | | | | | | | | | | | X | | | 2030-2037 |
| 7 | X | X | X | | | | | | | | X | X | X | X | | X | | | | | 2030-2037 |
| 8 | | | | | | | | X | X | | | | | | | | X | | | | 2024-2025 |
| 9 | | | | | | | | X | X | X | | | | | | | X | | | | 2026-2029 |
| 10 | | | | | | | | X | X | X | X | X | X | X | | | X | | | | 2030-2037 |
| 11 | | | | | | | | X | X | X | X | X | X | X | | | X | | X | | 2030-2037 |
| 12 | | | | | | | | X | X | X | X | X | X | X | | | X | | | X | 2030-2037 |

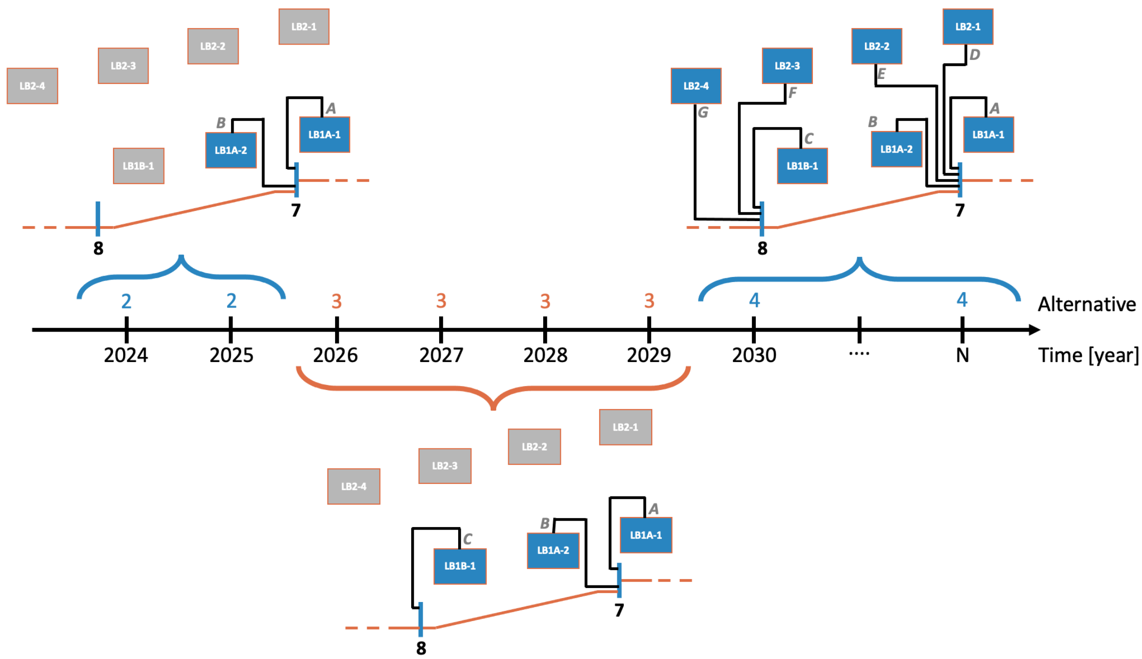


Figure 19: An illustrative example of a system solution, including implementation order and implementation time of the alternatives in the solution. Note: The supply situation prior to 2024, alternative 1, is not shown in the figure, but can be seen in Figure 18.

### 5.3.2 Comments on the Generation of Planning Alternatives

At last, the process on obtaining the measures, alternatives and system solutions, should be elaborated. What they all have in common, is that they follow the overall criteria of ensuring that no technical constraints are violated, both regarding supply voltage variations and power transfer capacities in cables and transformers.

Regarding the measures, all LV cables suggested built are $1kV$, $240mm^2 Al$ cables, and they are operated in a parallel of two such cables. Again, this is due to the current standard of Arva and a desire to plan for a maximum cable loading of 60% (limit set by Arva). Although measures A to N appears to be the same, except from transmission distance, it should be noted that the operational voltage level of a cable depends on what substation it is connected to. As such:

- *Existing substations:* The cables connected to the existing substations, namely 7 and 8, are operated with a voltage of $230V$.
- *New substations:* The cables connected to the newly built substation, 9, will be operated with a voltage of $400V$.This is also the case if the transformers at substations 7 and 8 are upgraded, as they are in alternative 5 (measure O).

Further, measures O to Q represent installing new transformers, while measures R-T represent the utilization of batteries for load levelling. The capacity ratings of the transformers and batteries are chosen based on what transformer loading is considered satisfactory. There are three maximum levels:

- 80%*:* This is the maximum transformer loading level set by Arva, when in the planning phase.
- 100%*:* This is the rated capacity of the transformer.
- 120%*:* This is the maximum transformer loading level set by Arva, during operation. Note: Such overloading is only acceptable for short periods of time.

Hence, as will be observed in Section 6, some of the alternatives will ensure a maximum loading of 80%, while others are barely within the 120%-limit. This will be subject for discussion.

Further, it should be noted that in terms of geographical location, substation 7 is located close to LB1A-1 and LB1A-2, while substation 8 is located close to LB1B-1. As such, it is reasonable that substation 7 supplies LB1A-1 and LB1A-2, and that substation 8 supplies LB1B-1, as suggested by measures A, B, and C. For the same reason, to minimize transmission distances, a potential new substation (measures P and Q) will be located “in the middle” of the new buildings of Molobyen.

Moreover, there is also a desire to investigate whether or not existing substations can handle the increased load demand and PV power production, and for how long.

If they have enough free capacity, costs could be avoided, or at least delayed. For instance, if technical requirements are satisfied in alternative 3, but not in 4, the system solution could be $1-2-3-7$, and as such the investment cost of a new substation can be both reduced (less capacity needed) and delayed by six years, compared to system solution $1-8-9-10$.

Finally, a short remark on the term *years valid* is provided. In Section 5.2.1, it was stated that loads and generation of construction stage 1A will come into operation in 2024, with the corresponding years for stage 1B and 2 being 2026 and 2030, respectively. The reasoning behind the chosen years, is simply based on the number of buildings to be constructed within the different stages. As such, the two buildings of construction stage 1A will be finished in the beginning of 2024, with the construction taking place in 2021-2023. When these are built, the construction of the single building of stage 1B is initialized. As there is only one building, only two years will be spent constructing it, and so it becomes operative in 2026. The last stage contains four buildings, with the construction of these taking four years. Thus, stage 2 becomes operative in 2030. Note: these "expected" years of construction are only estimates, as the construction stages given in [10] are simply presented in relation to order, not time and order.

## 5.4 Optimize Dispatch

Having defined the different alternatives, the next step is to check whether or not technical constraints are satisfied, through technical analyses. If an alternative does not include a battery, the load demand and PV generation of the different buildings become as presented in Section 5.2. However, if a battery is to be included, a model for optimal dispatch must be developed. Hence, large efforts have been put into the development and testing of such a model.

From initial simulations of the different alternatives presented in Section 5.3, it became apparent that certain alternatives caused surrounding transformers to become overloaded, mainly due to the large PV production. Thus, to avoid this, the main objective of the use of batteries is defined as:

*The objective of the utilization of batteries is to minimize power flows through the transformers in the system, i.e. minimize power flowing to and from the grid.*

This will be achieved through load levelling. As the objective includes minimizing power flows from the grid, the model will also facilitate self-consumption. In addition, PV curtailment will not be allowed. As such, the model facilitates for and enhances integration of renewables.

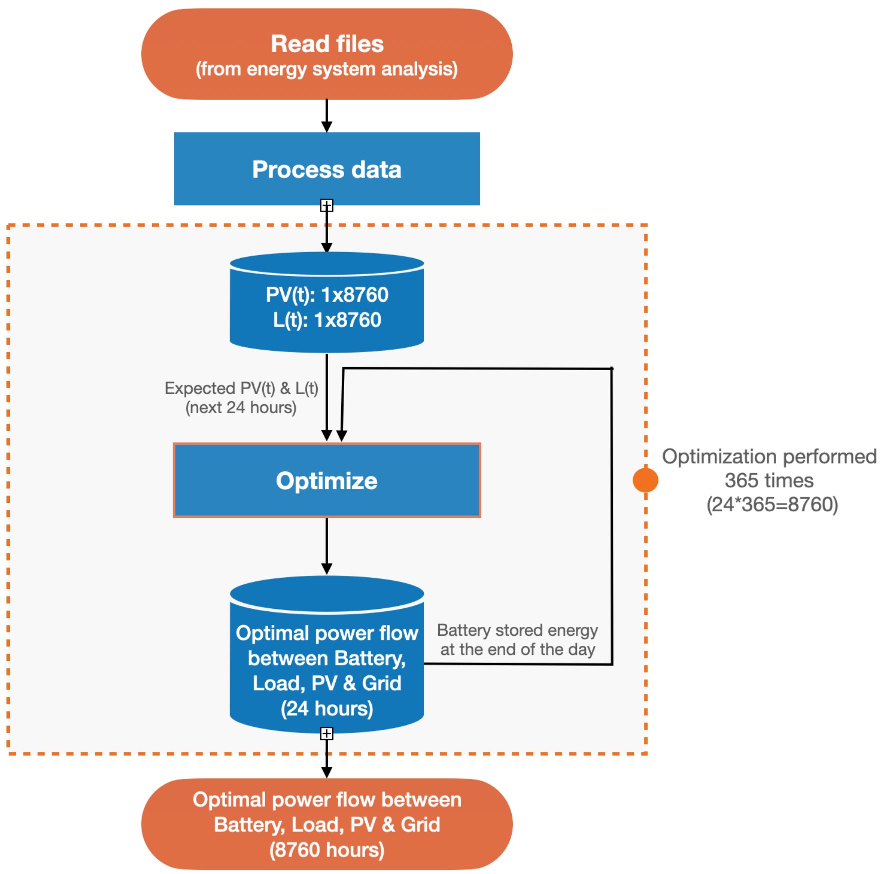


Figure 20: Flow chart illustrating the methodology for finding battery optimal dispatch. The block named *Optimize* is expanded upon in Section 5.4.1

Before the model itself is presented, a flow chart of the process going from simple data on load demand and PV production to finding optimal power flow between battery, load, PV and grid, is presented, see Figure 20. The model for the optimal dispatch is represented by the block named *Optimize* and the final model is presented in Section 5.4.1.

The different blocks of the flow chart are briefly presented below:

- **Read files:** The script starts of by reading the files containing the results from the energy system analysis: Two files, each containing the load demand of different elements within a building, along with solar PV production, throughout a year. More simply, these result files can be seen as two matrices: a $112173x9$ matrix and a $110245x8$ matrix. Here, the columns describe the power demand of the different elements, while the rows represent time. It should be noted that the reason why the number of rows in the two matrices does not match, is that the time step is not held constant.

- **Process data:** It is desirable to have a constant time step and an equal time step for both files. Thus, a script changing the varying time step into any desirable, constant time step has been developed. The script is based around the use of average values, and in this case a time step of 1 *hour* is chosen. The relevant elements representing load demand is then added together and stored as a 1x8760 vector, containing hourly load demand for an entire year. The solar PV production is also stored as a 1x8760 vector, with hourly PV production for an entire year. These are stored as L(t) and PV(t), respectively, as illustrated by the **third block**, from the top.

- **Optimize:** All of the values stored as L(t) and PV(t) will in turn be used as input for the optimization. Again, the model for the optimization will be presented in Section 5.4.1, but something worth noting already now is the input and output. As input, the model will take the expected load demand and PV production for the next 24 hours, i.e. the 24 first elements of L(t) and PV(t) for iteration 1, along with the battery stored energy at the end of the previous day. For the first iteration, the energy level will be set equal to the minimum SOC defined for the battery. The output will then be the optimal power flow between battery, load, PV and grid, for the next 24 hours. This is stored, before moving on to the next iteration, using elements 25 to 48 of L(t) and PV(t), along with the battery SOC at the end of the previous day (iteration 1), as input.

- **Optimal power flow ... (24 hours):** Stores the daily optimal power flow found through the optimization.
- **Optimal power flow ... (8760 hours):** In total, the optimization will be performed 365 times, one for each day (24 hour period) of the year. The results from each of these simulations are stored in this last block. As a result, the optimal power flow between battery, load, PV and grid, is obtained for 8760 hours, i.e. an entire year.

With the overall flow chart having been presented, the optimization model itself can be introduced. It should be noted that the *initial* model was not found satisfactory. Hence, several iterations and alterations have been performed in order to obtain a well-functioning model for battery optimal dispatch. The final model, used in the subsequent simulations, is presented in the following section, Section 5.4.1. The initial model, along with the most important iterations and alterations on the way to obtaining the final model, are presented in Appendix C.

### 5.4.1 Final Battery Optimal Dispatch Model

In order to develop a model for the battery optimal dispatch, the non-linear programming model presented in [29] has been used as an inspiration. This model has been extensively altered to fit the purpose of the situation of Molobyen. The intital model and the most important alterations are presented and described in Appendix C.

The final model, a QP with nine decision variables, is presented in the following. First, the decision variables are listed in Table 9. These variables are also illustrated in Figure 21. Note: $x_7(t)$ is also defined for $t = 25$. This is due to how the constraints, to be presented, are formulated.

Table 9: Decision variables.

| Variable | Description | Set of $x_{i,t}$ | Unit |
|---|---|---|---|
| $x_1(t)$ | Grid to load | $\{x_1(t)\|t \in \mathbb{N}, 1 \leq t \leq 24\}$ | Wh/h |
| $x_2(t)$ | Grid to batt. | $\{x_2(t)\|t \in \mathbb{N}, 1 \leq t \leq 24\}$ | Wh/h |
| $x_3(t)$ | PV to load | $\{x_3(t)\|t \in \mathbb{N}, 1 \leq t \leq 24\}$ | Wh/h |
| $x_4(t)$ | PV to batt. | $\{x_4(t)\|t \in \mathbb{N}, 1 \leq t \leq 24\}$ | Wh/h |
| $x_5(t)$ | PV to grid | $\{x_5(t)\|t \in \mathbb{N}, 1 \leq t \leq 24\}$ | Wh/h |
| $x_6(t)$ | Batt. to load | $\{x_6(t)\|t \in \mathbb{N}, 1 \leq t \leq 24\}$ | Wh/h |
| $x_7(t)^*$ | Batt. stored | $\{x_7(t)\|t \in \mathbb{N}, 1 \leq t \leq 25\}$ | Wh/h |
| $x_8(t)$ | Batt. to grid | $\{x_8(t)\|t \in \mathbb{N}, 1 \leq t \leq 24\}$ | Wh/h |
| $x_9(t)$ | Aux. var.: Max. min. PF | $\{x_9(t)\|t \in \mathbb{N}, 1 \leq t \leq 24\}$ | Wh/h |

$^*$As the time step is one hour, the "actual" unit of $x_7(t)$ is $Wh$.

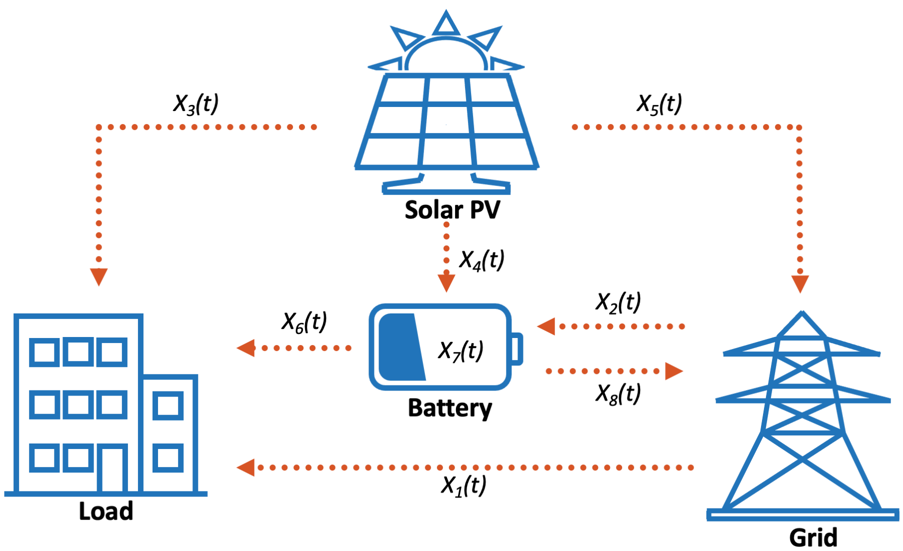


Figure 21: Supply topology of Molobyen with decision variables included.

The model is presented through Equations (4)-(15), with constants defined in Table 10. The auxiliary variable, $x_9(t)$, is always set equal to the maximum power flow (to or from the grid), due to how the auxiliary constraints, Equations (14) and (15), are formulated. Comments on the interpretation of $x_9(t)$ is provided in Appendix C.3.

**Objective function #1: Load levelling ($PV(t) \leq 0.95 \cdot Load(t)$)**

$$min \sum_{t=1}^{24} x_9^2(t) \tag{4}$$

**Objective function #2: Load levelling ($PV(t) > 0.95 \cdot Load(t)$)**

$$min \sum_{t=1}^{24} x_9^2(t) + k \cdot [x_6(t-1) + x_6(t) + x_8(t-1) + x_8(t)] \tag{5}$$

**Constraints and boundaries**:

A. *Battery stored energy conservation*

$$\eta \cdot x_2(t) + \eta \cdot x_4(t) - \frac{1}{\eta} \cdot x_6(t) - \frac{1}{\eta} \cdot x_8(t) + x_7(t) = x_7(t+1), \ 1 \leq t \leq 24 \tag{6}$$

B. *PV output and load conservation*

$$x_3(t) + x_4(t) + x_5(t) = PV(t), \qquad 1 \leq t \leq 24 \tag{7}$$

$$x_1(t) + x_3(t) + x_6(t) = L(t), \qquad 1 \leq t \leq 24 \tag{8}$$

C. *Battery max. and min. storage limits*

$$x_7(t) \leq \alpha \cdot B_{max}, \qquad 1 \leq t \leq 25 \tag{9}$$

$$x_7(t) \geq \gamma \cdot B_{max}, \qquad 1 \leq t \leq 25 \tag{10}$$

D. *Initial stored battery energy*

$$x_7(t) = Bprevday, \qquad t = 1 \tag{11}$$

E. *Battery maximum power constraint*

$$x_6(t) + x_8(t) \leq P_{max}, \qquad 1 \leq t \leq 24 \tag{12}$$

$$x_2(t) + x_4(t) \leq P_{max}, \qquad 1 \leq t \leq 24 \tag{13}$$

Aux.: *Auxiliary constraints for load levelling (peak shaving)*

$$x_1(t) + x_2(t) \leq x_9(t), \qquad 1 \leq t \leq 24 \tag{14}$$

$$x_5(t) + x_8(t) \leq x_9(t), \qquad 1 \leq t \leq 24 \tag{15}$$

All decision variables do also have a lower boundary of zero.

Table 10: Constants used in the optimization model.

| Parameter | Notation | Value |
|---|---|---|
| Penalty factor | $k$ | $10^7$ |
| Charge & discharge efficiency | $\eta$ | 90% |
| Upper batt. storage limit | $\alpha$ | 90% |
| Lower batt. storage limit | $\gamma$ | 10% |

### 5.4.2 Load and Generation Replication

Ideally, the output from the optimization should be used directly in NETBAS, but, again, this was not possible due to inadequate licenses. Hence, for the battery alternatives, load and generation must once more be modelled through maximum values and daily and yearly variation curves, as presented in Figure 12. There is, however, one major difference between the alternatives with and without batteries: the battery. Hence, it is a bit more challenging to model the behaviour of the load and PV for the battery alternatives.

To perform the replication, it is essential that the main operational benefit of the batteries, being load levelling, is captured. More specifically, the reduction in maximum power flows, caused by the batteries, must be preserved when going from time series in MATLAB to daily and yearly variation curves in NETBAS. This is obtained by ensuring that the difference between maximum PV production and maximum load demand for each of the months, as seen from the substations, are the same for the analyses in NETBAS and the results from MATLAB.

More specific details, in terms of formulas and additional information, can be found in Appendix C.4.

## 5.5 Technical Analysis

Having modelled the load demand and PV generation of all buildings, for each of the different alternatives, technical analyses are performed. The main goal of these are both to ensure satisfactory operation and to calculate losses. With satisfactory operation, the major focus is on avoiding overloading of cables and transformers, according to the desired limits defined in Section 5.3.2, and ensuring supply voltage variations to be within given limits, see Section 2.3.2.

These analyses are performed through power flow analyses in NETBAS, simulating operation for an entire year, with the results being on an hourly format. This is done for all alternatives, for the first and last year of the interval referred to as valid years. Results are presented in Section 6.2.

## 5.6 Cost Evaluation

The cost elements included in this thesis, for each of the alternatives, are the investment costs and the cost of losses. These are presented in Sections 5.6.1 and 5.6.2, respectively.

### 5.6.1 Investment Costs

The investment cost of the different measures involving new substations, transformers and cables are calculated using cost tables in REN's *Planlegginsbok for kraftnett: Kostnadskatalog distribusjonsnett* [6]. The relevant tables are included in Appendix D, see Tables 25, 26, 27 and 28. The investment cost of the measures involving batteries, were mapped in Section 3.1. The most important findings, being costs of batteries for grid application, including power electronics and servicing (15-20 years), are summarized in Table 11, along with their corresponding value in NOK/kWh.

Table 11: Battery prices. Exchange rate at the time of price estimates was $1USD = 9.20NOK$ (5 Oct. 2020, CleanTechnica) and $1USD = 8.59NOK$ (16 Dec. 2020, BloombergNEF). An average conversion rate of $1USD = 8.90NOK$ is utilized for the lower row in the table.

| Year | 2020 | 2021 | 2022 | 2023 | 2024 | 2025 | 2026 | 2027 | 2028 | 2029 | 2030 |
|---|---|---|---|---|---|---|---|---|---|---|---|
| Price [$\$/kWh$] | 300 | 287 | 275 | 264 | 254 | 246 | 239 | 232 | 227 | 224 | 221 |
| Price [$NOK/kWh$] | 2670 | 2554 | 2448 | 2350 | 2261 | 2189 | 2127 | 2065 | 2020 | 1994 | 1967 |

The general formula for the investment cost of a measure, $I$, can be formulated as:

$$I = (c_{cable} + \epsilon \cdot c_{trench}) \cdot L + C_{substation} + c_{battery} \cdot R_{kWh} \tag{16}$$

Here, $c_{cable}$ [$NOK/km$] and $c_{trench}$ [$NOK/km$] are the specific costs of cables and trenches, $L$ [$km$] the cable length, $C_{substation}$ [$NOK$] the cost of substations, $c_{battery}$ [$NOK/kWh$] the specific battery cost, and $R_{kWh}$ [$kWh$] the energy capacity rating of the battery. Also, $\epsilon$ is a unitless factor with the purpose of dividing trench costs equally between measures with cables that utilizes the same trench. I.e., if two cables to two different buildings are sharing a trench for most of the distance from the substation to their respective buildings, the two cables, and hence measures, should share the common trench cost equally. As such, $\epsilon$ is chosen based on the distance of which a cable shares a trench with other cables, and the distance of which it needs its own trench. It is important to note that the main purpose for doing this is:

- To avoid that costs of one specific trench is taken into account several times.
- To avoid that one measure, and hence alternative, is preferred as compared to another, simply due to that the latter takes into account all costs related to a common trench.

The investment costs are calculated and presented in Section 6.3.

### 5.6.2 Cost of Losses

For cases with no distributed generation, the maximum power loss will occur when the power demand is at its highest, typically during winter time. The cost can then be calculated as the sum of the cost of maximum power losses and the cost of energy losses, or more simply as the product of the maximum power loss and the equivalent cost of losses, $k_{pekv}$ [42]. As standard values of $k_{pekv}$ can be found through tables in [42], only the maximum power loss is needed in order to obtain the cost of power losses when using the latter formulation. The formula is given in Equation (17), with all relevant parameters listed in Table 12.

$$K_{losses} = (k_p + k_{wekv} \cdot T_t) \cdot \Delta P_{max} = k_{pekv} \cdot \Delta P_{max} \tag{17}$$

Table 12: Parameters used in Equations (17)-(22).

| Parameter | Unit | Description |
|---|---|---|
| $K_{losses}$ | $[NOK/yr]$ | Cost of losses |
| $k_p$ | $[NOK/kWyr]$ | Cost of maximum power losses |
| $k_{wekv}$ | $[NOK/kWh]$ | Equivalent yearly cost of energy losses |
| $k_{pekv}$ | $[NOK/kWyr]$ | Equivalent cost of losses |
| $\Delta W$ | $[kWh]$ | Yearly energy losses |
| $\Delta P_{max}$ | $[kW]$ | Maximum power losses |
| $\Delta P_{max}^{PV}$ | $[kW]$ | Maximum power losses during summer |
| $\Delta P_{max}^{L}$ | $[kW]$ | Maximum power losses during winter |
| $T_t$ | $[h]$ | Utilization time for losses, based on $P_{max}$ |
| $T_t^{PV}$ | $[h]$ | Utilization time for losses, based on $P_{max}^{PV}$ |
| $T_t^{L}$ | $[h]$ | Utilization time for losses, based on $P_{max}^{L}$ |

As mentioned, the cost relies on both maximum power losses and energy losses. The reason for this, is that the power losses do occupy some of the grid's available capacity, while the energy losses have to be produced, although it is not directly used to supply a load [42].

For Molobyen, however, the distributed generation (solar PV) is of such a size that it causes the maximum power loss to occur during summer time, for several of the defined alternatives. In these cases, the duration curve for the yearly losses becomes as illustrated in Figure 22. Note: The area of the orange rectangle equals the area of the blue rectangle, as this represents yearly energy losses, see Equation (18).

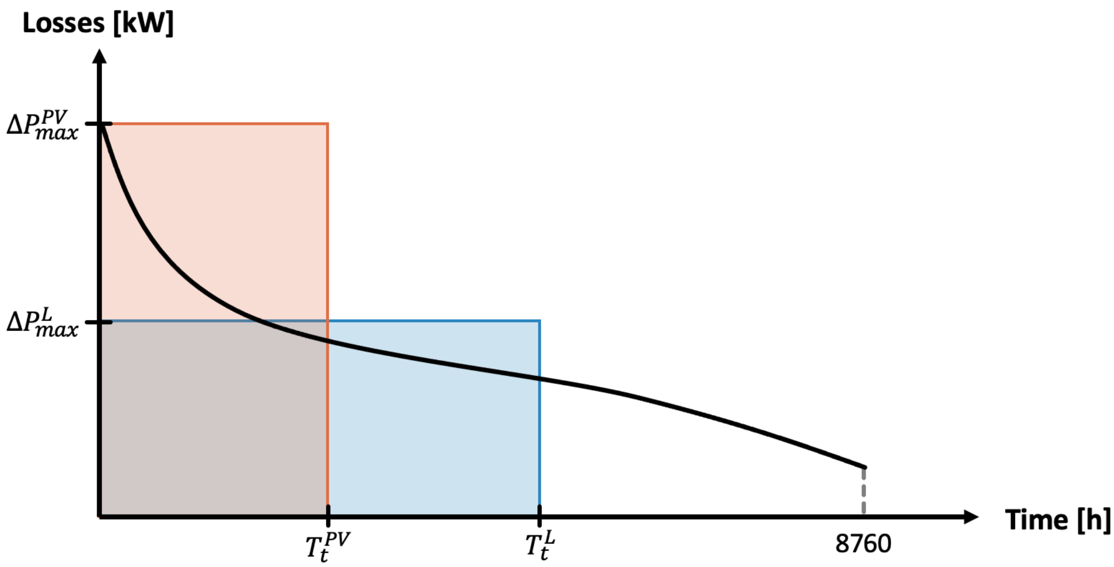


Figure 22: Utilization time for losses.

$$\Delta P_{max}^{PV} \cdot T_t^{PV} = \Delta P_{max}^{L} \cdot T_t^{L} = \Delta W. \tag{18}$$

As the cost of maximum power losses, $k_p$, from Equation (17), is based on losses occupying capacity all the way from a centralized power producer to a load, penalizing the power losses from local generation on equal terms can be considered excessive: These losses will only occupy capacity of the grid nearby the loads. Thus, in such cases, $k_p$ should be reduced accordingly. To handle this, the ratio between maximum power loss during the traditional high-loading periods (winter), $\Delta P_{max}^{L}$, and the maximum power loss during high PV production (summer), $\Delta P_{max}^{PV}$, is multiplied with $k_p$. The formulas for calculating the cost of losses, $K_{losses}$, and hence $k_{pekv}$, are presented in Equations (19) and (20), with all relevant parameters presented in Table 12 (Note: Equation (20) is the exact same as Equation (17)):

- If $\Delta P^{PV}_{max} >= \Delta P^{L}_{max}$:

$$\begin{aligned} K_{losses} &= k_p \cdot \frac{\Delta P^{L}_{max}}{\Delta P^{PV}_{max}} \cdot \Delta P^{PV}_{max} + k_{wekv} \cdot T^{PV}_t \cdot \Delta P^{PV}_{max} \\ &= \left( k_p \cdot \frac{\Delta P^{L}_{max}}{\Delta P^{PV}_{max}} + k_{wekv} \cdot T^{PV}_t \right) \cdot \Delta P^{PV}_{max} \\ &= k_{pekv} \cdot \Delta P^{PV}_{max} \end{aligned} \tag{19}$$

- If $\Delta P^{PV}_{max} < \Delta P^{L}_{max}$:

$$\begin{aligned} K_{losses} &= k_p \cdot \Delta P^{L}_{max} + k_{wekv} \cdot T^{L}_t \cdot \Delta P^{L}_{max} \\ &= (k_p + k_{wekv} \cdot T^{L}_t) \cdot \Delta P^{L}_{max} \\ &= k_{pekv} \cdot \Delta P^{L}_{max} \end{aligned} \tag{20}$$

Here, $k_p$ and $k_{wekv}$ can be extracted from tables in REN's *Planbok for kraftnett: Tapskostnader* [42], while $P^{PV}_{max}$ and $P^{L}_{max}$, along with the yearly energy loss, $\Delta W$, can be obtained from power flow analyses. $T^{PV}_t$ and $T^{L}_t$ are calculated through the power and energy losses, as:

$$T^{PV}_t = \frac{\Delta W}{\Delta P^{PV}_{max}} \tag{21}$$

$$T^{L}_t = \frac{\Delta W}{\Delta P^{L}_{max}} \tag{22}$$

As such, by using Equations (19) and (20), the equivalent cost of losses, $k_{pekv}$, can be calculated. From this, the cost of losses, $K_{losses}$, is found as the product of $k_{pekv}$ and the maximum power loss for the given year; independent of when this maximum loss occurs. In DYNKO, to be used for the socio-economic analyses, the cost of losses can be given as either of the following:

- The combination of maximum power loss, $\Delta P_{max}$ (kW), for each alternative and the equivalent cost of losses, $k_{pekv}$ (NOK/kW yr), for each of the years in the period of analysis

- The cost of losses, $K_{losses}$ (NOK/yr), for each alternative, for each of the years the alternative is valid

As $k_{pekv}$ will have a unique value for each alternative, for each year of its valid years, average values will have to be utilized if the first option is chosen. Hence, to obtain more accurate results, $K_{losses}$ is calculated for each of the different alternatives, for the first and last year of the period for which the respective alternatives are valid. I.e., the second option is utilized. Finally, all calculations and results are presented in Section 6.3.

## 5.7 Socio-Economic Analysis

The socio-economic analysis is performed using DYNKO, as introduced in Section 4.3. Here, an objective function consisting of investment costs and cost of losses is minimized, for a given period of analysis. This is performed for all possible system solutions (i.e., combination of alternatives), from which they are ranked from cheapest to most expensive solution. These results are presented in Section 6.4.

## 5.8 Overall Assessment and Ranking of Alternatives

Finally, all alternatives and system solutions are assessed through technical and economic considerations, both qualitatively and quantitatively. These considerations will be presented in Section 6.5.

# 6 Practical Application of the Proposed Grid Planning Framework

This section follows, to a large extent, the same structure as Section 5, see Figure 8, and presents the results from all calculations and simulations performed, together with some key observations. As the planning study was defined, the load and generation modelled, and the planning alternatives generated, in Sections 5.1, 5.2 and 5.3, respectively, this section will first present results from the battery dispatch optimization. From there on, the structure is the same as in Section 5.

## 6.1 Optimize Dispatch

Three of the alternatives defined involve utilization of batteries, namely Alternative 6, 11 and 12. Hence, for these, the load and generation modelling presented in Section 5.2 must be modified. This is done through using the battery optimal dispatch model, presented in Section 5.4.1. In the following, for each of these three alternatives, the power flow to and from the grid are presented before and after including a battery. The maximum power flow to and from grid, before and after the optimization, are also summarized below, in Table 13.

Table 13: Maximum power flow [kW] to and from grid, for all alternatives involving batteries, before and after including a battery.

| | **Power Flow From Grid** $[kW]$ | | | | **Power Flow To Grid** $[kW]$ | | | |
|---|---|---|---|---|---|---|---|---|
| | ALT 6 | | ALT 11 | ALT 12 | ALT 6 | | ALT 11 | ALT 12 |
| | TF 7 | TF 8 | TF 9 | TF 9 | TF7 | TF8 | TF9 | TF9 |
| W/ batt. | 349.2 | 252.2 | 601.4 | 601.4 | 901.6 | 684.5 | 1 586.1 | 1 586.1 |
| W/o batt. | 343.4 | 225.1 | 515.1 | 579.4 | 888.2 | 602.3 | 1 293.2 | 1 532.7 |

### 6.1.1 Alternative 6

The power flow through the transformer at substation 7, for alternative 6, with and without a battery, is presented in Figure 23. From this, a reduction in both the power flow to and from the grid can be observed.

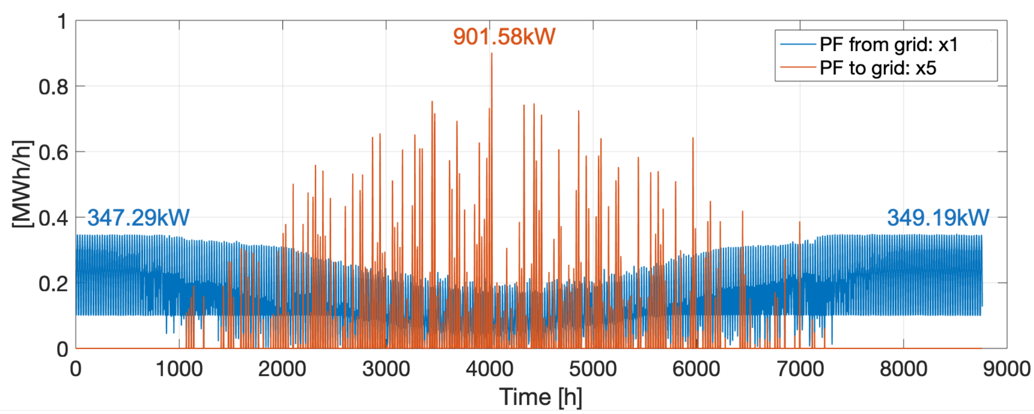


(a) Without battery

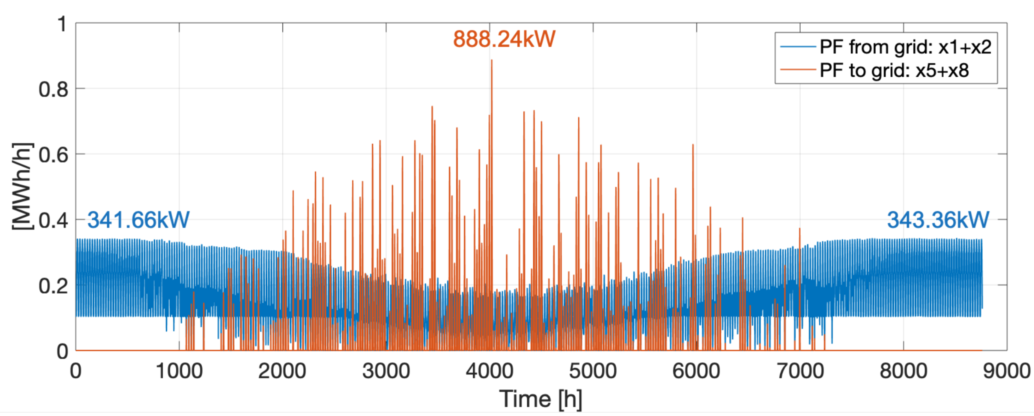


(b) With a 0.015MW/0.015MWh battery

Figure 23: Comparison of power flow to and from grid with and without batteries, for substation 7. Peak values for the power flow from grid during the start and the end of the year marked, along with the peak power flow to grid during summer time.

The power flow through the transformer at substation 8, for alternative 6, with and without a battery, is presented in Figure 24. From this, a reduction in both the power flow to and from the grid can be observed.

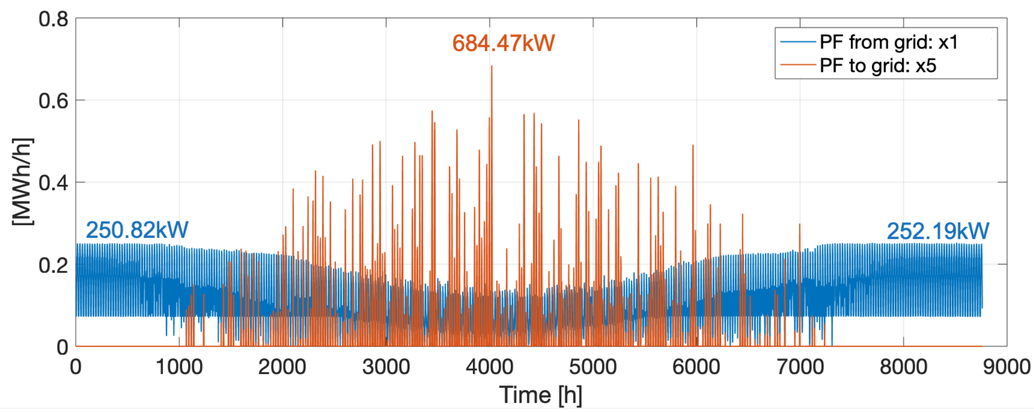


(a) Without battery

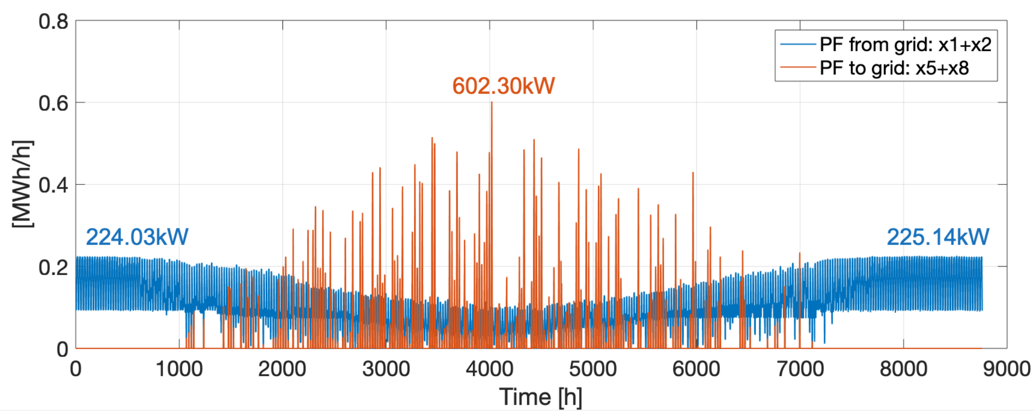


(b) With a 0.13MW/0.13MWh battery

Figure 24: Comparison of power flow to and from grid with and without batteries, for substation 8. Peak values for the power flow from grid during the start and the end of the year marked, along with the peak power flow to grid during summer time.

### 6.1.2 Alternative 11

The power flow through the transformer at substation 9, for alternative 11, with and without a battery, is presented in Figure 25. From this, a reduction in both the power flow to and from the grid can be observed.

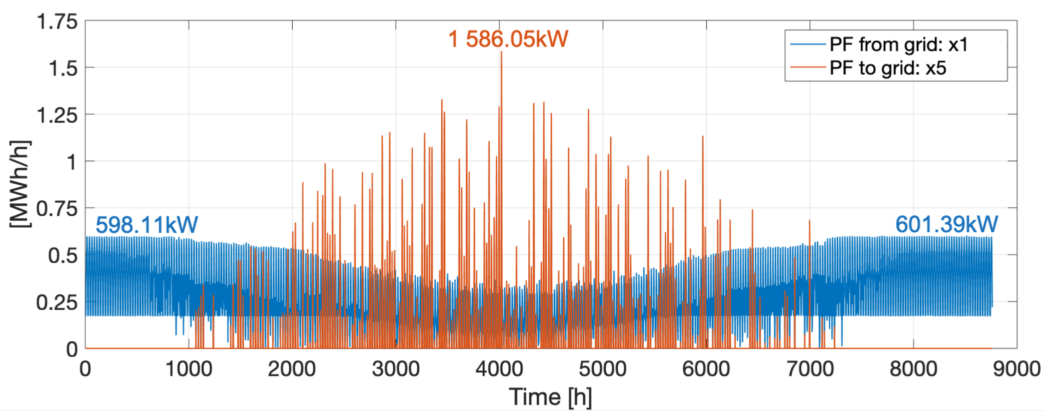


(a) Without battery

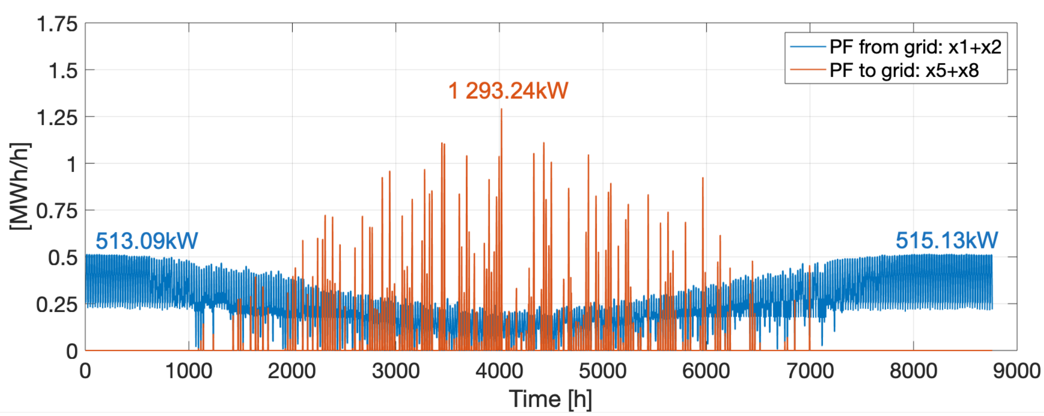


(b) With a 0.53MW/0.53MWh battery

Figure 25: Comparison of power flow to and from grid with and without batteries, for substation 9. Peak values for the power flow from grid during the start and the end of the year marked, along with the peak power flow to grid during summer time.

### 6.1.3 Alternative 12

The power flow through the transformer at substation 9, for alternative 12, with and without a battery, is presented in Figure 26. From this, a reduction in both the power flow to and from the grid can be observed.

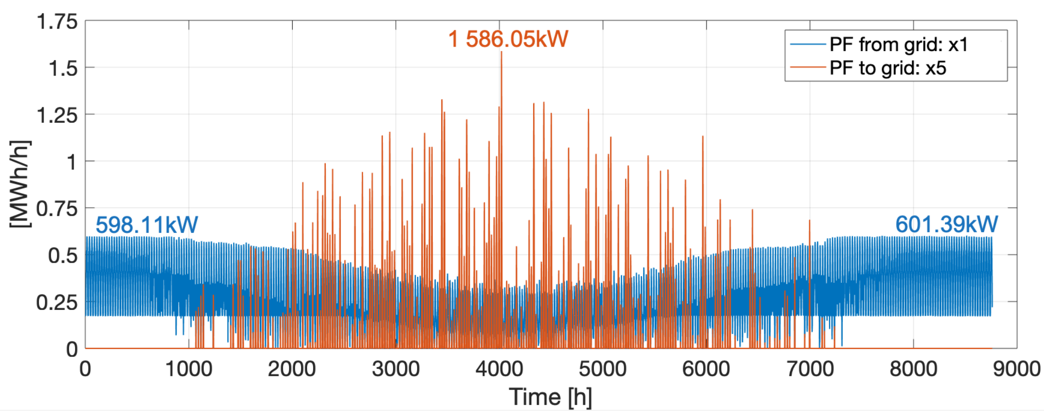


(a) Without battery

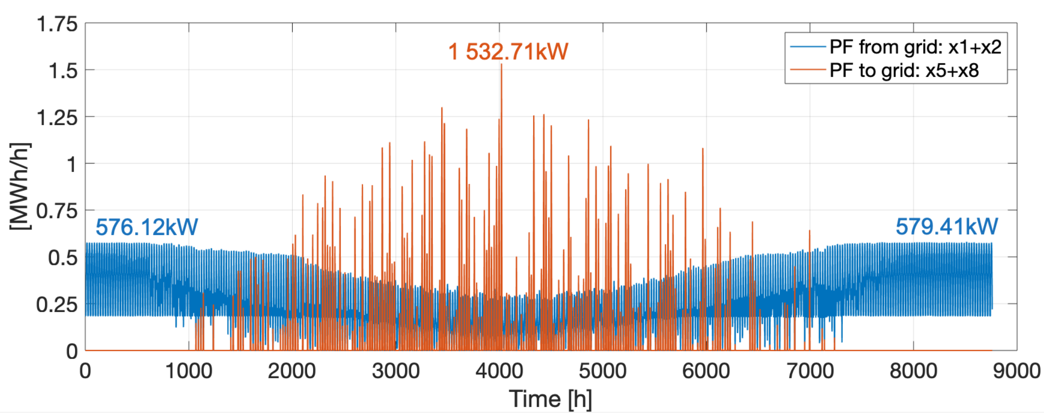


(b) With 0.06MW/0.06MWh battery

Figure 26: Comparison of power flow to and from grid with and without batteries, for substation 9. Peak values for the power flow from grid during the start and the end of the year marked, along with the peak power flow to grid during summer time.

### 6.1.4 Replication of Load and Generation

The power flow shown in the above figures must be replicated in NETBAS, through daily and yearly variation curves, along with maximum values. By following the method described in Section 5.4.2, the maximum values are calculated and presented in Table 14, while the daily variation for the load and the yearly variation for the solar PV, become as in Table 15. Note: There is close to no variation in the yearly load demand, i.e. the maximum load demand is approximately the same for every month. Hence, the yearly variation in load demand is not presented explicitly.

Table 14

| **Load: Max demand** $[kW]$ | | | | **PV: Max production** $[kW]$ | | | |
|---|---|---|---|---|---|---|---|
| ALT 6 | | ALT 11 | ALT 12 | ALT 6 | | ALT 11 | ALT 12 |
| TF 7 | TF 8 | TF 9 | TF 9 | TF7 | TF8 | TF9 | TF9 |
| 349.9 | 229.9 | 526.4 | 590.7 | 1 177.7 | 788.3 | 1 713.4 | 2 020.9 |

Table 15: Load and PV replication for the alternatives involving batteries. Here, TF X refers to the loads connected to transformer/substation X for the given alternative.

| | **Load: Daily var.** [%] | | | | | **PV: Yearly var.** [%] | | |
|---|---|---|---|---|---|---|---|---|
| | ALT 6 | | ALT 11 | ALT 12 | | ALT 6 | ALT 11 | ALT 12 |
| Hour | TF 7 | TF 8 | TF 9 | TF 9 | Month | TF 7&8 | TF 9 | TF 9 |
| 01:00 | 30.0 | 41.7 | 49.6 | 31.8 | Jan | 0.6 | 1.3 | 0.5 |
| 02:00 | 30.0 | 41.7 | 49.6 | 31.8 | Feb | 40.2 | 39.1 | 39.7 |
| 03:00 | 30.0 | 41.7 | 49.6 | 31.8 | Mar | 55.3 | 61.1 | 64.7 |
| 04:00 | 30.0 | 41.7 | 49.6 | 31.8 | Apr | 70.2 | 79.5 | 69.6 |
| 05:00 | 30.0 | 41.7 | 49.6 | 31.8 | May | 88.8 | 89.7 | 90.0 |
| 06:00 | 32.4 | 41.7 | 49.6 | 32.7 | June | 100 | 100 | 100 |
| 07:00 | 46.2 | 47.9 | 51.1 | 47.1 | July | 87.9 | 89.7 | 88.2 |
| 08:00 | 59.2 | 65.2 | 68.1 | 60.6 | Aug | 81.5 | 77.7 | 80.1 |
| 09:00 | 67.7 | 74.8 | 77.6 | 69.2 | Sept | 75.6 | 71.6 | 78.6 |
| 10:00 | 70.6 | 78.4 | 81.5 | 72.4 | Oct | 56.2 | 53.7 | 58.8 |
| 11:00 | 86.8 | 96.4 | 100 | 88.0 | Nov | 1.1 | 2.1 | 0.5 |
| 12:00 | 88.4 | 98.0 | 100 | 89.4 | Dec | 0.0 | 0.0 | 0.0 |
| 13:00 | 85.6 | 94.3 | 99.0 | 87.5 | | | | |
| 14:00 | 90.9 | 100 | 100 | 93.0 | | | | |
| 15:00 | 98.1 | 100 | 100 | 100 | | | | |
| 16:00 | 100 | 100 | 100 | 100 | | | | |
| 17:00 | 100 | 100 | 100 | 100 | | | | |
| 18:00 | 97.5 | 100 | 100 | 99.5 | | | | |
| 19:00 | 92.7 | 100 | 100 | 94.8 | | | | |
| 20:00 | 90.4 | 100 | 100 | 92.2 | | | | |
| 21:00 | 72.8 | 79.8 | 83.6 | 74.3 | | | | |
| 22:00 | 65.1 | 72.2 | 74.5 | 65.6 | | | | |
| 23:00 | 57.3 | 62.4 | 63.9 | 57.7 | | | | |
| 24:00 | 39.3 | 40.8 | 43.0 | 39.2 | | | | |

## 6.2 Technical Analysis

First, the maximum loading of the transformers and certain cables, along with voltage level of certain connection points, are presented, in Table 16. The simulations are performed for the first year of the years for which the respective alternatives are valid. This year is also specified in the first column. Further, as discussed in Section 5.3.2, the alternatives are developed to ensure that the maximum loading of the transformers do not exceed a given limit (80%, 100% or 120%). For clarity, the alternatives marked in green implies a maximum transformer loading of 80%, yellow implies a maximum transformer loading of 100%, and red implies a maximum transformer loading of 120%.

Table 16: Overview of alternative performance. For all alternatives, the simulations are performed for the first year of their period of validity. N/A means that a value is not applicable for the given alternative.

| Alt. | Max loading of TF | | | Max load. of cable to | | Max/min voltage [V] at | |
|---|---|---|---|---|---|---|---|
| | 7 | 8 | 9 | LB1A-1 | LB2-1 | LB1A-1 | LB2-1 |
| 1 (2023) | 30.6% | 45.6% | N/A | N/A | N/A | N/A | N/A |
| 2 (2024) | 55.0% | 46.1% | N/A | 59.17% | N/A | 249.7/237.4 | N/A |
| 3 (2026) | 55.7% | 65.6% | N/A | 59.15% | N/A | 249.7/237.3 | N/A |
| 4 (2030) | 101.2% | 119.3% | N/A | 59.31% | 63.24% | 249.1/236.1 | 249.8/236.9 |
| 5 (2030) | 64.7% | 74.4% | N/A | 36.05% | 38.51% | 409.8/400.9 | 410.2/401.4 |
| 6 (2030) | 99.5% | 99.8% | N/A | 59.31% | 63.24% | 249.1/236.1 | 249.8/236.9 |
| 7 (2030) | 57.0% | 67.6% | 78.0% | 59.18% | 40.35% | 243.7/241.3 | 391.4/385.3 |
| 8 (2024) | 30.9% | 46.0% | 28.5% | 37.70% | N/A | 391.9/386.0 | N/A |
| 9 (2026) | 31.6% | 47.0% | 42.8% | 37.72% | N/A | 391.6/385.4 | N/A |
| 10 (2030) | 33.3% | 48.9% | 103.9% | 37.83% | 40.43% | 390.5/383.6 | 390.7/384.1 |
| 11 (2030) | 33.0% | 48.9% | 79.7% | 37.83% | 40.43% | 390.5/383.6 | 390.7/384.1 |
| 12 (2030) | 33.0% | 48.9% | 99.3% | 37.83% | 40.43% | 390.5/383.6 | 390.7/384.1 |

Key observations from this table are:

- Regarding the transformer maximum loading, these are all within their given limits: Alternative 4 and 10 satisfy a maximum loading of 120%, alternative 6 and 12 satisfy a maximum loading of 100%, and the rest satisfy a limit of 80%. Also, note that alternatives 6, 11 and 12, which all involves batteries, are dimensioned to have maximum loading close to their respective limits of 100%, 80% and 100%.

- Regarding the loading of the cables to buildings LB1A-1 and LB2-1, these are all within or around the desired maximum loading of 60%. The only alternatives violating this limit are alternatives 4 and 6. Although parallel cables are used for these alternatives as well, the rated operating voltage is here $230V$, as compared to $400V$ for the other alternatives valid from 2030.

- Regarding the voltage variations at the connection points of buildings LB1A-1 and LB2-1, no voltage variation limits are violated. As stated in Section 2.3.2, a maximum deviation of $\pm 10\%$ from the rated voltage is considered satisfactory. Hence, for $230V$ connections, the voltage should be within the interval $[207V, 253V]$, with the corresponding interval for $400V$ being $[360V, 440V]$. Alternatives 2-4 and 6-7 utilizes $230V$, while alternatives 5 and 8-12 utilizes $400V$, and all alternatives satisfy their respective intervals.

- Finally, regarding future cable loading and voltages, these will remain the same for the years to come, as well. The reason for this is that the new buildings are assumed to have zero growth in both consumption and production.

Further, the losses, both in terms of energy and maximum power, are presented in Tables 17 and 18. For the columns denoted with $kW$ *(sum.)*, the first value is the maximum power loss during traditional high-loading periods (winter), while the value in the parenthesis is the maximum power loss during the summer. Further, the latter table is a continuation of the first, but it also presents the loading of the transformers at the end of the period of analysis, in 2037.

Table 17: Yearly losses: Energy losses in columns denoted *kWh* and maximum power losses during the winter and the summer in columns denoted *kW (sum.)*.

| Alt. | 2023 | | 2024 | | 2025 | |
|---|---|---|---|---|---|---|
| | kWh | kW (sum.) | kWh | kW (sum.) | kWh | kW (sum.) |
| 1 | 66 141.2 | 17.47 (5.11) | - | - | - | - |
| 2 | - | - | 80 005.6 | 21.30 (16.42) | 80 738.4 | 21.66 (16.46) |
| 3 | - | - | - | - | - | - |
| 4 | - | - | - | - | - | - |
| 5 | - | - | - | - | - | - |
| 6 | - | - | - | - | - | - |
| 7 | - | - | - | - | - | - |
| 8 | - | - | 82 770.2 | 19.88 (9.79) | 83 463.1 | 20.22 (9.84) |
| 9 | - | - | - | - | - | - |
| 10 | - | - | - | - | - | - |
| 11 | - | - | - | - | - | - |
| 12 | - | - | - | - | - | - |
| **Alt.** | **2026** | | **2029** | | **2030** | |
| | kWh | kW (sum.) | kWh | kW (sum.) | kWh | kW (sum.) |
| 1 | - | - | - | - | - | - |
| 2 | - | - | - | - | - | - |
| 3 | 88 467.1 | 23.44 (21.89) | 91 844.1 | 25.11 (22.14) | - | - |
| 4 | - | - | - | - | 122 090.9 | 32.58 (59.21) |
| 5 | - | - | - | - | 60 722.5 | 14.18 (26.50) |
| 6 | - | - | - | - | 120 211.3 | 31.96 (51.16) |
| 7 | - | - | - | - | 114 283.7 | 28.61 (37.65) |
| 8 | - | - | - | - | - | - |
| 9 | 86 397.5 | 21.00 (12.31) | 89 616.7 | 22.10 (12.51) | - | - |
| 10 | - | - | - | - | 102 263.7 | 24.58 (31.93) |
| 11 | - | - | - | - | 99 463.7 | 24.29 (21.37) |
| 12 | - | - | - | - | 102 245.0 | 24.49 (29.70) |

Table 18: This is a continuation of Table 17, and presents the losses for 2037. In addition, the transformer loadings are presented for 2037.

| Alt. | 2037 | | Max loading of TF | | |
|---|---|---|---|---|---|
| | kWh | kW (sum.) | 7 | 8 | 9 |
| 1 | - | - | - | - | - |
| 2 | - | - | - | - | - |
| 3 | - | - | - | - | - |
| 4 | 130 411.6 | 35.55 (59.08) | 101.5% | 119.3% | - |
| 5 | 64 025.6 | 15.23 (26.51) | 65.7% | 75.5% | - |
| 6 | 128 856.2 | 35.29 (51.03) | 99.4% | 100.8% | - |
| 7 | 122 250.7 | 31.41 (37.45) | 59.0% | 71.0% | 78.0% |
| 8 | - | - | - | - | - |
| 9 | - | - | - | - | - |
| 10 | 110 764.7 | 27.52 (31.95) | 35.6% | 52.5% | 103.9% |
| 11 | 107 964.7 | 27.23 (21.61) | 35.6% | 52.5% | 79.7% |
| 12 | 110 746.0 | 27.42 (29.88) | 35.6% | 52.5% | 99.3% |

Key observations from these tables are:

- Regarding the maximum power losses, the trend is that the maximum power loss occurs during winter time for all alternatives valid before the year of 2030, i.e. before all buildings are constructed. However, after 2030, the maximum power loss occurs during summer time, with the main reason being the large solar PV production. The only exception is alternative 11, where the utilization of a rather large battery manages to heavily reduce the peak power flows created by the large PV production.

- Regarding alternative 5, both the energy and power losses are significantly smaller compared to all other alternatives, for the years 2030 and 2037. The reason for this is that when upgrading the transformers, the LV voltage level is increased, from $230V$ to $400V$. As such, all new and existing cables connected to these transformers, can be operated at $400V$, yielding reduced losses.

- In addition, the max loading of the transformers are listed for the alternatives valid in 2037. Comparing these with the loading in 2030, transformers 7 and 8 have, in general, experienced a slight increase in loading, while transformer 9 remains unaffected. This is expected as the existing loads in the area assume a yearly increase in load demand, as opposed to the new loads of Molobyen, assuming the yearly increase in both demand and production to be zero.

  As a consequence of this, transformer 8, in alternative 6, will no longer stay within its desired limit of 100% loading. Due to this, it may be considered unacceptable and, hence, be discarded.

### 6.2.1 Yearly Variation in Transformer Loading

In order to obtain a better understanding of how the transformer loading varies throughout the year, the yearly transformer loading for certain alternatives are presented.

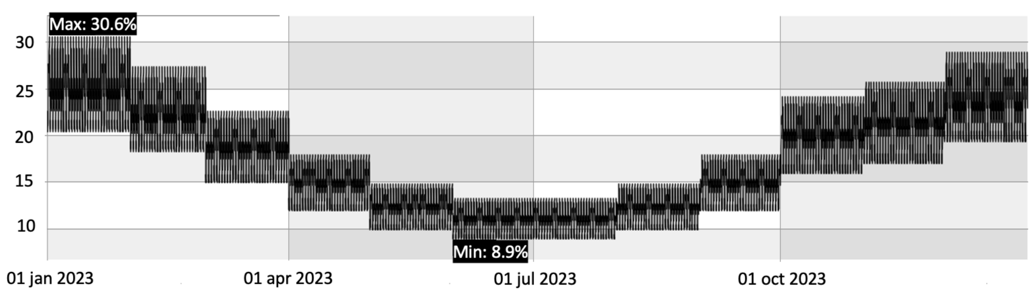


(a) Transformer 7

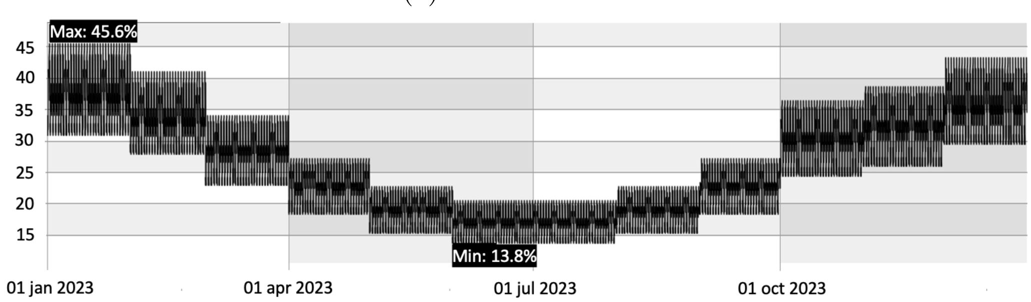


(b) Transformer 8

Figure 27: Transformer loading [%] for alternative 1, for year 2023.

In Figure 27, the transformer loading of the existing transformers, for alternative 1, are presented. At this point of time, in 2023, none of the seven buildings of Molobyen are constructed. Hence, the variation in loading is only due to existing loads in the area. As can be observed, the maximum loading for both transformers appear during the traditional high-loading period, i.e winter time. The maximum values, 30.6% and 45.6%, respectively, have already been listed in Table 16.

Moving forward, if only utilizing existing transformers to connect all buildings of Molobyen to grid, as suggested by alternative 4, the transformer loading becomes as in Figure 28. Here, it becomes clear that load demand during winter time, is no longer the cause of maximum transformer loading: Solar PV production is now the dimensioning factor. The maximum values observed in the plots have already been presented in Table 18. What this table does not show, however, is for how long the transformers are overloaded.

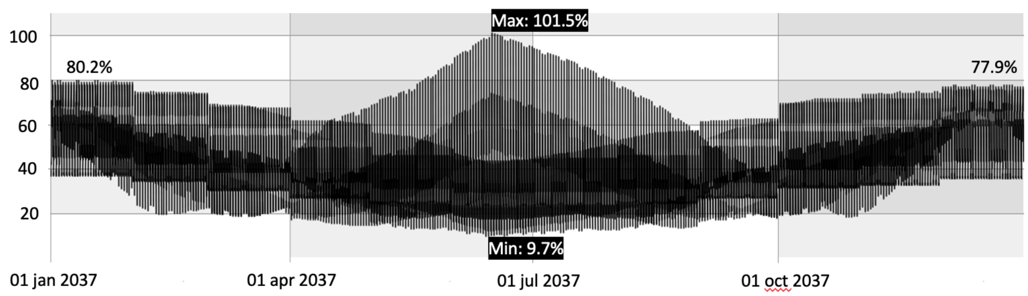


(a) Transformer 7

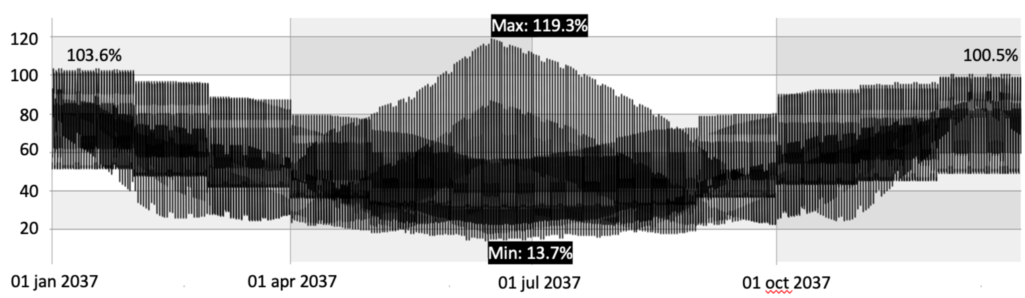


(b) Transformer 8

Figure 28: Transformer loading [%] for alternative 4, for year 2037.

To get an impression of for how long the transformers are overloaded, Figure 29 is provided. It is a more detailed version of Figure 28b, showcasing the day where the transformer experienced its heaviest overloading. As can be observed, although it is overloaded by almost 20%, this overload does not last for a substantial amount of time. The period, about 1.25 hours, is even acceptable, from an operational point of view. As stated by Arva, the maximum acceptable transformer loading, during operation, is set to (for short periods of time) 120%.

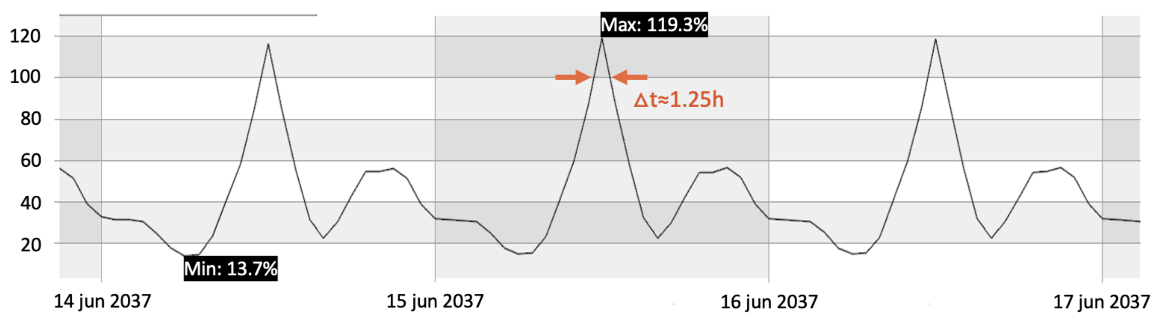


Figure 29: Loading [%] of transformer 8, in alternative 4, for year 2037. This is a more detailed version of Figure 28b.

Finally, to get an impression of the effect of upgrading the transformers, as suggested by alternative 5, Figure 30 is provided. Compared to alternative 4, in Figure 28, the maximum loading of both transformers have been reduced to well below 80%.

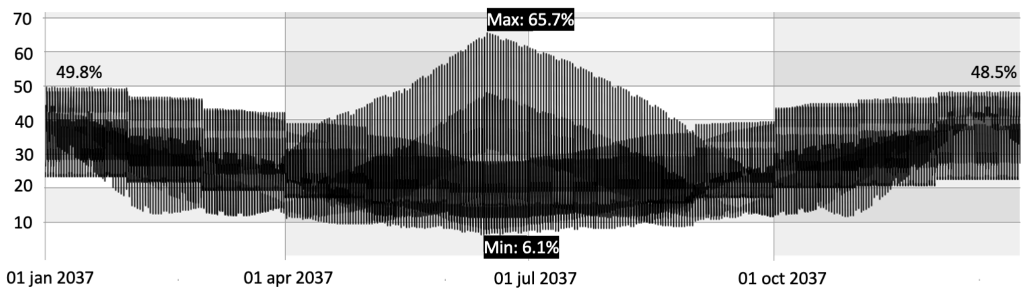


(a) Transformer 7

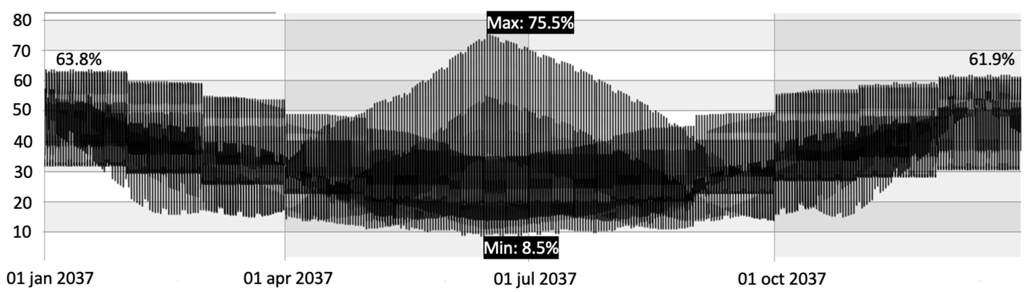


(b) Transformer 8

Figure 30: Transformer loading [%] for alternative 5, for year 2037.

## 6.3 Cost Evaluation

Using Equation (16), in Section 5.6.1, the investment cost of the different measures are calculated, and listed in Table 19. Note: If a measures does not include one of the cost elements listed in the equation, this element is set equal zero. The complete calculations are shown in Appendix E, Table 29.

Further, having mapped the yearly losses for the first and last year of the period for which the respective alternatives are valid, the yearly cost of losses, $K_{losses}$, can now be calculated. This is done according to Equations (19) and (20), in Section 5.6.2, and the results are listed in Table 20. Note: In the process of obtaining $K_{losses}$, also $k_{pekv}$ was calculated. These results are presented in Appendix F, Table 30. Also, in Appendix F, the values used for $k_p$ and $k_{wekv}$ are listed, see Table 31.

Table 19: Investment cost of the different measures.

| Measure | Cost [kNOK] | Measure | Cost [kNOK] |
|---|---|---|---|
| A | 173.374 | K | 134.846 |
| B | 44.579 | L | 35.837 |
| C | 152.826 | M | 87.329 |
| D | 71.600 | N | 115.778 |
| E | 57.674 | O | 845.144 |
| F | 77.679 | P | 596.584 |
| G | 78.332 | Q | 600.323 |
| H | 61.974 | R | 285.201 |
| I | 18.067 | S | 1042.457 |
| J | 38.513 | T | 118.014 |

Table 20: Yearly cost of losses, $K_{losses}$, calculated for all alternatives, for the first and last year of the respective intervals *Valid years*.

| Alt. | 2023 NOK/yr | 2024 NOK/yr | 2025 NOK/yr | 2026 NOK/yr | 2029 NOK/yr | 2030 NOK/yr | 2037 NOK/yr |
|---|---|---|---|---|---|---|---|
| 1 | 30 030.9 | - | - | - | - | - | - |
| 2 | - | 36 029.0 | 36 752.7 | - | - | - | - |
| 3 | - | - | - | 40 513.7 | 43 862.1 | - | - |
| 4 | - | - | - | - | - | 60 234.3 | 75 350.6 |
| 5 | - | - | - | - | - | 28 416.0 | 35 218.5 |
| 6 | - | - | - | - | - | 59 212.6 | 74 585.4 |
| 7 | - | - | - | - | - | 54 942.6 | 69 106.5 |
| 8 | - | 35 966.9 | 36 632.6 | - | - | - | - |
| 9 | - | - | - | 38 339.7 | 41 046.3 | - | - |
| 10 | - | - | - | - | - | 48 386.7 | 61 864.8 |
| 11 | - | - | - | - | - | 47 353.4 | 60 624.9 |
| 12 | - | - | - | - | - | 48 313.0 | 61 776.9 |

Some key considerations from this table, Table 20, are:

- The alternative with the lowest annual cost of losses is alternative 5. Again, this is because the voltage level is increased from $230V$ to $400V$ for all cables connected to substations 7 and 8.

- In general, for the years 2030-2037, the cost of losses are lower for the alternatives involving a new substation (Alt. 10-12), as compared to the ones utilizing existing substations and transformers (Alt. 4 and 6). In alternative 7, both existing and new substations are utilized, causing the cost of losses to be in between the costs for the aforementioned alternatives.

## 6.4 Socio-Economic Analysis

Having mapped the investment cost for each measure and the cost of losses for each alternative, DYNKO are utilized to obtain the total cost for each system solution, throughout the period on analysis. Some of the most important input parameters required for this optimization are listed below, along with some values:

- **Period of analysis**: 15 $years$.

- **Economic lifetime of measures**: Lifetime of measures including substations, transformers and cables chosen according to Svenska Elverksföreningen, through SINTEF Energi [43]: $L_{cable} = 35yr$, $L_{substations} = L_{transformers} = 25yr$. Lifetime of battery measures chosen based on discussion in Section 3.1: $L_{battery} = 15yr$.

- **Discount rate**: Chosen according to NVE's *Forenklede samfunnsøkonomiske vurderinger* [44]: 4.0%.

- **Investment cost for each measure**: Calculated in Section 6.3.

- **Yearly cost of losses for each alternative**: Calculated in Section 6.3.

- **Valid years for each alternative**: Chosen based on construction stages and listed in the last column of Table 8.

Running DYNKO, all possible system solutions are ranked from cheapest to most expensive, in Table 21, with all costs presented explicitly in Table 22. As in Section 6.2, the combination of alternatives (system solution) marked in green implies a maximum transformer loading of 80%, yellow implies a maximum transformer loading of 100%, and red implies a maximum transformer loading of 120%.

Table 21: All system solutions, ranked from cheapest (1) to most expensive (7).

| | Year | | | | | | | | | | | | | | |
|---|---|---|---|---|---|---|---|---|---|---|---|---|---|---|---|
| # | 23 | 24 | 25 | 26 | 27 | 28 | 29 | 30 | 31 | 32 | 33 | 34 | 35 | 36 | 37 |
| 1 | 1 | 2 | 2 | 3 | 3 | 3 | 3 | 4 | 4 | 4 | 4 | 4 | 4 | 4 | 4 |
| 2 | 1 | 2 | 2 | 3 | 3 | 3 | 3 | 5 | 5 | 5 | 5 | 5 | 5 | 5 | 5 |
| 3 | 1 | 2 | 2 | 3 | 3 | 3 | 3 | 6 | 6 | 6 | 6 | 6 | 6 | 6 | 6 |
| 4 | 1 | 2 | 2 | 3 | 3 | 3 | 3 | 7 | 7 | 7 | 7 | 7 | 7 | 7 | 7 |
| 5 | 1 | 8 | 8 | 9 | 9 | 9 | 9 | 10 | 10 | 10 | 10 | 10 | 10 | 10 | 10 |
| 6 | 1 | 8 | 8 | 9 | 9 | 9 | 9 | 12 | 12 | 12 | 12 | 12 | 12 | 12 | 12 |
| 7 | 1 | 8 | 8 | 9 | 9 | 9 | 9 | 11 | 11 | 11 | 11 | 11 | 11 | 11 | 11 |

Table 22: Costs of the different system solutions, from cheapest (1) to most expensive (7). Note: #1 refers to the system solution named #1 in Table 21; the same goes for #2, #3 and so on.

| # | Investment costs [kkr] | Cost of losses [kkr] | **Total [kkr]** | Annuity [kkr/yr] | Relative [%] |
|---|---|---|---|---|---|
| 1 | 265.1 | 574.1 | **839.2** | 75.5 | 100.0 |
| 2 | 541.1 | 392.0 | **933.1** | 83.9 | 111.1 |
| 3 | 395.0 | 569.4 | **964.4** | 86.7 | 114.8 |
| 4 | 481.8 | 544.8 | **1026.6** | 92.3 | 122.3 |
| 5 | 552.0 | 501.4 | **1053.5** | 94.7 | 125.4 |
| 6 | 607.0 | 501.0 | **1108.0** | 99.7 | 132.1 |
| 7 | 1022.0 | 495.6 | **1517.6** | 136.5 | 180.8 |

From these tables, Tables 21 and 22, some important considerations are:

- Although the system solution $1 - 2 - 3 - 4$ (#1) is by far the cheapest, it causes the transformer at substation 8 to operate at a loading of 119.3% in 2037, with the corresponding number for substation 7 being 101.5% (see Table 18). For substation 8, this is very close to what Arva considers acceptable during operation, i.e. 120% loading for short periods of time. Also, considering future growth in load demand or potential new installations of solar PV of the existing buildings in the area, this system solution appears to impose a high risk of violating the technical constraints. Hence, it should be considered discarded.

- System solution $1 - 2 - 3 - 5$ (#2) has an investment cost that is almost 40% larger than the third cheapest solution (#3), $1 - 2 - 3 - 6$, but as its cost of losses is by far the lowest of all system solutions, it comes out as the second cheapest solution. In addition, it ensures a maximum loading of 80%, throughout the period of analysis. Solution #3 targeted a maximum loading of 100%, but in 2037, the transformer at substation 8 violated this limit, with a maximum loading of 100.8%. As this system solution involves the use of batteries, in alternative 6, the simple solution to this is to increase the battery energy capacity, but this would make this system solution more expensive. Thus, based on the above, system solution $1 - 2 - 3 - 5$ is better than solution $1 - 2 - 3 - 6$, both in terms of technical and economic considerations.

- For system solutions $1-2-3-7$ (#4) and $1-8-9-10$ (#5), a new substation is constructed (subst. 9). The first has a lower investments cost, both due to the fact that the new transformer requires a lower capacity and that its time of investment can be delayed by six years (from 2024 to 2030). However, as this implies the use of existing substations (230V), the cost of losses area about 10% higher, as compared to solution #5. This leaves the total costs pretty similar, but as system solution #4 is both slightly cheaper, and ensures a maximum transformer loading of 80%, this is the preferable solution of these two.

- System solution $1-8-9-12$ (#6) and $1-8-9-11$ (#7) involves the use of batteries and a new substation. Although there is a slight reduction in the cost of losses, the investment costs become very high, making these system solutions the most expensive of the solutions investigated. In addition, from a technical point of view, system solutions #2, #3 and #4 can be considered better than, or equally good as, #6, while solutions #2 and #4 can be considered better than, or equally good as, #7.

### 6.4.1 Sensitivity Analysis: Battery Lifetime

As discussed in Section 3.1, there are uncertainties regarding the economic lifetime of batteries. From [34], an interval of 15-20 years was found realistic. For the above analysis, the more conservative number was chosen, and so the battery lifetime was set to 15 years. To investigate what impact this lifetime has on the results, a socio-economic analysis was also performed using the more optimistic lifetime of 20 years. This did, however, not affect the rank of the system solutions, as the rank remained as in Table 21. Regarding the costs, these were slightly altered, see Table 23. As can be observed, the investment cost of all system solutions involving batteries, here #3, #6 and #7, are reduced, but not to such an extent that they become cheaper than other, less expensive system solutions.

Table 23: Costs of the different system solutions, from cheapest (1) to most expensive (7). Note: #1 refers to the system solution named #1 in Table 21; the same goes for #2, #3 and so on. Battery economic lifetime is here set to 20 years.

| # | Investment costs [kkr] | Cost of losses [kkr] | **Total [kkr]** | Annuity [kkr/yr] | Relative [%] |
|---|---|---|---|---|---|
| 1 | 265.1 | 574.1 | **839.2** | 75.5 | 100.0 |
| 2 | 541.1 | 392.0 | **933.1** | 83.9 | 111.1 |
| 3 | 373.8 | 569.4 | **943.2** | 84.8 | 112.4 |
| 4 | 481.8 | 544.8 | **1026.6** | 92.3 | 122.3 |
| 5 | 552.0 | 501.4 | **1053.5** | 94.7 | 125.4 |
| 6 | 597.7 | 501.0 | **1098.7** | 98.8 | 130.9 |
| 7 | 951.0 | 495.6 | **1446.6** | 130.1 | 172.4 |

## 6.5 Overall Assessment and Ranking of Alternatives

From the considerations made in the previous sections, some conclusions can be drawn (see Tables 21 and 22):

- The construction of a new substation (subst. 9) imposes a large investments cost (new MV cable+substation), which is not justified by the reduction in cost of losses. In addition, a new substation will not manage to keep the maximum loading under 80%, nor under 100%, on its own. Hence, system solutions $1-8-9-10$ (#5), $1-8-9-12$ (#6) and $1-8-9-11$ (#7) are inferior, as compared to the solutions utilizing existing grid.

- Although system solution $1-2-3-4$ (#1) is the cheapest solution, it imposes a risk of future, unacceptable transformer loading. Hence, it seems reasonable to proceed with a more expensive system solution that reduces the maximum loading to below 80%. As such, system solution $1-2-3-5$ (#2) appears as the most promising solution. A high investment cost is required to upgrade the existing transformers (at subst. 7 and 8), but this is well justified by the reduction in cost of losses.

As such, based on the above results and discussion, the optimal construction plan becomes:

*2024:*

A. 2 LV cables from subst. 7 to LB1A-1
B. 2 LV cables from subst. 7 to LB1A-2

*2026:*

C. 2 LV cables from subst. 8 to LB1B-1

*2030:*

D. 2 LV cables from subst. 7 to LB2-1
E. 2 LV cables from subst. 7 to LB2-2
F. 2 LV cables from subst. 8 to LB2-3
G. 2 LV cables from subst. 8 to LB2-4
O. Upgrade transformers at subst. 7 and 8 to 1250 and 800kVA, resp.

This yields a total cost, within the period of analysis, of **933.1 kkr**.

# 7 General Evaluation of Results and Framework

This section provides general considerations regarding the final results and the grid planning framework utilized. More detailed evaluations of the results were presented together with the results, in Section 6. Ultimately, the major limitations deteriorating the results, are listed.

## 7.1 Final Results

System solution $1-2-3-5$ (#2) appears as the most promising solution, considering the combination of technical and socio-economic factors. This involves utilizing the existing transformers in the area for the first two construction stages, while upgrading these transformers in 2030 to handle the last construction stage. A large investment cost is required for this system solution, but this is justified by the reduction in cost of losses. The main reason for this reduction, is the increase in operating voltage level, from $230V$ to $400V$, of the cables connected to existing loads. This illustrates the value of operating with a higher voltage level.

Some other considerations related to the results are provided below:

- **The investment cost of batteries is too high**: Utilizing batteries as a permanent solution to handle the increase in load demand and PV production, does not appear to be an ideal solution. In this case, the more "traditional" solution of upgrading existing transformers proved to be better, both from a technical and economic perspective. Further, the optimal system solution of those considering batteries, was solution $1-2-3-6$ (#3). As alternative 6 involves installing a BESS at two different locations, the installation costs, and hence investment costs, can be expected to be higher for this alternative, as compared to the other alternatives considering batteries (alt. 11 and 12). This is not accounted for in the economic analyses, and an inclusion of this may deteriorate the current rank of system solution $1-2-3-6$ (#3).

- **Including interruption costs should prove beneficial for battery alternatives**: The cost of energy not supplied is not considered quantitatively, but it could be expected that the battery alternatives could see these costs being reduced: If an outage occurs, a fully charged battery could supply end-users that otherwise would have been affected by this outage.

- **Power rating of batteries**: The cost of batteries have been considered to be a function of the energy capacity rating, hence the power rating can be, and is, chosen arbitrary for the benefit of the model. Here, all batteries have had their power rating chosen "equal" to the energy capacity rating (e.g. 0.53MW/0.53MWh). This is a simplification, as the actual cost of BESSs depends on both energy capacity and power rating. A more realistic battery cost function may cause an increase in the costs. At the same time, in most of the simulated cases, the power rating can be heavily reduced without affecting the results, in terms of reduction in maximum power flow to and from the grid. Hence, it is not known to what extent a more realistic model would affect the current results.

- **Different operating voltages**: For the alternatives using both existing transformers and a new transformer, certain buildings will be connected to the grid through cables having an operating voltage of 230V, while for others the operating voltage will be 400V. This is because new and old cables connected to existing transformers will have an operating voltage of 230V, while the cables connected to a new transformer will be operated at 400V. As 400V is typically utilized for new installations, using 230V should be avoided, if possible.

## 7.2 Planning Framework

The planning framework used, presented in Figure 8, combines elements from the traditional passive grid planning framework, in Figure 3, and from the research-based active grid planning framework, in Figure 5. Hence, certain parts of the framework used should fit the current practice of grid companies, while other parts could represent something new. Particularly, the inclusion of batteries as active measures should be highlighted, as this is a significant part of planning of active distribution networks.

This, and other (potentially) new elements, are summarized below:

- **Load and generation modelling through time series**: Load demand and PV generation were modelled using time series, with hourly values for an entire year. This is opposed to a more traditional approach, considering only the worst-case operating states: the case of maximum demand with no generation and the case of minimum demand with maximum generation.
- **Active measures (batteries)**: The use of active measures (here: batteries) for handling the increased load demand and PV generation, are considered as potential solutions to the grid planning problem. This is very much opposed to traditional grid reinvestments.
- **Battery optimal dispatch model**: As the use of batteries are considered, a model capturing the operational benefits of batteries was developed. The model itself is based around battery optimal dispatch, with an objective of providing load levelling.
- **(Technical analysis) Simulating operation for entire years**: By utilizing the module "Timesanalyse" (or "hourly analysis") within NETBAS, power flow analyses were run for entire years, with the results being on an hourly format. One of the main advantages of this, is that the actual yearly energy losses can be obtained. Hence, there is no need to use estimated values for utilization time for losses when calculating the cost of losses.
- **Calculation of cost of losses**: For several alternatives, high PV production was the cause of maximum transformer loading. As discussed in Section 5.6.2, when this is the case, the cost of maximum power losses, $k_p$, should be scaled down. This is a new approach, as compared to the traditional approach of utilizing the formula in Equation (17), no matter the case.

## 7.3 Limitations

Some considerations should also be made regarding potential limitations impacting the quality of the results. These are summarized below:

- **Expected load demand and PV production**: All results are based on the expected load demand and PV production from the energy system analysis [13]. The actual validity of these numbers are not investigated in this work, as it is outside of the scope of this thesis. Anyhow, there is a certain uncertainty related to the future load demand and PV production, hence a more probabilistic approach to the modelling of these should be considered.

- **Replication of PV and load**: The replication of PV and load in NETBAS do manage to capture the peak power sent to and from the grid, each month. However, information on the daily variation in PV production is lost. This is due to NETBAS only allowing a change in the installed PV capacity, along with the maximum and minimum production for each month of the year. The main issue with this is that the PV production will appear very consistent and predictable, comparable to a normal distribution. I.e. during the summer, it will appear as there is an increasing amount of power sent back to the grid each day, until the yearly peak is reached, from where it decreases by a small amount each day. In reality, however, the power sent back to the grid may be at its monthly maximum one day, but the next day it may be reduced to almost zero, due to cloudy weather. Hence, in NETBAS, it will appear as there is a higher frequency of very large power flows to the grid, than there is in reality. This will make for increased energy losses, making the values listed in Table 17 and 18, artificially high. This is especially prominent for alternatives including batteries, as the stable power flows caused by load levelling will not be perfectly replicated in NETBAS.

- **Degradation of batteries**: For the technical analyses, battery degradation is not considered. As degradation causes the available battery capacity to be reduced over time, the battery alternatives defined may be slightly over-performing, as compared to reality. To circumvent this limitation, the battery capacity could have been reduced by e.g. 1 or 2%, each year of operation.

- **Model for battery optimal dispatch**: Several models for battery optimal dispatch were developed and tested in order to obtain a final well-functioning model. Whether or not this is the best possible model, in terms of achieving the objective defined for the utilization of batteries, is not known. The objective was defined as minimizing power flows to and from the grid, in Section 5.4. Hence, the battery model represents a potential limitation.

- **General uncertainty regarding investment costs**: The investment costs related to the different alternatives are mainly based on values found in [6]. These numbers should be reliable, but there is a significant uncertainty related to the investment cost of alternatives including batteries; both with regards to the current price and to the future price.

# 8 Conclusion and Future Work

## 8.1 Conclusion

In this work, the grid connection of an area to be developed, in Bodø, has been investigated. A grid planning framework combining elements from the traditional passive grid planning and from research-based active grid planning frameworks, has been established and utilized. The major new elements included, as compared to the traditional framework, are:

- active measures, in terms of batteries,
- the use of time series, both for load and generation modelling and for power flow analyses, and
- the approach for calculating cost of losses.

In addition, a model for battery optimal dispatch was developed, in order to capture the operational benefits of batteries. All these elements could be adopted in the current grid planning process of grid companies, although the use of optimization may need some time to mature before it becomes viable.

Further, different alternatives for grid connection of the given area were defined, and technical and socio-economic analyses performed, in order to obtain an optimal system solution. The use of BESSs were promising, as these were very capable of reducing maximum power sent back to the grid, from the solar PVs. However, the optimal system solution did not include the use of BESSs. Although the most promising solution involving batteries ($1-2-3-6$ (#3)) was only about 3% more expensive than the optimal solution ($1-2-3-5$ (#2)), it suffered from not being capable of reducing transformer loading to below 80%. Hence, the more traditional approach of upgrading existing transformers, appeared as a better solution than installing batteries, both from a technical and economic perspective.

Two of the major limitations of this work, are the absence of quantitative considerations regarding interruption costs and the loss of information in the process of replicating load demand and PV generation. As discussed in the previous section, both these limitations are affecting alternatives involving batteries in a negative manner. If the time series from MATLAB could have been used directly in NETBAS and interruption costs were considered, all system solutions involving batteries could have increased their respective rank, in Table 21. At the same time, not including battery degradation affects the battery in a positive manner, but whether or not this counteracts the negative impact of the other limitations, is not known.

## 8.2 Future Work

Ultimately, some suggestions for future work are presented. The suggestions include both elements that would improve the framework used and elements that would increase the quality of the results. These are listed below:

- **Probabilistic load and generation modelling:** The load demand and PV generation are assumed to be exactly as given in the time series from the energy system analysis [13]. Although this can be seen as a step towards a more active distribution grid planning, if compared to only considering worst-case operating conditions, it remains a deterministic approach to load and generation modelling. To avoid dimensioning the grid with respect to operating situations that are potentially not likely to occur, a more probabilistic approach should be considered utilized.

- **Risk analysis:** By including the probability of outcomes and their potential consequences, in the technical analyses, risk analyses could be performed.

- **New cases:** Through talks held with BE Varme, it became apparent that district heating was expected to cover the area's heat demand. Hence, this is assumed to be true. However, it could be interesting to consider a supply situation where district heating is not utilized at all. This could reduce the maximum power fed back to the grid, due to an increased load demand. Also, a case considering optimal interaction between the district heating network and the electricity grid, could make for interesting findings. For instance, in times of high solar PV production, the solar PV could be allowed to also cover some of the heating and cooling demand (originally covered by DH), to reduce the power fed back to the grid.

- **More alternatives:** Additional alternatives could be investigated in order to improve the probability of finding the optimal system solution. For instance, if reliability is considered, the use of two new substations could be included as an alternative. This would reduce the expected cost of energy not supplied, particularly if operated in a mesh network. In addition, while a single new substation did not even manage to keep the maximum transformer loading below 100%, two new substations would certainly reduce the loading to well below 80%.

- **Investigate alternatives for load and PV replication:** To avoid losing any information, the data sets from MATLAB should be used directly as input to the technical analyses. This can potentially be done in NETBAS, but an alternative may be performing the power flow analyses in another software, such as MATLAB or Python.

- **Investigating reliability:** Interruption costs are not considered quantitatively. As this is an important element in order to obtain an optimal socio-economic solution, it should be included before actually implementing any measures.

- **Reverse power flow:** As the PV production is causing power to be fed back to the grid, it is essential to ensure that the grid can handle reverse power flows. For instance, it must be ensured that circuit breakers are capable of handling bidirectional power flows.

# References

[1] S. Klyapovskiy, S. You, H. Cai, and H.W. Bindner. Incorporate flexibility in distribution grid planning through a framework solution. *International Journal of Electrical Power & Energy Systems*, vol. 111: pp. 66–78, 2019.

[2] I. B. Sperstad, E. Solvang, and O. Gjerde. Framework and methodology for active distribution grid planning in norway. In *2020 International Conference on Probabilistic Methods Applied to Power Systems (PMAPS)*, pages 1–6, 2020.

[3] I. B. Sperstad. *Framework and methodology for active distribution grid planning in Norway*, CINELDI/SINTEF Energy Research, Trondheim, Project memo, 2020.

[4] E. Tønne. *Planning of the Future Smart and Active Distribution Grids*. PhD thesis, Department of Electric Power Engineering, Norwegian University of Science and Technology, Trondheim, 2016.

[5] F. Pilo, S. Jupe, F. Silvestro, C. Abbey, A. Baitch, B. Bak-Jensen, C. Carter-Brown, G. Celli, K. El Bakari, M. Fan, P. Georgilakis, T. Hearne, L. Ochoa, G. Petretto, and J. Taylor. *Planning and optimization methods for active distribution systems*. CIGRE WG C6.19, 2014.

[6] SINTEF Energi AS. *Planleggingsbok for kraftnett: Kostnadskatalog distribusjonsnett*, 2019.

[7] I. B. Sperstad, M. Istad, H. Sæle, M. Korpås, I. Oleinikova, S. Hänninen, S. Motta, K. Panagiotou, C. Papadimitriou, V. Efthymiou, C. Træholt, and M. Marinelli. Cost-benefit analysis of battery energy storage in electric power grids: Research and practices. In *Proceedings of 2020 IEEE PES International Conference and Exhibition on Innovative Smart Grid Technologies*, United States, 2020. IEEE. 2020 IEEE PES Innovative Smart Grid Technologies Europe, IEEE-PES-ISGT-Europe 2020 ; Conference date: 25-10-2020 Through 28-10-2020.

[8] R. Li, W. Wang, Z. Chen, J. Jiang, and W. Zhang. A review of optimal planning active distribution system: Models, methods, and future researches. *Energies*, 10(11), 2017.

[9] K. Sand, K. Berg, A. Hammer, and K. Ingebrigtsen. Veileder for kost/nytte-vurderinger ved integrasjon av batteri i distribusjonsnettet. SINTEF Energi AS, 2020.

[10] Schmidt Hammer Lassen (SHL) Architects. *Bodø Masterplan/Molokvartalet/*. Available: https://bodo.kommune.no/getfile.php/1312352-1560430843/Plan%2C%20bygg%20og%20 eiendom/Kart%20og%20arealplaner/Arealplaner/Områdeplan/Utviklingsområde%20Vest/Bodø%20booklet_FINAL_screen.pdf [Accessed on 07.12.2020].

[11] FME ZEN. *New city – new airport, Bodø*. Available: https://fmezen.no/airport-redevelopment-bodo/ [Accessed on 06.12.2020].

[12] Bodø Kommune. *Fjernvarme*. Available: https://bodo.kommune.no/fjernvarme/category3193.html [Accessed on 06.12.2020].

[13] J. Clauss. *ZEN WP3.3 Energy system analysis Breivika Vest in Bodø*. FME ZEN, 2020.

[14] EQUA. *IDA Indoor Climate and Energy*. Available: https://www.equa.se/en/ida-ice [Accessed on 06.12.2020].

[15] American Society of Heating, Refrigerating and Air-Conditioning Engineers. *International Weather for Energy Calculations, v 2.0*. Available: https://www.ashrae.org/technical-resources/bookstore/ashrae-international-weather-files-for-energy-calculations-2-0-iwec2 [Accessed on 06.12.2020].

[16] E. Øye. *Results from summer researcher project related to pilot Utviklingsområde Breivika Vest*, CINELDI/SINTEF Energy Research, Trondheim, Project memo, 2020.

[17] SINTEF Energi AS. *Planleggingsbok for kraftnett: Systematikk ved planlegging av kraftnett*, 2010.

[18] Olje og energidepartementet. *Forskrift om produksjon, omforming, overføring, omsetning, fordeling og bruk av energi m.m. (energilovforskriften)*. 1990.

[19] H. B. Gooi. Class Lecture, Topic: "Network Applications Functions". EE6510, Nanyang Technological University, Singapore, 2019.

[20] M. Albadi. *Power Flow Analysis*. 2019.

[21] IEC. *Quality of the electricity supply*. Available: `http://www.electropedia.org/iev/iev.nsf/display?openform&ievref=617-01-07` [Accessed on 05.12.2020].

[22] NVE. *Quality of electricity supply*. Available: `https://www.nve.no/norwegian-energy-regulatory-authority/network-regulation/quality-of-electricity-supply/` [Accessed on 05.12.2020].

[23] NVE. *Forskrift om leveringskvalitet i kraftsystemet*. Available: `https://lovdata.no/dokument/SF/forskrift/2004-11-30-1557` [Accessed on 05.12.2020].

[24] K. Sand. 2008 Norwegian quality of supply survey - State of art and reported needs. *Renewable Energy and Power Quality Journal*, 1, 2010.

[25] NVE. *Omfang av henvendelser om leveringskvalitet*. Available: `http://publikasjoner.nve.no/rapport/2018/rapport2018_39.pdf` [Accessed on 05.12.2020].

[26] *EN50160 Voltage characteristics of electricity supplied by public electricity networks*, CENELEC, 2010.

[27] M. Larruskain, I. Zamora, O. Abarrategui, A. Iraolagoitia, M. Gutiérrez, E. Loroño, and F. Bodega. Power transmission capacity upgrade of overhead lines. *Electricity Today*, 19, 01 2007.

[28] L. C. Nichols. Effect of overloads on transformer life. *Electrical Engineering*, 53(12):1616–1621, 1934.

[29] M. Z. Degefa, H. Sæle, J. A. Foosnæs, and E. Thorshaug. Seasonally variant deployment of electric battery storage systems in active distribution networks. In *24th International Conference and Exhibition on Electricity Distribution : CIRED 2017 - Proceedings*. IET Digital Library, 2017.

[30] X. Luo, J. Wang, M. Dooner, and J. Clarke. Overview of current development in electrical energy storage technologies and the application potential in power system operation. *Applied Energy*, 137:511–536, 2015.

[31] Neoen. *Hornsdale Power Reserve: Our vision*. Available: https://hornsdalepowerreserve.com.au/our-vision/ [Accessed on 06.04.2021].

[32] H. Chen, T. N. Cong, W. Yang, C. Tan, Y. Li, and Y. Ding. Progress in electrical energy storage system: A critical review. *Progress in Natural Science*, 19(3):291–312, 2009.

[33] Bloomberg New Energy Finance. *Battery Pack Prices Fall As Market Ramps Up With Market Average At $156/kWh In 2019*. Available: https://about.bnef.com/blog/battery-pack-prices-fall-as-market-ramps-up-with-market-average-at-156-kwh-in-2019/ [Accessed on 13.04.2021].

[34] Z. Shahan. *Tesla Megapack, Powerpack, & Powerwall Battery Storage Prices Per KWh — Exclusive*. Available: https://cleantechnica.com/2020/10/05/tesla-megapack-powerpack-powerwall-battery-storage-prices/ [Accessed on 13.04.2021].

[35] Bloomberg New Energy Finance. *Battery Pack Prices Cited Below $100/kWh for the First Time in 2020, While Market Average Sits at $137/kWh*. Available: https://about.bnef.com/blog/battery-pack-prices-cited-below-100-kwh-for-the-first-time-in-2020-while-market-average-sits-at-137-kwh/ [Accessed on 13.04.2021].

[36] J. Fernando. *Volume Weighted Average Price (VWAP) Definition*. Available: https://www.investopedia.com/terms/v/vwap.asp [Accessed on 14.04.2021].

[37] J. Nocedal and S. J. Wright (1999). *Numerical Optimization*. New York, Springer.

[38] NVE. *Kraftsystemdata*. Available: nve.no/energiforsyning/energiforsyningsdata/kraftsystemdata/ [Accessed on 02.12.2020].

[39] Volue. *Powel Netbas*. Available: powel.com/electric-utility/assets/Netbas [Accessed on 02.12.2020].

[40] MathWorks. *What is MATLAB?*. Available: https://www.mathworks.com/discovery/what-is-matlab.html [Accessed on 08.06.2021].

[41] E. Solvang. Class Lecture, Topic: ”Systematikk ved planlegging av kraftnett”. ELK-11, Norwegian University of Science and Technology, Trondheim, 2020.

[42] SINTEF Energi AS. *Planleggingsbok for kraftnett: Tapkostnader (2019)*. Available: https://www.ren.no/doc/api/rest/download/fef/2373b1ba-b807-4470-b36f-8bf89742ed2a?filename=Tapskostnader.pdf.

[43] SINTEF Energi. *Analyse ved vedlikeholds- og fornyelsesbehov*. Available: https://www.ren.no/doc/api/rest/download/fef/a8aa1b56-24ca-44a1-9c4a-7a838d21f24d?filename=Analyse%20av%20vedlikeholds-%20og%20fornyelsesbehov.pdf [Accessed on 02.06.2021].

[44] NVE. *Forenklede samfunnsøkonomiske vurderinger*. Available: https://www.nve.no/energiforsyning/nett/kraftsystemutredninger/veiledningsmateriale/forenklede-samfunnsokonomiske-vurderinger/ [Accessed on 02.06.2021].

[45] J. Machowski, J.W. Bialek, and J.R. Bumby (2008). *Power System Dynamics: Stability and Control*. John Wiley & Sons.

[46] G. Parkinson. *Revealed: True cost of Tesla big battery, and its government contract*. Available: https://reneweconomy.com.au/revealed-true-cost-of-tesla-big-battery-and-its-government-contract-66888/ [Accessed on 06.04.2021].

# Appendix

## A The Power Flow Problem

All electrical networks consist of several interconnected transmission lines and transformers. The combination of these different models can be used to model the whole network through the nodal network equation, Equation (23) [45].

$$\begin{bmatrix} \underline{I}_1 \\ \vdots \\ \underline{I}_i \\ \vdots \\ \underline{I}_N \end{bmatrix} = \begin{bmatrix} \underline{Y}_{11} & \cdots & \underline{Y}_{1i} & \cdots & \underline{Y}_{1N} \\ \vdots & \ddots & \vdots & & \vdots \\ \underline{Y}_{i1} & \cdots & \underline{Y}_{ii} & \cdots & \underline{Y}_{iN} \\ \vdots & & \vdots & \ddots & \vdots \\ \underline{Y}_{N1} & \cdots & \underline{Y}_{Ni} & \cdots & \underline{Y}_{NN} \end{bmatrix} \begin{bmatrix} \underline{V}_1 \\ \vdots \\ \underline{V}_i \\ \vdots \\ \underline{V}_N \end{bmatrix} \tag{23}$$

Here, suffices $i$ and $j$ represent the node numbers, $N$ the total number of nodes in the network, $\underline{V}_i$ the voltage at node $i$, $\underline{I}_i$ the current injection at node $i$, $\underline{Y}_{ij}$ the mutual admittance between nodes $i$ and $j$, and $\underline{Y}_{ii}$ the self-admittance of node $i$.[45]

From this, the active ($P_i$) and reactive power ($Q_i$) injected at node $i$, are found to be:

$$\begin{aligned} P_i &= V_i^2 Y_{ii} cos\theta_{ii} + \sum_{j=1;j\neq i}^{N} V_i V_j Y_{ij} cos(\delta_i - \delta_j - \theta_{ij}), \\ Q_i &= -V_i^2 Y_{ii} sin\theta_{ii} + \sum_{j=1;j\neq i}^{N} V_i V_j Y_{ij} sin(\delta_i - \delta_j - \theta_{ij}), \end{aligned} \tag{24}$$

where $\delta$ and $\theta$ are defined through the node voltage and mutual admittance, respectively, as $\underline{V}_i = V_i \angle \delta_i$ and $\underline{Y}_{ij} = Y_{ij} \angle \theta_{ij}$. These equations, Equation (24), are the ones governing the flow of power through the many parallel routes between generators and loads, of the meshed transmission networks. The inputs of this power flow problem, are the set of load and generation data. Now, due to the non-linearity of Equation (24), iterative methods, such as the Gauss-Seidel method or the Newton-Raphson method, must be applied to find the solution; namely the voltage magnitude and angle at the different system nodes. Further, these results can be used to obtain all other relevant system quantities, including real and reactive power flows, power losses, and voltage drops.[45]

## B System Boundary of Planning Study

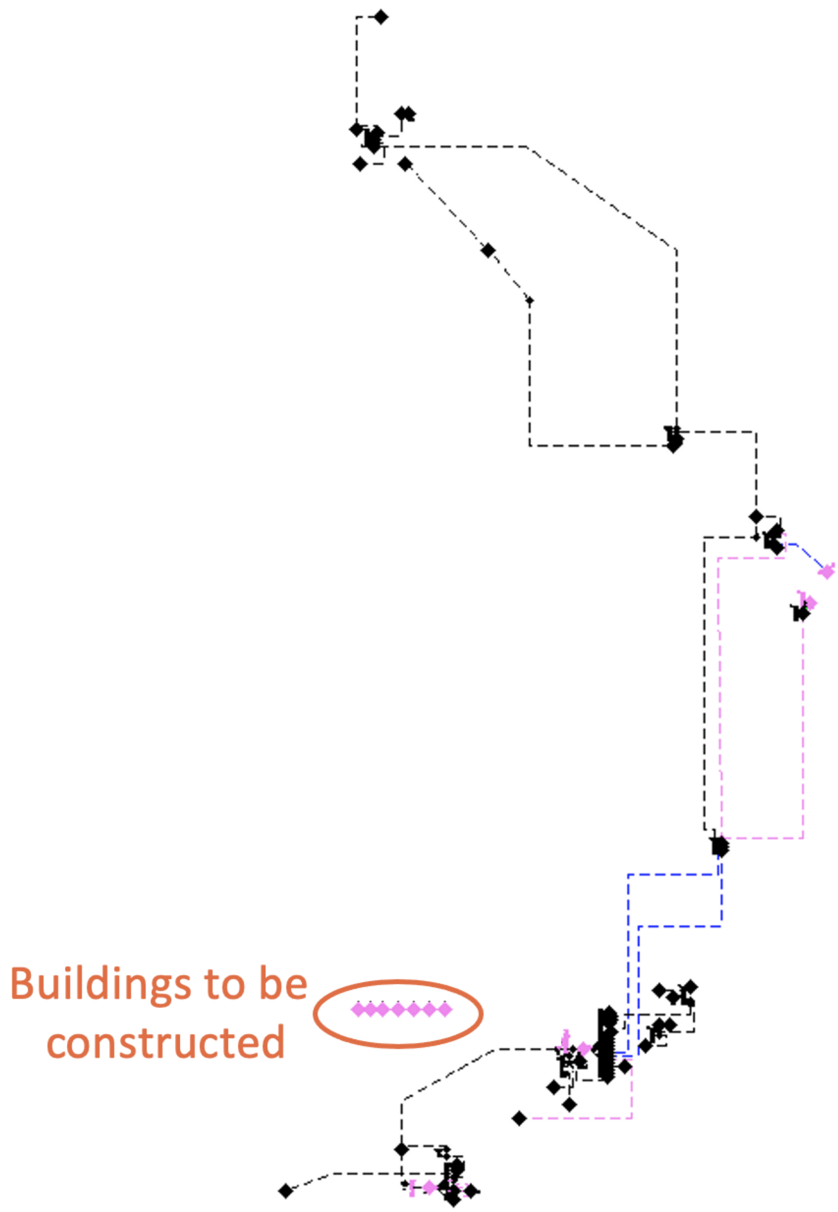


Figure 31: System boundary of the planning study (screenshot from NETBAS). See also the zoomed-in version in Figure 10.

# C Battery Optimal Dispatch Model

In the following, first, the initial model will be presented. Then, the most important iterations, and alterations, on the way to obtaining the final model are summarized. The final model was presented in Section 5.4.1. Ultimately, some considerations regarding the auxiliary variable and regarding the process of replicating PV and load, are provided.

## C.1 Initial Battery Optimal Dispatch Model

In order to develop a model for the battery optimal dispatch, the non-linear programming model presented in [29] has been used as an inspiration. This model has been altered to fit the purpose of the situation of Molobyen, with the major difference being that it is has been reformulated as a linear programming model. Another motivation behind this change is simplicity and reduced computational efforts.

The decision variables defined for the model are listed in Table 24 and illustrated in Figure 32. Note: $x_7(t)$ is also defined for $t = 25$, due to the formulation of the constraints.

Table 24: Decision variables.

| Variable | Description | Set of $x_i(t)$ | Unit |
|---|---|---|---|
| $x_1(t)$ | Grid to load | $\{x_1(t)\|t \in \mathbb{N}, 1 \leq t \leq 24\}$ | Wh/h |
| $x_2(t)$ | Grid to batt. | $\{x_2(t)\|t \in \mathbb{N}, 1 \leq t \leq 24\}$ | Wh/h |
| $x_3(t)$ | PV to load | $\{x_3(t)\|t \in \mathbb{N}, 1 \leq t \leq 24\}$ | Wh/h |
| $x_4(t)$ | PV to batt. | $\{x_4(t)\|t \in \mathbb{N}, 1 \leq t \leq 24\}$ | Wh/h |
| $x_5(t)$ | PV to grid | $\{x_5(t)\|t \in \mathbb{N}, 1 \leq t \leq 24\}$ | Wh/h |
| $x_6(t)$ | Batt. to load | $\{x_6(t)\|t \in \mathbb{N}, 1 \leq t \leq 24\}$ | Wh/h |
| $x_7(t)^*$ | Batt. stored | $\{x_7(t)\|t \in \mathbb{N}, 1 \leq t \leq 25\}$ | Wh/h |
| $x_8(t)$ | Aux. var.: Max. min. PF | $\{x_8(t)\|t \in \mathbb{N}, 1 \leq t \leq 24\}$ | Wh/h |

$^*$As the time step is one hour, the "actual" unit of $x_7(t)$ is $Wh$.

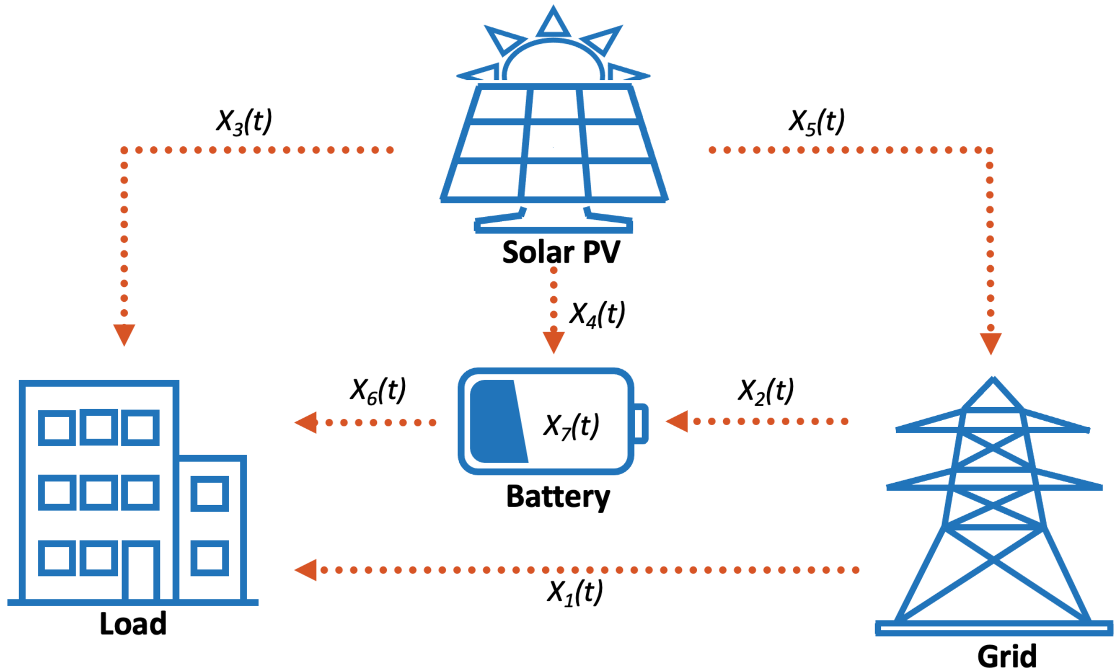


Figure 32: Supply topology of Molobyen with decision variables included.

The model itself is defined below, through Equations (25)-(35). The constants in the model, $\eta$, $\alpha$ and $\gamma$, are defined in Table 10. The auxiliary variable, $x_8(t)$, will always be set equal to the maximum power flow in the system, i.e. the power to or from the grid, due to how the auxiliary constraints, Equations (34) and (35), are defined. The auxiliary variable was explicitly presented in Section 5.4.1, under the name $x_9(t)$.

**Objective function:** ***Reduce power flows to and from grid***

$$min \sum_{t=1}^{24} x_8(t) \tag{25}$$

**Constraints and boundaries**:

A. *Battery stored energy conservation*

$$\eta \cdot x_2(t) + \eta \cdot x_4(t) - \frac{1}{\eta} \cdot x_6(t) + x_7(t) = x_7(t+1), \qquad 1 \le t \le 24 \tag{26}$$

B. *PV output and load conservation*

$$x_3(t) + x_4(t) + x_5(t) = PV(t), \qquad 1 \le t \le 24 \tag{27}$$

$$x_1(t) + x_3(t) + x_6(t) = L(t), \qquad 1 \le t \le 24 \tag{28}$$

C. *Battery max. and min. storage limits*

$$x_7(t) \le \alpha \cdot B_{max}, \qquad 1 \le t \le 25 \tag{29}$$

$$x_7(t) \ge \gamma \cdot B_{max}, \qquad 1 \le t \le 25 \tag{30}$$

D. *Initial stored battery energy*

$$x_7(t) = Bprevday, \qquad t = 1 \tag{31}$$

E. *Battery maximum power constraint*

$$x_6(t) \le P_{max}, \qquad 1 \le t \le 24 \tag{32}$$

$$x_2(t) + x_4(t) \le P_{max}, \qquad 1 \le t \le 24 \tag{33}$$

Aux.: *Auxiliary constraints for peak shaving*

$$x_1(t) + x_2(t) \le x_8, \qquad 1 \le t \le 24 \tag{34}$$

$$x_5(t) \le x_8, \qquad 1 \le t \le 24 \tag{35}$$

All decision variables do also have a lower boundary of zero.

## C.2 Battery Optimal Dispatch Model: Iterations and Alterations

In order to obtain a well-functioning model for battery optimal dispatch, the initial model presented in the previous section had to undergo several alterations. In the following, the major iterations on the way to the final model are presented, including why the different versions of the model appeared promising, as well as potential errors with the respective versions.

- **Initial model: LP with eight decision variables:** This model was presented explicitly in Section C.1. For the initial simulations and tests, to avoid any battery size-related problems, a very large battery was chosen: a $10MW/100MWh$ Li-ion battery. This approach revealed promising results in the beginning: The model converged and the power sent back to the grid was reduced to zero. However, as socio-economic considerations are to be made when deciding upon what measures to initiate, it would not be worth considering to install batteries of such sizes. For instance, in terms of capacity, this battery would to be comparable to the Hornsdale Power Reserve ($100MW/129MWh$). Located in Australia, it aims to "stabilise the South Australian electricity grid, facilitate integration of renewable energy in the State and reduce the chance of load-shedding events" [31]. The aim of the energy storage system of Molobyen should, to a certain extent, facilitate integration of renewable energy (solar PV), but it will not contribute to e.g. stabilising the county of Nordland. In addition, the cost of the Hornsdale Power Reserve project was an estimated €56 *million*, in 2017 [46].

  As such, the battery size was reduced for further testing of the model. This did, however, cause the battery to reach its capacity limit in the early hours each day, due to the large PV production. Further, as the load demand is quite low, the battery was unable to discharge much of its energy before the hours of peak PV production. This made the battery incapable of making any actual impact on the power peaks.

- **LP with nine decision variables:** To circumvent the problem of having an almost fully-charged battery at all times, the battery was also allowed to dispatch its energy back to the grid. As such, the battery was given the opportunity of discharging during night time, hence increasing its free capacity, in order to handle the worst peak power flows appearing in the middle of the day. Mathematically, to obtain such a behavior, either $x_2$ could be allowed to be negative or a new decision variable could be defined. To avoid having to redefine the auxiliary constraints, a new decision variable was defined, $x_8(t)$. Again, this represents the power flow from the battery to the grid. The auxiliary variable from the original model, named $x_8(t)$, was renamed to $x_9(t)$. To a certain extent, this did resolve the problem, but an underlying problem regarding the objective function revealed itself. When minimizing the sum of the auxiliary variable, $x_9(t)$, the peak power flow is not necessarily being minimized. Such an objective function would rather minimize the *energy* sent over the grid, each day. For instance, if the optimal objection function value for a given day is 24, the model will not care whether this is split equally over each time step or divided unequally: i.e. whether $x_9(t)$ is set to 1 for all 24 time steps, or set to 0 for the twelve first time steps and to 2 for the last twelve. This could cause the peak power flow over the grid not to be reduced at all.

- **QP with nine decision variables (1):** In order to penalize such a behaviour, the model was reformulated as a quadratic programming (QP) problem. Using the example above, the sum of $x_9(t)$ squared would become 24 for the case where $x_9(t) = 1$ for all 24 time steps, as compared to 48 for the other case. As such, load levelling, and hence a reduction in the maximum power flows, would be achieved.

- **Final model: QP with nine decision variables (2):** Initially, this did seem to resolve all problems. When running tests, having connected all loads and solar PVs to one transformer and a rather large battery, the model did converge and the results revealed no logical errors. However, when running tests utilizing smaller batteries, another issue was revealed: As the objective is to minimize the power flows over the grid, the model will find it beneficial to curtail some of the PV production at times where the production is higher than the load and the battery is fully charged. With no curtailment variable having been defined, directly curtailing the PV production will not be allowed. Hence, the model chooses to supply the load with power from the solar PVs by sending it through the battery, charging and discharging it at the same time step, rather than directly from the PV panels. As such, the power sent back to the grid will be reduced, due to power losses caused by charging and discharging the battery.

The major issue with such a behaviour, is that the battery is being forced to charge and discharge at the same time step. As this is not possible, the model must be modified in a way to punish such a behaviour. This is done through adding the term $k \cdot [x_6(t-1) + x_6(t) + x_8(t-1) + x_8(t)]$ to the objective function, where $k$ is chosen as a very high number (here: $10^7$). As the unwanted behaviour only occurred during times where the PV production surpassed the load demand, the condition $PV(t) > 0.95 \cdot Load(t)$ must be met, in order for the new term to be added. The qualitative interpretation of this modification is that the battery is prevented from discharging energy during times where the PV production surpasses the load demand. This is reasonable as it will be desirable to satisfy the load demand directly through solar PV, rather than through discharging a battery, as this will cause more of the PV production to be sent back to the grid. In addition, under the same conditions, supplying the grid with power from the battery would contribute to increased power flows over the grid, as opposed to the objective of the model. As such, it is both reasonable and desirable to prevent the battery from discharging at times where the PV production surpasses the load demand.

This version of the model revealed itself as the most promising and was the one utilized for all simulations involving batteries. It was presented explicitly in Section 5.4.1.

- **NLP with nine decision variables:** An attempt was also made to solve the optimization problem through nonlinear programming (NLP). The major advantage with such a model is that it can easily handle the problem of charging and discharging occurring at the same time step, through the nonlinear constraint shown in Equation (36).

$$(x_2(t) + x_4(t)) \cdot (x_6(t) + x_8(t)) = 0, \qquad 1 \le t \le 24 \tag{36}$$

Although, when implementing this model, it did converge to a feasible solution, it did not manage to find the optimal solution. Several optimization algorithms were utilized (most prominent: interior point algorithm), along with allowing an increased number of maximum function evaluations and maximum iterations, but the optimal solution could not be found. Also, the model was fed with different starting/initial points, all being feasible. However, a feasible starting point does not imply finding the global optimal solution. In general, the process of obtaining "good" initial points, that will (almost) guarantee an optimal solution, can be extensive and time-consuming. Due to this, no more efforts were made and the above approach, *QP with nine decision variables (2)*, was considered sufficient.

### C.3 Comments on the Auxiliary Variable (Final Model)

In this section, some efforts are given to ensure a correct interpretation of the auxiliary variable, $x_9(t)$. Note: In the initial model, presented in Appendix C.1, the auxiliary variable was referred to as $x_8(t)$. As can be seen from the auxiliary constraints, when minimizing $x_9^2(t)$, $x_9(t)$ will always be set equal to the binding auxiliary constraint. This means that for each time step, it will be set equal to the maximum minimum power flow over the grid, i.e. the largest of the power flows to and from the grid, after having tried to minimize both. This is illustrated in Figure 33 and can be expressed as in Equation (37). Note: as power cannot flow to and from the grid at the same time, for each time step either $x_1(t) + x_2(t)$ or $x_5(t) + x_8(t)$ will be zero.

$$x_9(t) = max\{min(x_1(t) + x_2(t)),\ min(x_5(t) + x_8(t))\}, \qquad 1 \leq t \leq 24 \qquad (37)$$

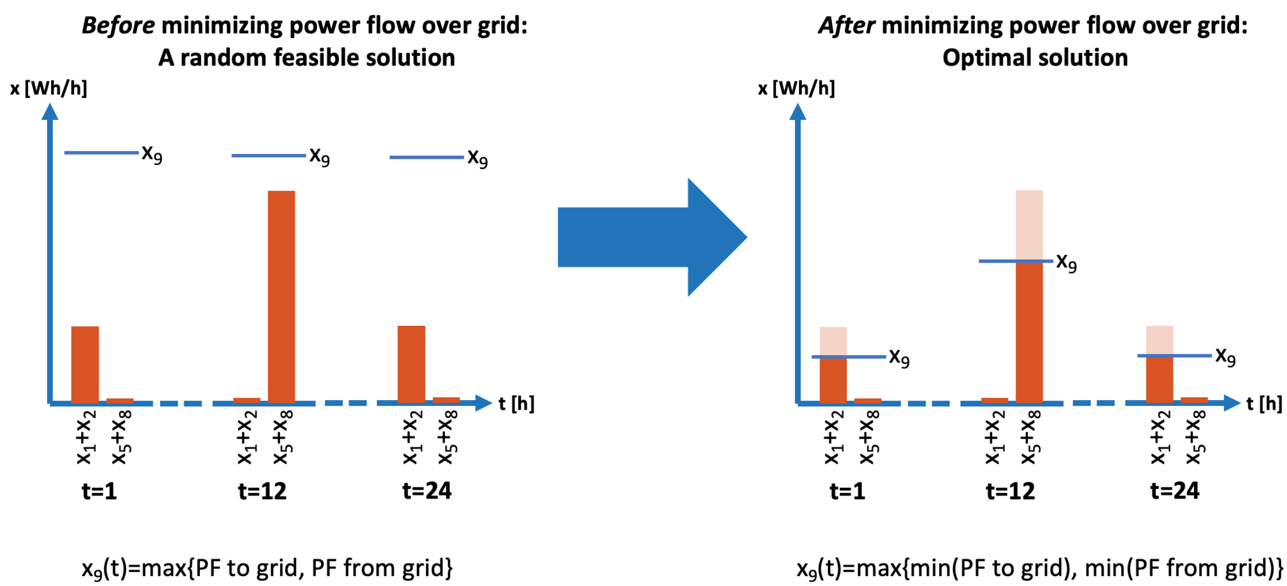


Figure 33: Illustration on how the auxiliary variable can be interpreted.

## C.4 Replication of Load Demand and PV Generation

Specific information on performing the load and PV replication in NETBAS, is found below.

**For the load**:

- Maximum load demand, as seen from the nearby substation, is calculated as:

$$Max\ load = Max\ load\ before\ optimization - PFFG\ reduction$$

- Daily variation is set equal a typical day during winter time
- Yearly variation remains as before, i.e. close to no variation

**For the solar PV**:

- Maximum PV production, as seen from the nearby substation, is calculated as:

$$\begin{aligned} Max\ PV =& Max\ PV\ before\ optimization - PFTG\ reduction \\ & - \frac{Max\ PFFG\ at\ 12:00}{Max\ PFFG} \cdot PFFG\ reduction \end{aligned}$$

- Yearly variation: Maximum value for each month is calculated as (note: *Max* refers to the maximum value within the month investigated):

$$Max\ PV\ (month) = \frac{(Max\ PFTG + Max\ PFFG\ at\ 12:00)}{Max\ PV\ before\ optimization}$$

Here, PFFG refers to *power flow from grid* and equals $x_1(t) + x_2(t)$ (defined in previous section), while PFTG refers to *power flow to grid* and equals $x_5(t) + x_8(t)$ (also defined in previous section). To avoid any confusion, these parameters are further discussed below:

- $Max\ load/Max\ PV$: Maximum load demand/PV production as seen from the substation of which the load/PV is connected, after the optimization. The maximum load demand/PV production is divided between the buildings in the same manner as was done in Section 5.2.

- $Max\ load/PV\ before\ optimization$: Maximum load demand/PV production as seen from the substation of which the load/PV is connected. For instance, when all buildings are connected to the same substation (subst. 9), the maximum load equals $0.62MW$, while the maximum PV equals $2.1MW$.

- $PFFG\ reduction$: Difference between maximum power flow from grid before optimization and maximum power flow from grid after optimization.

- $PFTG\ reduction$: Difference between maximum power flow to grid before optimization and maximum power flow to grid after optimization.

- $Max\ PFFG/Max\ PFFG$: Maximum power flow from/to grid.

- $Max\ PFFG\ at\ 12:00$: Chosen as the power flow from grid at 12:00, at the same day as $Max\ PFFG$ appears. Note: In NETBAS, 12:00 is pre-defined as the time of maximum PV production.

Having found the daily and yearly variation curves and maximum power demand/production as seen from the substation, each of the buildings connected to the given substation is modelled to have these daily and yearly variations. As stated under $Max\ load/Max\ PV$, the maximum load and maximum generation, as seen from each substation, is divided between the buildings connected to the given substation, as done in Section 5.2.

# D Cost Tables

## D.1 Costs of Prefabricated Substations

Table 25: Costs related to *prefabricated* substations for $12kV$. All values from [6].

| Type | Materiell [kr/stk] | Montør [kr/stk] | Maskin [kr/stk] | Anlegg [kr/stk] | Prosjektering [kr/stk] | Andre [kr/stk] | Totalt [kr/stk] |
|---|---|---|---|---|---|---|---|
| 315kVA | 207 758 | 26 157 | 5 280 | 3 771 | 20 110 | 11 975 | **275 050** |
| 500kVA | 262 359 | 27 336 | 5 280 | 3 145 | 20 110 | 11 930 | **330 160** |
| 800kVA | 314 475 | 27 926 | 5 280 | 3 145 | 20 110 | 11 930 | **382 865** |
| 1250kVA | 392 942 | 28 515 | 5 280 | 3 245 | 20 110 | 12 187 | **462 279** |
| 1600kVA | 405 502 | 29 695 | 5 280 | 3 245 | 20 110 | 12 187 | **476 018** |

## D.2 Costs of Cable Systems

Table 26: Costs related to 230/400V cable systems. All values from [6, p.12].

| Type | Materiell [kr/km] | Montør [kr/km] | Maskin [kr/km] | Anlegg [kr/km] | Prosjektering [kr/km] | Totalt [kr/km] |
|---|---|---|---|---|---|---|
| TFXP 4x25 Al | 29 991 | 22 562 | 7 126 | 2 106 | 46 675 | **108 459** |
| TFXP 4x50 Al | 41 397 | 22 725 | 7 126 | 2 106 | 46 675 | **120 029** |
| TFXP 4x95 Al | 82 907 | 11 066 | 4 654 | 6 592 | 36 678 | **141 897** |
| TFXP 4x150 Al | 112 267 | 11 211 | 4 654 | 8 265 | 36 678 | **173 075** |
| TFXP 4x240 Al | 161 378 | 11 006 | 4 654 | 8 265 | 35 834 | **221 137** |

Table 27: Costs related to 12kV cable systems (in trenches). All values from [6, p.15].

| Type | Materiell [kr/km] | Montør [kr/km] | Maskin [kr/km] | Anlegg [kr/km] | Prosjektering [kr/km] | Totalt [kr/km] |
|---|---|---|---|---|---|---|
| TSLE/-F 3x1x50 Al | 137 422 | 15 837 | 5 621 | 6 592 | 12 646 | **178 118** |
| TSLE/-F 3x1x150 Al | 193 052 | 20 260 | 5 621 | 8 265 | 15 244 | **242 442** |
| TSLE/-F 3x1x240 Al | 249 044 | 20 260 | 5 621 | 8 265 | 15 244 | **298 434** |
| TSLE/-F 3x1x400 Al | 346 203 | 21 102 | 5 621 | 16 911 | 15 244 | **405 081** |
| TSLE/-F 3x1x630 Al | 572 844 | 21 102 | 5 621 | 21 932 | 15 244 | **636 743** |

### D.3 Costs of Trenches

Table 28: Costs related to trenches. All values from [6, p.18].

| Type | Materiell [kr/km] | Montør [kr/km] | Maskin [kr/km] | Anlegg [kr/km] | Prosjektering [kr/km] | Andre [kr/km] | Totalt [kr/km] |
|---|---|---|---|---|---|---|---|
| Byområde | - | - | 145 625 | 360 677 | 35 338 | 253 591 | **795 231** |
| Forstad | - | - | 121 100 | 162 810 | 35 338 | 199 001 | **518 249** |
| Landsbygd | - | - | 147 092 | 125 220 | 35 338 | 81 823 | **389 473** |
| Tillegg for jordledning ($50mm^2$ Cu) forlagt i grøft | 42 345 | 253 | - | 2 106 | 2 042 | - | **46 745** |

## E Investment Cost Calculations for All Measures

Table 29: Investment cost of the different measures.

| Meas. | Calculation | Cost [kNOK] |
|---|---|---|
| A | $(2 \cdot 221\ 137 kr/km + 1.00 \cdot (795\ 231 kr/km + 46\ 745 kr/km)) \cdot 0.135 km$ | $=$ 173.374 |
| B | $(2 \cdot 221\ 137 kr/km + 0.20 \cdot (795\ 231 kr/km + 46\ 745 kr/km)) \cdot 0.073 km$ | $=$ 44.579 |
| C | $(2 \cdot 221\ 137 kr/km + 1.00 \cdot (795\ 231 kr/km + 46\ 745 kr/km)) \cdot 0.119 km$ | $=$ 152.826 |
| D | $(2 \cdot 221\ 137 kr/km + 0.10 \cdot (795\ 231 kr/km + 46\ 745 kr/km)) \cdot 0.136 km$ | $=$ 71.600 |
| E | $(2 \cdot 221\ 137 kr/km + 0.30 \cdot (795\ 231 kr/km + 46\ 745 kr/km)) \cdot 0.083 km$ | $=$ 57.674 |
| F | $(2 \cdot 221\ 137 kr/km + 0.25 \cdot (795\ 231 kr/km + 46\ 745 kr/km)) \cdot 0.119 km$ | $=$ 77.679 |
| G | $(2 \cdot 221\ 137 kr/km + 0.25 \cdot (795\ 231 kr/km + 46\ 745 kr/km)) \cdot 0.120 km$ | $=$ 78.332 |
| H | $(2 \cdot 221\ 137 kr/km + 0.15 \cdot (795\ 231 kr/km + 46\ 745 kr/km)) \cdot 0.109 km$ | $=$ 61.974 |
| I | $(2 \cdot 221\ 137 kr/km + 0.30 \cdot (795\ 231 kr/km + 46\ 745 kr/km)) \cdot 0.026 km$ | $=$ 18.067 |
| J | $(2 \cdot 221\ 137 kr/km + 0.25 \cdot (795\ 231 kr/km + 46\ 745 kr/km)) \cdot 0.059 km$ | $=$ 38.513 |
| K | $(2 \cdot 221\ 137 kr/km + 1.00 \cdot (795\ 231 kr/km + 46\ 745 kr/km)) \cdot 0.105 km$ | $=$ 134.846 |
| L | $(2 \cdot 221\ 137 kr/km + 0.40 \cdot (795\ 231 kr/km + 46\ 745 kr/km)) \cdot 0.046 km$ | $=$ 35.837 |
| M | $(2 \cdot 221\ 137 kr/km + 1.00 \cdot (795\ 231 kr/km + 46\ 745 kr/km)) \cdot 0.068 km$ | $=$ 87.329 |
| N | $(2 \cdot 221\ 137 kr/km + 0.65 \cdot (795\ 231 kr/km + 46\ 745 kr/km)) \cdot 0.117 km$ | $=$ 115.778 |
| O | $462\ 279 kr + 382\ 865 kr$ | $=$ 845.144 |
| P | $462\ 279 kr + (298434 kr/km + 795231 kr/km + 46745 kr/km) \cdot 0.109 km$ | $=$ 596.584 |
| Q | $476\ 018 kr + (298434 kr/km + 795231 kr/km + 46745 kr/km) \cdot 0.109 km$ | $=$ 600.323 |
| R | $(15 kWh + 130 kWh) \cdot 1966.9 NOK/kWh$ | $=$ 285.201 |
| S | $530 kWh \cdot 1966.9 kr/kWh$ | $=$ 1042.457 |
| T | $60 kWh \cdot 1966.9 kr/kWh$ | $=$ 118.014 |

## F Calculation of Cost of Losses

Table 30: Equivalent cost of losses, $k_{pekv}$, in $NOK/kWyr$, calculated for all alternatives, for the first and last year of all the intervals *Valid years*.

| Alt. | 2023 | 2024 | 2025 | 2026 | 2029 | 2030 | 2037 |
|---|---|---|---|---|---|---|---|
| 1 | 1719.0 | - | - | - | - | - | - |
| 2 | - | 1691.5 | 1696.8 | - | - | - | - |
| 3 | - | - | - | 1728.4 | 1746.8 | - | - |
| 4 | - | - | - | - | - | 1017.3 | 1275.4 |
| 5 | - | - | - | - | - | 1072.3 | 1328.5 |
| 6 | - | - | - | - | - | 1157.4 | 1461.6 |
| 7 | - | - | - | - | - | 1459.3 | 1845.3 |
| 8 | - | 1809.2 | 1811.7 | - | - | - | - |
| 9 | - | - | - | 1825.7 | 1857.3 | - | - |
| 10 | - | - | - | - | - | 1515.4 | 1936.3 |
| 11 | - | - | - | - | - | 1949.5 | 2226.4 |
| 12 | - | - | - | - | - | 1626.7 | 2067.5 |

Table 31: Parameter values relevent for calculating cost of losses. All values are extracted from [42].

| Parameter | 2023 | 2024 | 2025 | 2026 | 2029 | 2030 | 2037 |
|---|---|---|---|---|---|---|---|
| $k_p$ $[NOK/kW\ yr]$ | 587 | 606 | 627 | 649 | 730 | 762 | 799 |
| $k_{wekv}$ $[NOK/kWh]$ | 0.299 | 0.289 | 0.287 | 0.286 | 0.278 | 0.290 | 0.360 |

Erlend Øye

A Practical Application of an Active Distribution Grid Planning Framework

Norwegian University of
Science and Technology